# Channelised and Open-slope processes of mass sediment transport: their morphological and seismic characterisation from selected Atlantic high productivity regions

**Dissertation**

**zur Erlangung des Grades**
**Doktor der Naturwissenschaten**
**(Dr. rer. Nat)**

**im Fachbereich 5**
**der Universität Bremen**

**vorgelegt von**
**Andrew Akwasi Antobreh**
**Bremen**
**2005**

## General outline of the thesis

The text of this thesis is structured as follows: Chapter 1 provides a general introduction of the study, starting with a brief overview of mass sediment transport processes. The main objectives of the thesis are then outlined, followed by an introduction to the regional setting of the study areas and their geological significance for the study objectives. The data and methods employed for the study are then discussed with more details provided for the seismic data acquisition and the processing methods used. The main research findings of the thesis are presented in three individual manuscripts which form Chapters 2, 3 and 4. Finally, Chapter 5 which is the last chapter, summarises the main conclusions of this research and also presents suggestions for future work. Brief outlines of the three manuscripts are presented below:

**Chapter 2: Morphology, seismic characteristics and development of Cap Timiris Canyon, offshore Mauritania: a newly discovered canyon preserved off a major arid climatic region.** Andrew A. Antobreh, Sebastian Krastel. *Marine and Petroleum Geology (in Press, accepted 10 June 2005).*

In Chapter 2 a combined interpretation of Hydrosweep swath bathymetry and high resolution multi-channel seismic reflection data is used to investigate the development of Cap Timiris Canyon. The detailed study of canyon morphology and seismic structure has allowed a closer examination of the processes leading to canyon formation as well as the role the canyon has played in the sediment dynamics of the margin. The study suggests a possible link between canyon development and a potential major fluvial system which flowed in the adjacent land, and this is discussed with the view to providing a new framework for understanding the paleo-climatic evolution of the adjacent Sahara Desert since Neogene time.

**Chapter 3: Mauritania Slide Complex: morphology, seismic characterisation and processes of formation** Andrew A. Antobreh, Sebastian Krastel

*To be submitted to International Journal of Earth Sciences.*

Chapter 3 describes and analyses in detail the main morphological elements of Mauritania Slide Complex based on recently acquired Parasound sediment echosounder data and high resolution multi-channel seismic reflection data. The data have afforded a better framework for studying the slide which is more complex than previously reported. The spatial and temporal relationships between the main slide morphological elements as well as factors

governing slide mobility and geometry have been discussed. The study also investigates slide pre-conditioning and potential trigger mechanisms for slide development.

**Chapter 4: Sedimentation processes along the slope and rise offshore Uruguay inferred from reconnaissance high resolution seismic reflection survey**

Andrew A. Antobreh, Sebastian Krastel and Volkhard Spieß. *To be submitted to Marine Geology*

In Chapter 4, reconnaissance high resolution multichannel seismic reflection data are used to investigate sedimentation processes in the slope and rise areas of the Uruguayan margin. The margin is characterised by extensive mass sediment movements resulting from sediment failures in the slope area. The types of gravity-driven processes are identified and the causes of sediment instabilities examined. The processes of mass sediment movement are investigated and discussed in relation to sea level fluctuations and bottom current circulation.

# Table of contents

**Chapter 1: General Introduction**

1.1 Processes of submarine mass sediment transport: a brief overview ……1

1.1.1 Submarine canyons as sediment drainage systems……2

1.1.2 Submarine slides as process of open slope mass sediment transport ……4

1.2 Main objectives of study……...8

1.3 Setting and geological significance of the selected study areas……9

1.3.1 The NE Atlantic margin off Mauritanian……...9

1.3.2 The SW Atlantic margin off Uruguay……..11

1.4 Data and Methods……...13

1.4.1 The Hydrosweep swath bathymetry system……14

1.4.2 The Parasound sediment echosounder system……14

1.4.3 The Bremen high resolution multi-channel seismic reflection (MCS) system…15

1.4.3.1 Data acquisition……15

1.4.3.2 Data processing and display……..17

**Chapter 2: Morphology, seismic characteristics and development of Cap Timiris Canyon, offshore Mauritania: a newly discovered canyon preserved off a major arid climatic region**

Andrew A. Antobreh, Sebastian Krastel

*Marine and Petroleum Geology (in Press, accepted 10 June 2005)*

2.1 Abstract……...23

2.2 Introduction……24

2.3 Geological setting……...26

2.3.1 Margin physiography……...26

2.3.2 Structural setting and stratigraphy……...27

2.3.3 Onshore Quaternary coastal geology and Paleoclimate……...…28

2.4 Data and Methods……...29

2.5 Morphological characteristics……30

2.5.1 General Morphology……30

2.5.1.1 Upper Cap Timiris Canyon……...32

2.5.1.2 Lower Cap Timiris Canyon……...32

2.5.2 Longitudinal depth profiles and variations in canyon relief……34

2.6 Seismic structure……36

2.6.1 Upper Cap Timiris Canyon……..……36
2.6.2 Lower Cap Timiris Canyon……..……40
2.7 Discussions…….....…….…45
2.7.1 Structural controls on canyon development…….……45
2.7.2 Style and patterns of meander development……46
2.7.3 Canyon incision……49
2.7.4 Terrace formation……...…….....……50
2.7.5 Origin and age of Cap timiris Canyon…….……54
2.7.6 Sediment transport processes and canyon preservation……...……56
2.8 Conclusions…….……58
2.9 Acknowledgements…….……60
References……60

**Chapter 3: Mauritanian Slide Complex: morphology, seismic characterisation and processes of formation**

Andrew A. Antobreh and Sebastian Krastel

*To be submitted to International Journal of Earth Sciences*

3.1 Abstract……...……64
3.2 Introduction…….……65
3.3 Geological setting and oceanography…….67
3.3.1 Margin physiography……...……67
3.3.2 Structural setting……...……..68
3.3.3 Sources of sediment supply to the margin……...……68
3.3.4 Oceanography……..……69
3.4 Data and Methods……..……70
3.4.1 The Parasound system……..……70
3.4.2 The high resolution MCS system…….71
3.5 Echosounder characteristics and seafloor morphology of the Mauritania Slide Complex……..……..71
3.5.1 Echosounder characteristics…….……71
3.5.1.1 The headwall and proximal depositional areas…….……71
3.5.1.2 Main debris flow depositional area……...……76
3.5.2 Seafloor morphology of the Mauritania Slide Complex…….……76
3.6 Seismic characteristics……..……..78

3.6.1 Headwall and proximal depositional areas……..……..78
3.6.2 Main debris flow depositional area……..……84
3.7 Discussions…….……87
3.7.1 Controls on slide geometry and mobility…….……87
3.7.2 Sedimentary environments and pre-conditioning for slide development.……88
3.7.3 Timing of slide events and failure mechanisms……...……90
3.7.4 Possible trigger mechanisms for slide development……91
3.7.4.1 Excess pore pressure……..……92
3.7.4.2 Earthquake as possible trigger mechanism……92
3.7.4.3 Diapirism as a possible trigger mechanism and its influence on recent slide development…….……93
3.8 Conclusions…….……96
3.9 Acknowledgements…….97
References…….97

**Chapter 4: Sedimentation processes along the slope and rise offshore Uruguay inferred from reconnaissance high resolution seismic reflection survey**

Andrew A. Antobreh, Sebastian Krastel and Volkhard Spieß

*To be submitted to Marine Geology*

4.1 Abstract…….……..……...…101
4.2 Introduction…….……..……102
4.3 Physiography and oceanographic setting……..……..……...…104
4.4 Seismic data…….……105
4.5 Results and interpretation…….…….…….…….……...…106
4.5.1 Continental slope…….…….…….…….……106
4.5.2 Continental rise……...……...……108
4.6 Discussions……..……..113
4.6.1 Patterns of debris flow deposition……..……113
4.6.2 Source of the debris flows and pre-conditioning for mass sediment failure ….114
4.6.3 Possible trigger mechanisms for the mass sediment movement……115
4.6.4 Sea level fluctuations and bottom current influence on sedimentation……..…116
4.6.5 Influence of recent structural deformation on sedimentation…….……118
4.7 Conclusions……...……121
4.8 Acknowledgements……...……122

**Chapter 5: Summary and perspectives**……...……125
**General acknowledgements**……..……130

# 1 General Introduction

## 1.1 Processes of mass sediment transport: a brief overview

Submarine mass sediment transport events have been recognised globally as important geological events responsible for moving large volumes of sediments from shelf and slope areas into the deep sea, as well as shaping most continental margins, e.g. the eastern Scotian margin (Piper and Ingram, 2003), the New Jersey continental margin (McHugh et al., 2002), the Norwegian-Greenland Sea continental margins (Vorren et al., 1998) and the northwest African continental margin (Weaver et al., 2000; Wynn et al., 2000). Consequently, they provide very useful indications about the prevailing dynamic sedimentary conditions in an area. In addition, because of their widespread and often episodic nature, mass sediment transport events are perceived as being important components of the modern stratigraphic record, and have been studied in connection with global climatic cycles, including sea level changes (e.g. McHugh et al., 2002).

Submarine slope failures give rise to a variety of gravity-driven sediment flow processes whose end members are generally recognised as slides, slumps, debris flows and turbidity currents (Fig.1.1). The definitions of theses terms as well as their usage have been discussed by several authors (e.g., Dingle, 1977; Embley and Jacobi, 1977; Bates and Jackson, 1987; McHugh et al., 2002). Under this context, the term ‘slide’ applies to any mass or block that moves downslope on a planar glide plane or shear surface and which shows no internal deformation (Dingle, 1977; McHugh et al., 2002). The term ‘slump’ refers to any block that moves downslope on a concave-up glide plane or shear surface and undergoes rotational movement causing minimal to substantial internal deformation. Thus, whereas slides are characterised by translational movement, slumps on the other hand represent rotational movement. On moving downslope, a slide block may break up into a number of smaller blocks of various sizes through brittle deformation forming a ‘debris slide’ (McHugh et al., 2002). The term ‘debris flow’ refers to an incoherent sediment mass containing abundant coarse grained material which is transported downslope via laminar flow (Bates and Jackson, 1987). Motion in debris flows is supported by matrix strength (Elverhoi et al., 2000). Further downslope, debris flows may evolve into turbidity currents as the flow assumes turbulent flow behaviour (Fig. 1.1).

As a further clarification of terminology, the term ‘slide’ has also been used extensively in literature (e.g. Hampton et al., 1996; Canals et al., 2004b; Wynn et al., 2000; Bryn et al., 2005) to refer to submarine landslides, which involve the mass movement of sediments resulting from large-scale slope failures. In this thesis the term ‘slide’ has been

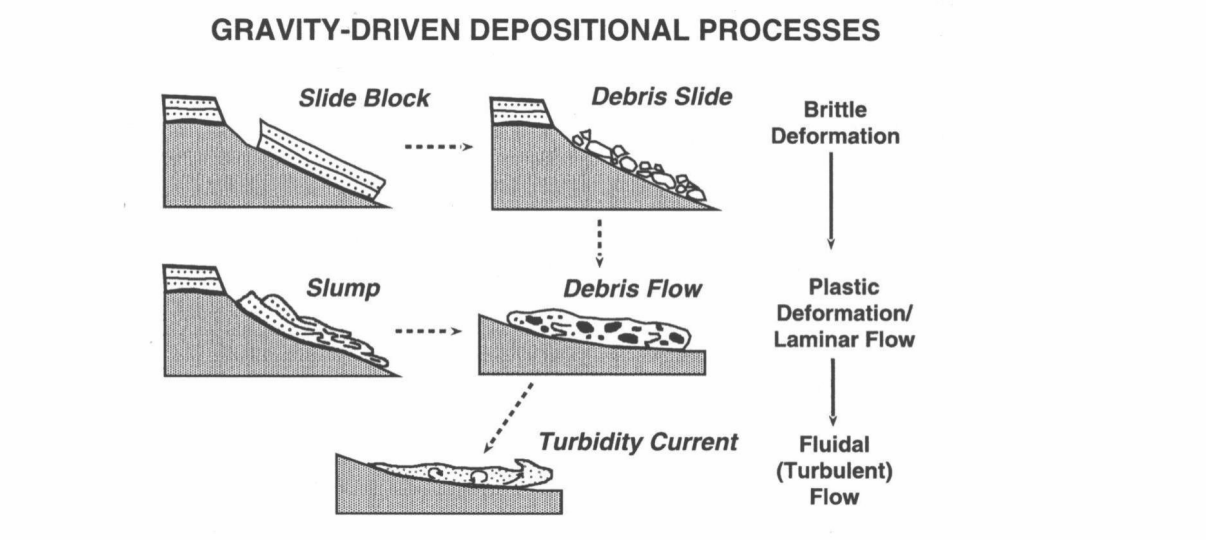


***Figure 1.1:*** *Schematic diagram showing end-member types of gravity-driven depositional processes that transport sediment into the deep sea (after McHugh et al., 2002)*

variously applied both as an end member gravity-driven process (as earlier defined), and also to refer to submarine landslides where appropriate. Along many Atlantic margins, the most conspicuous mechanisms through which remobilized submarine mass sediments are transported into the deep sea occur in the form of channelised sediment flows, where the sediments are funnelled into canyon systems and transported downslope as slides/slumps, debris flows and turbidity currents, or as submarine landslides which are commonly associated with large-scale sediments failures in open slope environments.

### 1.1.1 Submarine canyons as mass sediment drainage systems

Submarine canyons have been recognised globally on both convergent and divergent continental margins (e.g. Lewis and Barnes, 1999; Laursen and Normark, 2002; Babonneau et al., 2002; McHugh et al., 2002) as important sediment drainage systems for transporting mass sediments from slope and shelf areas into the deep sea. Consequently, canyons have been studied as important archives for documenting the sedimentation process history of an area (e.g. Bouma, 2001; Damuth, 1994). Furthermore, canyons are increasingly being studied as modern analogues for deepwater hydrocarbon reservoirs because they are often associated with sand-rich turbidites (Clark and Pickering, 1996; Posamentier, 2003; Abreu et al., 2003).

Along most Atlantic continental margins, submarine canyon systems are easily recognised as narrow submarine valleys that deeply incise shelf and slope areas, often extending several kilometres in length into the deep sea e.g. the NW African margin (Rona, 1971; Jacobi and Hayes, 1982; Weaver et al., 2000; Wynn et al., 2000) and the South Atlantic

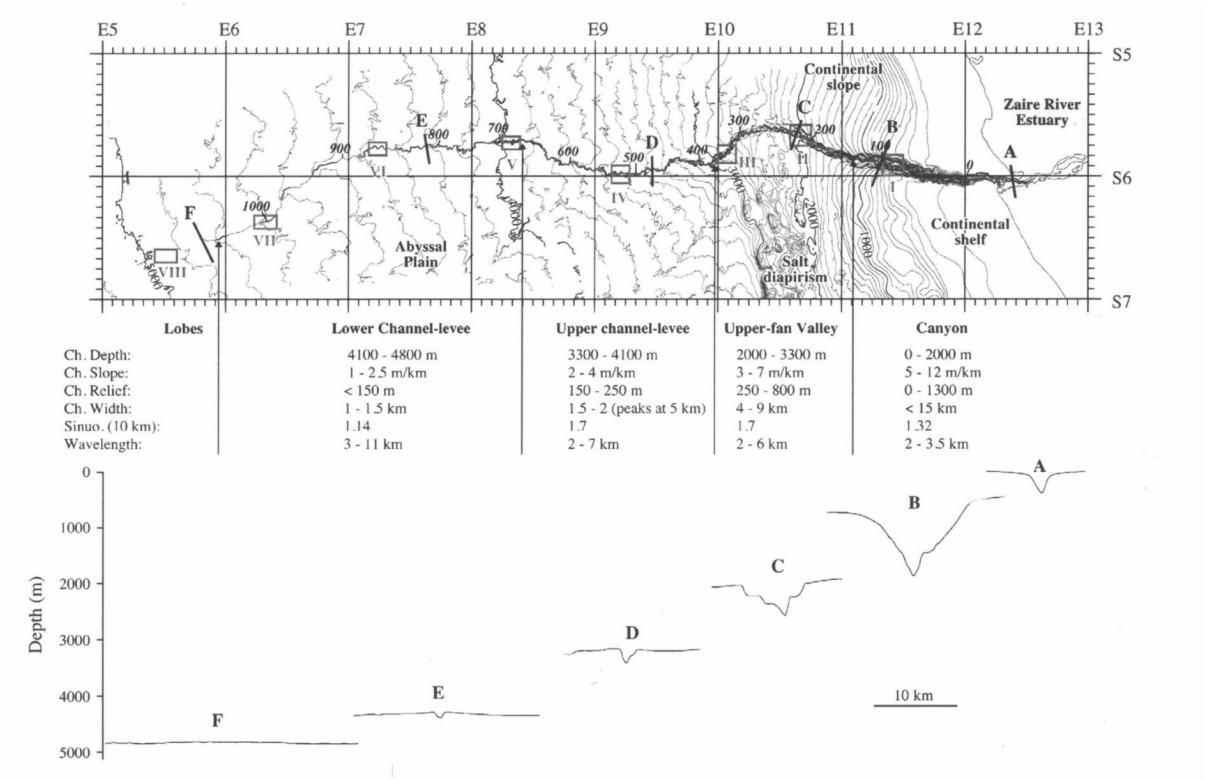


***Figure 1.2:*** *Bathymetric contour map of the Zaire Fan showing the canyon and channel segments as well as variations in cross-sectional morphology from the river mouth to the distal lobe on the lower fan (after Babonneau et al., 2002)*

margins (Lonardi and Ewing, 1971; Damuth, 1994). Submarine canyons commonly display many fluvial features including tributaries, meander and braided patterns, as well as terraces. They typically appear V-shaped in profile (Fig.1.2), and are often incised into bedrock (Damuth, 1994; Hagen et al., 1994).

Submarine canyons are primarily erosive features, and are dominated by sediment transport processes (Stow and Mayall., 2000). In deeper waters, the canyons may pass into channel systems as sediment deposition begins to dominate (Stow and Mayall., 2000; Barboneau et al., 2002; Canals et al., 2004a). The transition from canyon segment to channel segment in canyon-channel systems is typically characterised by the development of channel levees along channel flanks (Fig. 1.2). The channels are generally shallower and U-shaped. At their deep sea terminations, canyon-channel systems are characterised by the development of submarine fans. The large spatial extent of submarine fan systems, e.g. the Amazon Fan (Damuth and Kumar, 1975), the Bengal Fan (Curray, 1994) and the Mississippi Fan (Weimer, 1991), provides clear evidence of the importance of submarine canyons as efficient conduits for moving large sediment materials from shelf and slope areas into the deep sea.

Several hypotheses have been advanced to explain the origin of submarine canyons, and these are mostly associated with mass sediment flows as well as turbidity currents and

bottom currents (e.g. Lonardi and Ewing, 1971; Damuth and Kumar, 1975). The origin of many passive margin submarine canyons, e.g. Amazon Canyon, Monterrey Canyon and Zaire Canyon, has been traced to major terrestrial river systems which were able to erode their way across an emergent shelf during major periods of glacial sea level lowstand in order to deliver their load directly into the slope areas and beyond (Damuth and Kumar 1975; McHugh et al., 1998). Such submarine canyons are believed to have been most active during past periods of sea level lowstands, since they were then coupled to the river systems, and hence received direct supplies of terrigenous sediment discharges (Damuth, 1994; Hagen et al., 1994; Babonneau et al., 2002).

In addition to receiving sediments directly from connecting fluvial point sources, submarine canyons may also trap sediments transported by along slope currents as well as offshore wind-blown sediments. Often steep canyon walls become unstable and fail into the canyons thereby introducing slide/slump and debris flow materials which are incorporated into the canyon mainstream for downslope transport. This process is the most common cause of canyon widening (Posamentier, 2003). Tectonic activities and earthquakes are also known to temporarily initiate renewed turbidity flow activities within canyons, even during stages of canyon inactivity, as documented by the 1755 Lisbon earthquake which triggered massive turbidity currents along the Setubal Canyon (Thomson and Weaver, 1994).

In spite of the large strides made in marine geophysical research over the last few decades, several large submarine canyons may, however, still remain undocumented and hidden from detection. This is evidenced by, for example, the recent discovery of a large submarine meandering canyon off Mauritania, the Cap Timiris Canyon, which is one of the central themes of this study.

### 1.1.2 Submarine slides as processes of open slope mass sediment transport

Submarine slides (also known as submarine landslides) have been defined as the downward and outward movement of slope-forming materials, wherein shear failure occurs along one or several surfaces (Hampton et al., 1996; Weaver et al., 2000). The phenomena may involve a complexity of large slope failures, and may typically include elements of sliding, slumping and debris flows (Hampton et al., 1996; Wynn et al., 2000; Canals et al., 2004b).

Slides occur globally (Fig. 1.3) and affect all types of continental margins including passive, e.g. the eastern Scotian margin (Piper and Ingram, 2003), the New Jersey continental margin (McHugh et al., 2002) and the Norwegian-Greenland Sea continental margins (Bugge,

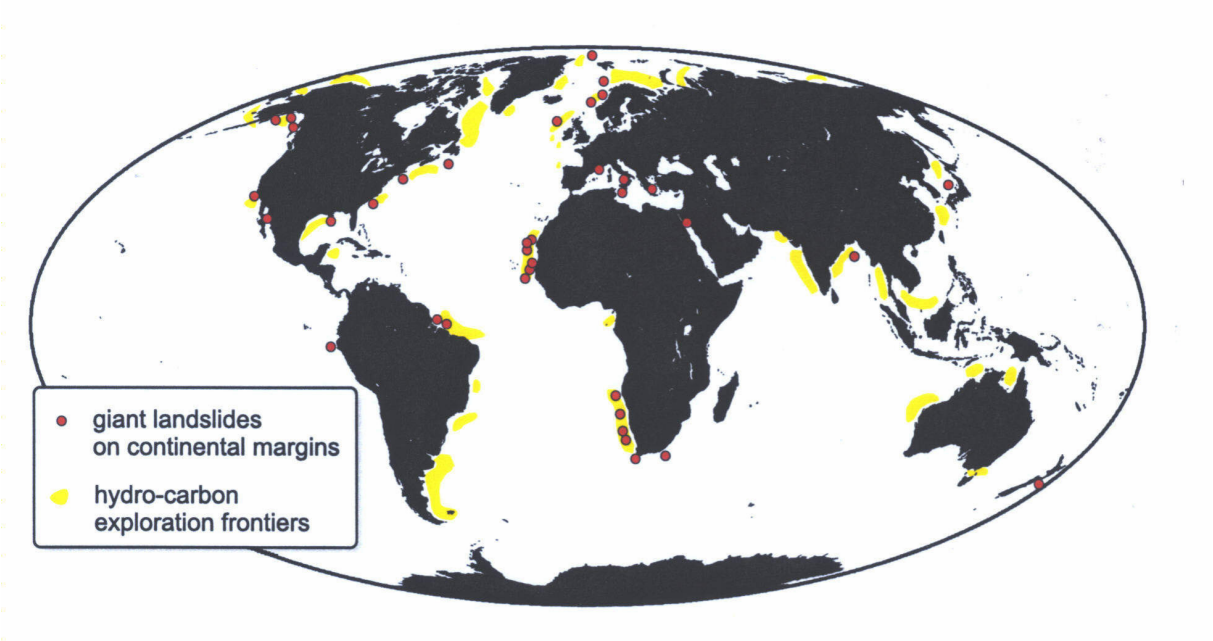


***Figure 1.3:*** *Global distribution of major submarine landslides on continental margins and location of frontier areas of hydrocarbon exploration (after Stow et al., 2000)*

1983; Vorren et al., 1998) as well as active margins, e.g. NE Mediterranean Sea (Lykousis et al., 2002) and Japan Sea (Lee et al., 1996). They have been recognised in various areal dimensions ranging from relatively smaller slides <1000 km², e.g. the Afen Slide off northwest of Shetlands Islands (Wilson et al., 2004) and the Gebra Slide off the Trinity Peninsula margin, Antarctica (Imbo et al., 2003) to giant slides affecting areas > 10 000 km², e.g. the Canary Slide (Canals et al., 2004b) and the Storegga Slide off western Norway (Bugge, 1983; Haflidason et al., 2004, Canals et al., 2004b). Slides, therefore, constitute one of the most important mechanisms for mass sediment movement from shelf and slope areas into the deep sea, and also play a very important role in the evolution of submarine landscape (Hampton et al., 1996; McAdoo et al., 2000).

Submarine slides constitute a major geo-hazard to coastal settlements because of their potential to displace large volumes of water, and thus generate or amplify destructive tsunami waves (Dawson, 1999; Fryer et al., 2003; Trifunac et al., 2003; Fine et al., 2004). As interest of the oil industry extends further into deeper waters, a good understanding of processes of submarine slide development has become increasingly imperative, especially, in geo-hazard assessment studies for engineering and environmental projects required for offshore economic resource exploitation and installations (Baraza et al., 1999, Piper and Ingram, 2003). Another reason why the study of slides is important for the oil industry is because slides are capable of significantly affecting the architectural characteristics, and hence sedimentological properties of channel systems and channel-levee complexes associated with potential deep sea

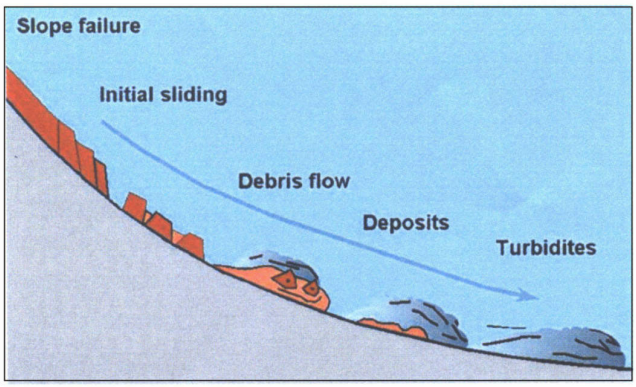


***Figure 1.4:*** *Schematic representations of the different stages of a submarine slide formation from slope failure to turbidite deposition (after Bryn et al., 2005)*

hydrocarbon reservoirs (Barley, 1999; Lastras et al., 2004). Consequently, major efforts have in recent years been dedicated towards understanding the dynamics, triggering mechanisms and products of submarine slides e.g. the COSTA Project (Canals et al.., 2004b) and the several studies connected with large slides on the Norwegian margin (e.g. Bugge, 1983; Laberg and Vorren, 2000; Haflidason et al., 2004).

A number of studies (e.g. Varnes, 1958; Hampton et al., 1996 and Canals et al., 2004b) have documented and discussed the main features that characterise submarine slides. Slides are typically recognised by the presence of a headwall scar at the upper part of a rupture surface where the sediment failure occurred and downslope mass sediment movement began. The displaced slide material may remain intact, deformed or break up into discrete blocks which may disintegrate completely into a debris flow and subsequently into turbidity currents (Fig. 1.4). Seismic interpretations of submarine slides (e.g. Lykousis et al., 2002; Lastras et al., 2004; Haflidason et al., 2004) show that headwall scars commonly occur as steep truncations in the well-layered slope stratigraphy (Fig. 1.5). The resulting debris flow deposits are acoustically identified by their transparent to chaotic internal reflections which are typically distinctive from surrounding well-layered sediments. Their upper surfaces are commonly characterised by hyperbolic or irregular reflections, often becoming hummocky and smoothening out in more distal parts. Individual debris flow units may assume various shapes and sizes ranging from small lenses to extensive sheet-like as well as massive bodies. The seismic characterisation of slides is, however, often complicated by variability in the sliding processes arising mainly from slide pre-conditioning geological controls (Hampton et al., 1996; Canals, 2004b).

When submarine slides result from slope failures in lithologically homogeneous sediment the rupture surface is often concave upward and the slide is termed a ‘rotational

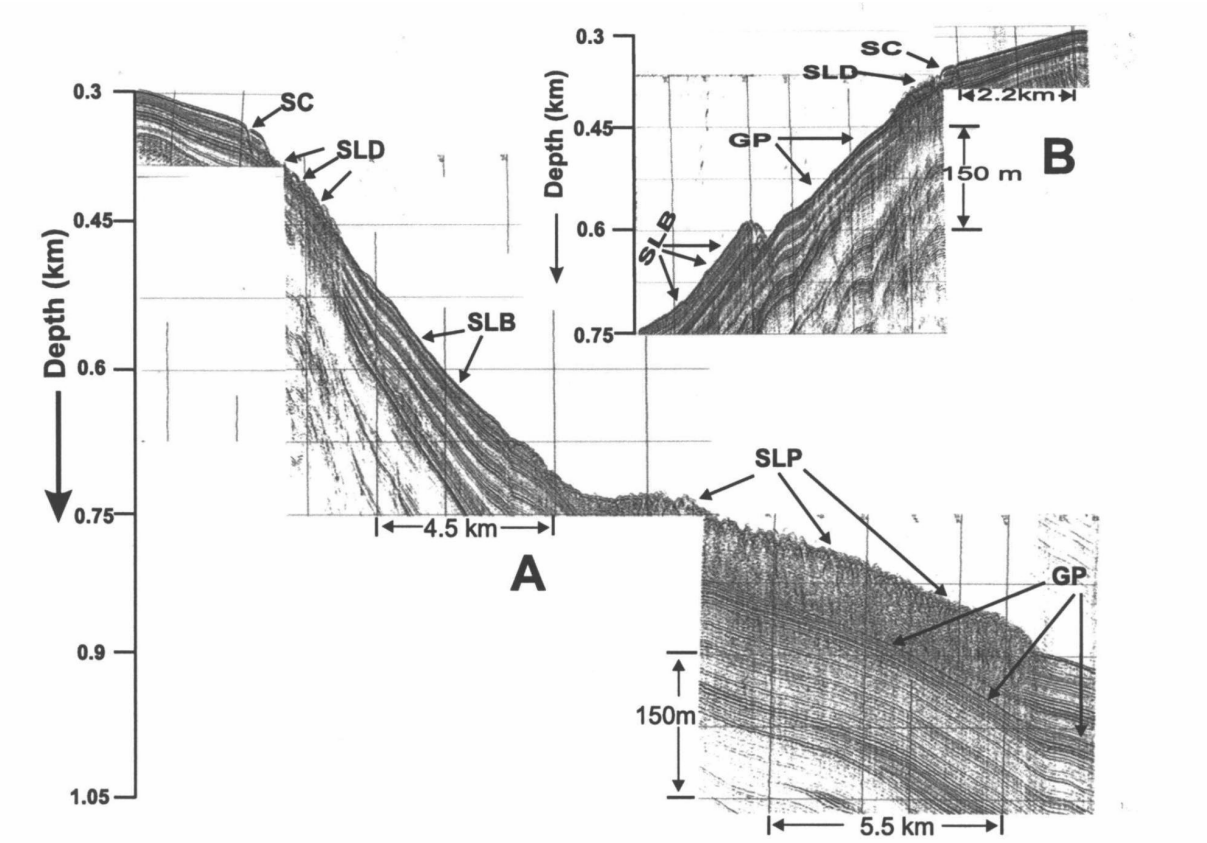


***Figure 1.5:*** *Air-gun seismic profile showing the appearance and characteristics of a slide from the North Aegean trough (Mediterranean) (modified after Lykousis et al., 2002). Headwall scar debris (SLD) at the foot of the scar (SC), glide plane (GP), slab slide (SLB) and the lower part of the slide (SLP) showing chaotic and hyperbolic reflectors.*

slide'. However, many slope sediments are inhomogeneous and have bedded weak layers which may control sediment failures and give rise to 'translational slide', characterised by a planar rupture surface. Yet still, slides may commonly develop from a series of slope failures that are initiated from downslope and progress upslope to give rise to 'retrogressive slides'.

A number of different factors have been cited as the immediate trigger mechanisms responsible for initiating submarine slide formation. These include, among others, earthquakes, sediment loading, excess pore pressures, gas hydrates, sea level fluctuations, diapirism and tectonic movements, or a combination of two or more of the factors (Hampton et al., 1996; Hühnerbach et al., 2004; Canals et al., 2004b). Though slope oversteepening may also constitute a potential trigger mechanism for sediment failure (e.g. Klaucke and Cochonat, 1999; Canals et al., 2004b), most submarine slides have been shown to occur on very low to moderately steep slopes between 2° - 5° or even <2° (McAdoo et al., 2000; Hühnerbach et al., 2004, Canals, 2004b), thus suggesting that slope angles in general do not provide a good indication about a margin's susceptibility to sliding.

**1. 2 Main objectives of study**

The present study investigates mass sediment transport processes based primarily on hydro-acoustic (Hydrosweep swath bathymetry and Parasound sediment echosounder) and high resolution multi-channel seismic reflection data acquired from two geologically unique Atlantic margin high productivity regions:

(i) off Mauritania, located on the eastern Atlantic margin of NW Africa (Fig. 6), and

(ii) off Uruguay, on the southwest Atlantic margin of South America (Fig. 1.7).

The data were acquired during two different expeditions by RV Meteor Cruises M49/2 and M58/1 offshore South America in February 2001 and NW Africa in April/May 200,3 respectively.

The main study objectives of the thesis include:

(i) to identify and seismically characterise the various forms of mass sediment movements in the high productivity regions, particularly submarine slides and canyon systems and their main morphological components, ,

(ii) to map their spatial and, if possible, temporal extent,

(iii) to determine the causes and triggers of the mass sediment movement events,

(iv) to evaluate the role of the events in the sedimentation process history of the various regions, and

(v) to evaluate their significance with respect to the morphological and oceanic boundary conditions in high productivity systems as well as their relationships with paleo-climatic events.

Studying geologically recent events have the advantage of being much better constrained than older events in terms of resulting morphologies, deposits, dynamics, impacts and ages (Canals et al., 2004b). As the selected study areas offer good potential for studying geologically recent mass transport events (Lonardi and Ewing, 1971; Weaver et al., 2000; Wynn et al., 2000, Hensen et al., 2003), the investigations should be well suited for achieving the main objectives of the thesis. The main results are intended to be integrated into other research findings within the interdisciplinary Project C2 of the Research Center Ocean Margins (RCOM), University of Bremen, with the aim of establishing a complete picture of mass transfer in high productivity regions, including their transport pathways as well as spatial and temporal relationships.

## 1.3 Setting and geological significance of the selected study areas

The selected study areas, i.e. the Mauritanian margin and the Uruguayan margin, are both strongly influenced by high rates of sediment accumulation related to oceanic high productivity leading to extensive mass sediment movement processes. However, the two areas exhibit marked differences in regional setting. For example, whereas the Mauritanian margin is strongly influenced by hyper-arid climatic conditions and additionally receives huge quantities of offshore wind-blown aeolian sediments, the Uruguayan margin is a fluvial-dominated margin and currently the site of huge quantities of terrigenous fluvial discharges.

As these are poorly surveyed areas, current knowledge about the sedimentary dynamics in the areas are limited, having been largely derived from more regional based studies (e.g. Lonardi and Ewing, 1971; Jacobi and Hayes, 1982; Klaus and Ledbetter, 1988). The following brief introduction of the geological and oceanographic setting of the selected areas is intended to highlight the geological significance of the study areas for achieving the study objectives.

### 1.3.1 The NE Atlantic margin off Mauritania

The Mauritanian margin is located off the Sahara Desert, a presently major arid climatic region and currently receives no significant fluvial sediment input (Fig. 1.6). However, major mass sediment movement events involving submarine canyon processes and slide formation have been documented along the margin (Rona, 1971; Jacobi, 1976; Jacobi and Hayes, 1982; Wynn et al., 2000). The margin has been the site of large sediment accumulations mainly from upwelling-induced sedimentation and offshore wind-blown aeolian sediment sources from the adjoining Sahara Desert (Sarnthein et al., 1982; Weaver et al., 2000). Previous studies of the margin (e.g. Rona, 1971; Jacobi, 1976; Jacobi and Hayes 1982, Wynn et al., 2000) showed the presence of areas of intense canyon processes which alternate with large scale slide development along the margin. However, as the mass sediment movement processes have not been adequately surveyed, they have remained poorly understood.

The Mauritanian margin lies within the Senegal Mauritania Basin, the largest of a series of marginal basins emplaced along the NW African margin during the Mesozoic opening of the Atlantic ocean (Jansa and Wiedmann, 1982). The basin is filled by a thick succession of Mesozoic-Cenozoic terrigenous to shallow marine sediments known to attain maximum depths of more than 10 km below the lower slope off Mauritania (Wissmann, 1982). The shelf width is typically between 25-50 km, but widens up to >100 km immediately

to the north of Cap Timiris following a sharp seaward offset of the shelf edge (Fig. 1.6). The shelf break occurs at water depth of 50 – 100 m from where it passes into the slope with gradient typically between 1° - 3° , but which locally reaches up to 6° north of Cap Timiris. The entire continental rise off Mauritania is very broad, and occurs at water depths of 2000 – 3000 m. Off Cap Timiris, and northwards, the slope and rise areas are characterised by several

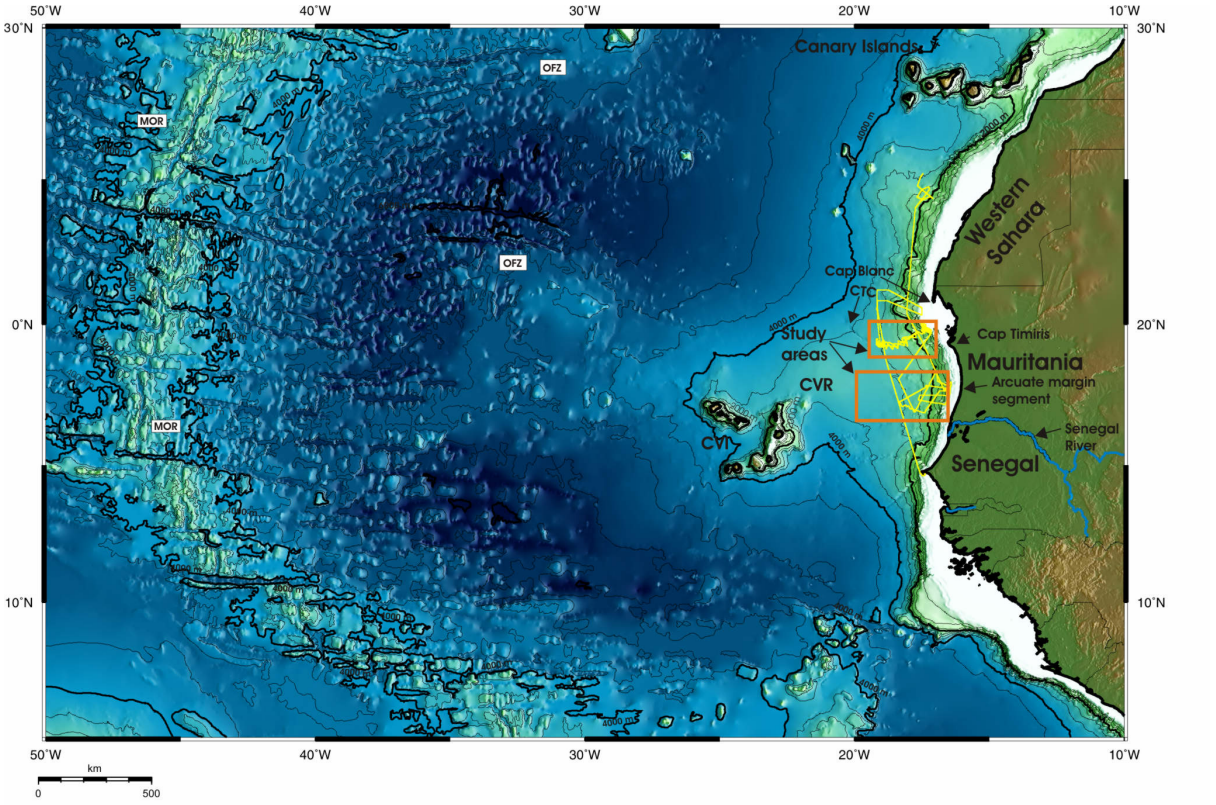


***Figure 1.6:*** *General bathymetry of NW African continental margin (Gebco, 2003) showing the location of the study areas along the Mauritanian margin (shown in two boxes) in relation to regional structure and bathymetry (contours at 500 m intervals). RV Meteor Cruise M58/1 track lines are shown in yellow lines. OFZ = oceanic fracture zones, MOR = Mid Oceanic Ridge, CVI = Cape Verde Islands, CVR = Cape Verde Rise, CTC = Cap Timiris Canyon.*

seamounts and basement highs (Jacobi and Hayes, 1982; Wynn et al., 2000). In the south, the rise is dominated by the extensive Cape Verde Rise (Fig. 1.6) which gradually elevates into the Cape Verde Islands at its crest. The region is dissected by several E-W trending oceanic fracture zones some of which are thought to have continental extensions to the margin (Wissmann, 1982).

As demonstrated by Vörösmarty et al. (2002) through a study of potential paleo-drainage patterns off NW Africa, the Cap Timiris area possibly constituted the estuary of a major ancient river which is now extinct, hence suggesting that parts of the margin may have previously been supplied with significant terrigenous fluvial sediments. In addition the mouth

of the Senegal River is believed to have been located near 18° 30'N during Miocene/Pliocene time, where it discharged large quantities of sediment thought to have triggered salt halokinesis (Wissmann, 1982) in the area. The mouth of the river has since migrated southwards to its present location near latitude 16°05'N, i.e. at the boundary between Mauritania and Senegal. As most of the sediment discharges into the coast by the river are swept southwards by nearshore currents (Seibold and Hinz, 1974), the river is currently unlikely to contribute significantly to sediment inputs into the Mauritanian margin.

The current regime along the outer shelf and slope of the Mauritanian margin, i.e., at <200 m water depth, is controlled by the southward-flowing Canary Current. Off Cap Blanc, the current splits up into two, as the dominant fraction is diverted towards the southwest whilst the remaining fraction continues further south to form the Guinea Current (Sarnthein et al., 1982). The Canary Current is underlain by the northward-flowing South Atlantic Central Water (SACW) which operates between ~150 – 400 m water depth. This current system is in turn underlain by the southward-flowing North Atlantic Central Water (NACW) which operates down to ~600 – 700 m water depth.

Though the deeper waters are less well studied (Sarnthein et al., 1982; Longdale, 1982), they are thought to be controlled by the southward-flowing North Atlantic Deep Water (NADW), which operates down to ~3500 – 4000 m water depths, and the underlying northward-flowing Antarctic Bottom Water (AABW). Present current velocities of the deep waters are thought to be generally weak, i.e. 1-6 cm/s, but they are known to increase significantly up to ~20 cm/s in areas where current circulation is topographically constricted (Lonsdale, 1982).

Though upwelling activities are mainly dominant along the outer shelf and shelf edge, they may locally extend offshore for hundreds of kilometres (Van camp et al., 1991; Gabric et al., 1993). The resulting biogenic sediment material is mainly deposited on the upper and mid-slope areas at water depths of ~1000 – 1500 m (Fütterer, 1983) where sedimentation rates may attain ~10 – 20 cm/1000 yr (Martinez et al., 1999).

### 1.3.2 The SW Atlantic margin off Uruguay

The Uruguayan margin is located near the estuary of the Rio de la Plata, and hence a strongly river-dominated margin (Fig. 1.7). Huge quantities of terrigenous sediments discharged into the South Atlantic by the Rio de la Plata are swept northwards from the estuary by longshore currents, and deposited at the Uruguayan continental shelf and slope (Lonardi and Ewing, 1971, Spiess et. al., 2002). The high rate of sediment accumulation is able to retain high

amount of water leading to low sediment rigidity. In addition, the margin is the site of high primary productivity and organic sedimentation arising from prevailing dynamic conditions in the surface waters (Behrenfeld and Falkowski, 1997; Hensen et al., 2003). Consequently, the Uruguayan margin is characterized by sediment instabilities and extensive mass sediment movement processes (Klaus and Ledbetter, 1988; Spiess et. al., 2002). Klaus and Ledbetter (1988) identified large mass flow deposits east of the Rio de la Plata and the adjacent abyssal plain based on their interpretations of 3.5 kHz echograms in their regional study of deep-sea sedimentary processes in the Argentine Basin. Furthermore, interpretations of Parasound sediment echosounder data from the area (e.g. Bleil et al.,1994; Hensen et al., 2003) also suggested frequent and extensive downslope mass movements of near-surface sediments in the margin.

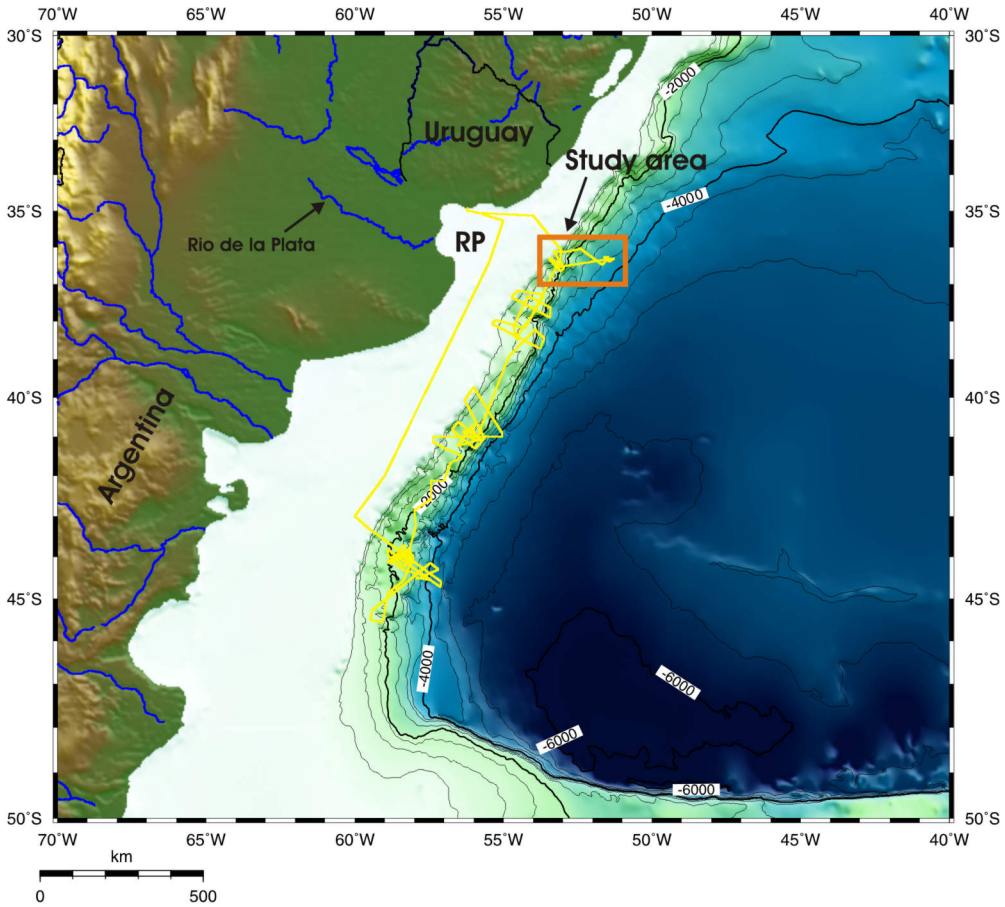


***Figure 1.7:*** *General bathymetry of SW Atlantic continental margin (Gebco, 2003) showing the location of the study area along the Uruguayan margin (shown in box). Contours are at 500 m intervals. RV Meteor Cruise M49/2 track lines are shown in yellow lines. RP = Rio de la Plata estuary. Blue lines = location of major rivers.*

Structurally, the Uruguayan margin is situated at the northwestern part of the continental rim of the extensive Argentine Basin. The physiography and sedimentary structure of the margin have been described by Lonardi and Ewing (1971) and Ewing and Lonardi

(1971). The width of the shelf offshore Uruguay is <150 km but it gradually increases up to more than 300 km south of 38° S (Fig. 1.7). The shelf break occurs at 130 – 150 m water depth from where it passes into a broad slope which becomes even broader northwards along the margin. The slope gradient is typically between 1° - 2.5°, but may locally increase to between 3° - 3.5°. The continental rise is characterised by a low to gentle gradient and it occurs from below ~2900 m water depth. Several canyons incise the slope and rise off the Rio de la Plata.

The Uruguayan margin is set within one of the most dynamically active regions of the South Atlantic, i.e. the confluence region of intensely mixing oceanic currents (Fig. 1.7) where the northward-flowing cold Antarctic water masses of the Falkland (Malvinas) Current meet the southward-flowing warm and saline tropical waters of the Brazil Current (Peterson and Stramma, 1991). The front separating these mixing water masses, which also controls the dynamics of the upper-level current regimes, currently migrates between 32° and 40° S in response to the relative strengths of the currents (Olson et al., 1988). The intense mixing leads to increases in current velocities extending to the seafloor, and at the same time give rise to high primary productivity (Antoine et al., 1996; Peterson et al., 1996). The increased current velocities are also thought to be the main cause for the winnowing and re-distribution of the large volumes of terrigenous sediment supplied to the Uruguayan margin by the Rio de la Plata (Peterson et al., 1996).

The confluence region is also set within the crossroads of a number of major deep-water masses including the northward-flowing Antarctic Intermediate Water (AAIW) and the southward-flowing North Atlantic Deep Water (NADW) which operates between 500 – 4000 m water depths. The Antarctic Bottom Water (AABW) which forms a strong deep-water circulation gyre centred around the Argentine Basin, controls the current regime from water depths below 3800 – 4000 m (Reid, 1989; Flood and Shor, 1988; von Lom-Keil et al., 2002).

## 1.4 Data and Methods

Data used in this thesis are based mainly on Hydrosweep swath bathymetry, Parasound sediment echosounder and high resolution multi-channel seismic reflection (MCS) data acquired during two separate cruises: R/V Meteor Cruises M49/2, off Uruguay in February 2001, and M58/1 off NW Africa in April/May 2003 (Figs. 6, 7). The research expeditions were undertaken by the University of Bremen. In general, systems for collecting all three data types were operated simultaneously in each of the two cruises during seismic profiling. Altogether, the amount of data processed and analysed for this study comprises

some 1000 km length of bathymetry data and more than 2,400 km length of Parasound and seismic profiles.

### 1.4.1 The Hydrosweep swath bathymetry system

The Hydrosweep swath bathymetric system is a hull-mounted multibeam echosounder which is permanently installed on the R/V Meteor. The system generates 59 pre-formed acoustic beams for sampling the seafloor at a frequency of 15.5 kHz. The beams are transmitted over an angle of 90°, and thus allows the system to map a seabed swath of width equal to two times the water depth (Grant and Schreiber, 1990). The system is able to suppress refraction effects on the outer beams by employing a patented calibration process which compares depth values of the central and outer beams in order to calculate a mean sound velocity from the best fit between the two values. The mean velocity is then used for all depth computations, hence minimizing residual errors to values less than 0.5% of water depth.

The bathymetry data was processed using the public domain software Multibeam System (Caress and Chayes, 1996) which has both automatic and interactive editing tools for correcting navigation data as well as depth values. After the automatic tools had been used to remove all bad outer beams and abnormal depth values, the time-intensive interactive editing was then carried out to delete any remaining artefacts. Following processing, the data were gridded and then imaged as contour plots using the public domain software package, GMT (Wessel and Smith, 1998).

### 1.4.2 The Parasound sediment echosounder system

The Parasound system (Grant and Schreiber, 1990) is a high frequency sediment echosounder which, like the Hydrosweep system, is also hull-mounted and permanently installed on the R/V Meteor. The system utilizes the so-called parametric effect through the emission of two high amplitude, high frequency sound waves in order to generate an operational secondary sound wave of the difference frequency which lies between 2.5 – 5.5 kHz. This secondary sound wave is focused within an emission cone of 4° opening angle, and consequently results in a footprint diameter of ~7% of the water depth, thereby affording a better horizontal resolution than conventional 3.5 kHz systems. In addition, the broader signal bandwith of the system provides a better vertical resolution, which is in the order of a few decimeters. Depending on the type of sediment and attenuation, depth of penetration may vary between 0 - 200 m. The system is compensated for roll, pitch and heave as a means of ensuring vertical sound emission. The Parasound data were digitally recorded using the

ParaDigMA acquisition system (Spiess, 1993) and then stored in a compressed SEGY format for further processing. A band pass frequency filter of 2.0 – 6.0 kHz was applied during processing before display.

### 1.4.3 The Bremen high resolution multi-channel seismic (MCS) reflection system

The multi-channel seismic reflection system of the University of Bremen has been specially designed to acquire high-resolution seismic data through optimizing all system components and procedural parameters. An outline of the system used during RV Meteor Cruise M58/1 (Fig. 1.8) is provided as an example.

#### 1.4.3.1 Data acquisition

During both cruises, the MCS data were acquired using a 1.7 l GI-Gun as the primary seismic source and a 0.16 l Watergun as a secondary source. However, in the case of M49/2 a 0.4 l GI-Gun was in use as a third seismic source as well. The Watergun and the GI-Guns were operated in an alternating mode at different frequencies of 200 – 1600 Hz and 100 – 500 Hz respectively, with a high pressure air of 150 bar (2150 PSI). During M49/2 Cruise, the guns were triggered at a time interval between 9 - 11.5 s. With an average ship speed of 6.0 – 6.5 knots, a shot distance of ~30 – 38 m between shots was obtained for the Watergun while the shot distance for the individual GI-Guns was twice this distance because both GI-Guns were recorded with the same recording unit.. In the case of M58/1 Cruise, the average ship speed was 6 knots and the guns were shot every 9 – 10 s leading to a distance of 28 – 31 m between shots of the same source.

An oil-filled Syntron streamer, equipped with separately programmable hydrophone subgroups, was employed to receive the seismic signals. During cruise M49/2 the streamer had a lead-in cable of 30 m length and a stretch section of 100 m length as well as six active sections each 100 m long. The hydrophone subgroups were assigned different lengths in order to optimize resolution and bandwith of the received signals and also to avoid destructive interferences. During the cruise, 48 groups, each with a length of 6.25 m and a group spacing of 12.5 m, were employed for recording the GI-Gun data while another 48 channels with a length of ~2m and a group spacing of 12.5m were used for recording the Watergun data. The streamer was attached with 5 Multi Trak and 5 DigiBird Remote Units (RUs) each equipped with adjustable wings which were remotely controlled with a PC-based control unit to maintain the streamer at 3 m water depth. In the case of M58/1 Cruise, the streamer had a lead-in cable of 45 m length connected to a stretch section of 50 m length which was then

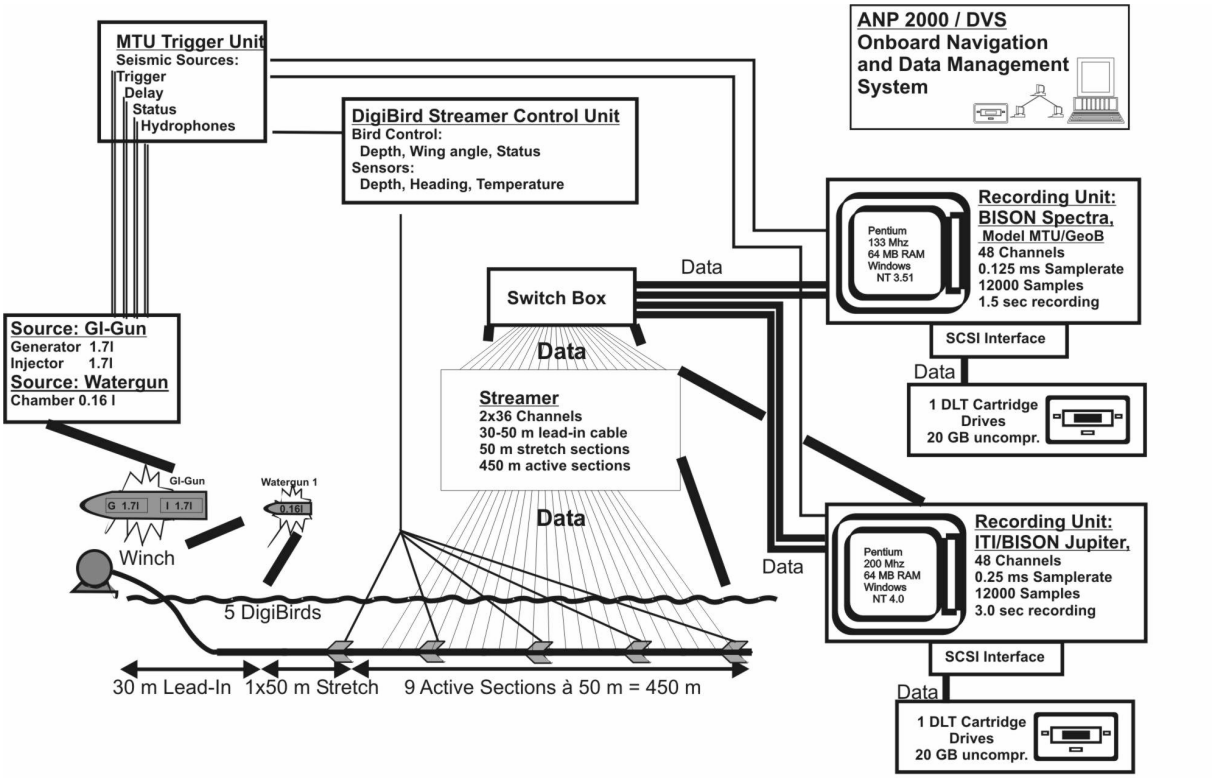


***Figure 1.8:*** *Outline of the high resolution multi-channel seismic data acquisition system used during RV Meteor Cruise M58/1 (after Shultz, H.D. and cruise participants, 2003)*

followed by nine active sections each of 50 m length. 36 channels each were used for recording the GI-GUN and Watergun data, respectively. The setup of the channels (group spacing and length) was identical to the values given above for cruise M49/2. The streamer was attached with only 5 DigiBird RUs, though one did not function most of the time. Again the RUs were remotely operated to keep the Syntron steamer at 3 m water depth.

The data were digitally recorded using two separate 48-channel recording units: a Jupiter/ITI/Bison seismograph for the GI-Gun data and a Bison Spectra seismograph for the Watergun data. The Jupiter/ITI/Bison seismograph allows online display of data (shot gather) as well as demultiplexing and data storage in SEG-Y format. During both cruises the GI-Gun data were recorded at a sampling frequency of 4 kHz for 3 s time. Pre-amplifiers were set to 48 dB and low-cut filters to 4 Hz. Though all 48 channels were written on tape, in the case of M58/2 no data was available for the last 12 channels, as only 36 channels were used.

The Bison Spectra has the same essential features as the first unit and was specially designed for the University of Bremen. It permits a continuous operation mode for acquiring very high-resolution seismic data (sampling with up to 20 kHz). The recording unit also allows online display of data (shot gather) as well as demultiplexing and data storage in SEG-Y format. During both cruises the Watergun data were recorded at a sampling frequency of 8 kHz over a recording length of 1.5 s. Pre-amplifiers were set to 60 dB, and analogue filters to 16 Hz (low-cut) and 2000 Hz (high-cut). The data were stored on DLT 4000 cartridge tapes.

#### 1.4.3.2 Data processing and display

The MCS data were processed using a combination of 'in-house' softwares, developed at the University of Bremen, and the commercial 'Vista' (Seismic Image Software Ltd.) software. Only data sets for the 1.7 l GI-Gun were completely processed and then analysed for the study as they afforded deeper penetration and reasonably good resolution of the sedimentary features within the upper ~600 m (800 ms TWT) of the upper sedimentary cover.

As a first step geometry processing was carried out using a University of Bremen custom software package (Zühlsdorff, 1999) for CDP-sorting and static correction of the seismic data in order to account for both lateral and vertical movements of the streamer. The input data included: (i) shot number and time information, (ii) navigation data, (iii) depth data of the birds, and (iv) heading data of the birds. The algorithm initially involved a time interpolation to resample all data to the same time interval. The navigation and heading data were then applied to calculate reflection midpoints between source and receiver positions for each trace. The CDP's were then defined as small circles(bins) with distinct sizes and distances along the cruise track. Each reflection midpoint was next assigned to one CDP bin with the minimum distance to the center of the bin. Consequently, a CDP number was determined for each shot and recording number. This was followed by calculation of static correction time for each trace based on the lateral linear interpolation of depth information of the birds for each receiver. 'Vista' (Seismic Image Software Ltd.) software was then utilised for the main data processing.

The static correction time and CDP number data were exported into 'Vista' and then written into the trace headers of each record. Delay corrections were then applied to the data followed by velocity analysis to establish stacking velocities for NMO corrections and CDP-stacking. However, it emerged during the initial velocity analyses that a constant velocity of 1500 m/s could be applied for most of the data processing as the data were mostly collected from deep water environments (>1000 m water depths) using a relatively short streamer

length. A CMP spacing of 10 m was applied throughout for the data sets leading mostly to 8-10 and 7-8 fold coverages for the M49/2 and M58/1 seismic profiles respectively. The stacked sections were filtered with a bandpass frequency filter (frequency content: 55/110 – 600/800). The sections were time migrated and then muted. Finally, the commercial software package, Kingdom Suite (Seismic Micro Technology, Inc.) was used to display and interpret the sections.

## References

Abreu, V., Sullivan, M., Mohrig, D., and Pirmez, C. (2003). Lateral accretion packages (LAPS): an important reservoir element in deep water sinuous channels. Marine and Petroleum Geology 20, 631-648.

Antoine, D., Andre, J. M., and Morel, A. (1996). Oceanic primary production. 2. Estimation at global scale from satellite (coastal zone color scanner) chlorophyll. Global Biogeochem. Cycle 10, 43-55.

Babonneau, N., Savoye, B., Cremer, M., and Klein, B. (2002). Morphology and architecture of the present canyon and channel system of the Zaire deep-sea fan. Marine and Petroleum Geology 19, 445-467.

Baraza, J., Ercilla, G., and Nelson, C. H. (1999). Potential geologic hazards on the eastern Gulf of Cadiz slope (SW Spain). Marine Geology 155, 191-215.

Barley, B. (1999). Deepwater problems around the world. Leading Edge 18, 488-494.

Barusseau, J. P., Ba, M., Descamps, C., Diop, E. H. S., Giresse, P., and Saos, J.-L. (1995). Coastal evolution in Senegal and Mauritania at $10^3$, $10^2$ and 10-year scales: Natural and human records. Quaternary International 29/30, 61-73.

Bates, R. L., and Jackson, J. A. (1987). "Glossary of Geology." Amer. Geol. Inst., Alexandria, USA.

Behrenfeld, M. J., and Fakowski, P. G. (1997). Photosynthetic rates derived from satellite-based chlorophyll concentration. Limnol. Oceanogr. 42, 1-20.

Bouma, A. H. (2001). Fine-grained submarine fans as possible recorders of long- and short-term climatic changes. Global and Planetary Change 28, 85-91.

Bryn, P., Berg, K., Forsberg, C. F., Solheim, A., and Kvalstad, T. (2005). Explaining the Storegga Slide. Marine and Petroleum Geology 22, 11-19.

Bugge, T., (1983). Submarine slides on the Norwegian continental margin, with special emphasis on the Storegga area. Publ. Cont. Shelf Inst. 110, 152.

Canals, M., Casamor, J. L., Lastras, G., Monaco, A., Acosta, J., Berne., S., Loubrieu, B., Weaver, P. P. E., Grehan, A., and Dannielou, B. (2004a). The role of canyons in strata formation. Oceanography 17, 80-91.

Canals, M., Lastras, G., Urgeles, R., Casamor, J. L., Mienert, J., Cattaneo, A., De Batist, M., Haflidason, H., Imbo, Y., Laberg, J. S., Locat, J., Long, D., Longva, O., Masson, D. G., Sultan, N., Trincardi, F., and Bryn, P. (2004b). Slope failure dynamics and impacts from seafloor and shallow sub-seafloor geophysical data: case studies from COSTA project. Marine Geology 213, 9-72.

Caress, D. W., and Chayes, D. N. (1996). Improved Processing of Hydrosweep Multibeam Data on the R/V Maurice Ewing. Marine Geophysical Researches 18, 631-650.

Clark, J. D., and Pickering, K. T. (1996). "Submarine channels; Processes and Architecture." Vallis Press, London.

Curray, J. R. (1994). Sediment volume and mass beneath the Bay of Bengal. Earth and Planetary Science Letters 94(1-2), 71-77.

Damuth, J. E. (1994). Neogene gravity tectonics and depositional processes on the deep Niger Delta continental margin. Marine and Petroleum Geology 11, 320-346.

Damuth, J. E., and Kumar, N. (1975). Amazon cone: Morphology, sediments, age and growth pattern. Geological Society of America Bulletin 86, 873-878.

Dawson, A. G. (1999). Linking tsunami deposits, submarine slides and offshore earthquakes. Quaternary International 60, 119-126.

Dingle, R. V. (1977). The anatomy of a large submarine slump on a sheared continental margin (SE Africa). J. Geol. Soc. London 134, 293-310.

Elverhoi, A., Habitz, C. B., Dimakis, P., Mohring, D., Marr, J., and Parker, G. (2000). On the dynamics of subaqueous debris flows. Oceanography 13, 109-117.

Embley, R. W., and Jacobi, R. D. (1977). Distributions and morphology of large sediment slides and slumps on Atlantic continental margins. Mar. Geotechnol. 2, 205-228.

Ewing, M., and Lonardi, A. G. (1971). Sediment transport and distribution in the Argentine Basin. 5. Sedimentary structure of the Argentine Margin, Basin and related provinces. In: L.H. Ahrens et al. (Eds.), Physics and Chemistry of the Earth. Pergamon Press, Oxford. pp. 123-251.

Fine, I. V., Rabinovich, A. B., Bornhold, B. D., Thomson, R. E., and Kulikov, E. A. (2005). The Grand banks landslide-generated tsunami of November 18, 1929: preliminary analysis and numerical modeling. Marine Geology 215, 45-57.

Flood, R. D., and Shor, A. N. (1988). Mud waves in the Argentine Basin and their relationship to regional bottom circulation patterns. Deep-Sea Research 35, 943-971.

Fryer, G. J., Watts, P., and Pratson, L. F. (2003). Source of the great tsunami of 1 April 1946: a landslide in the upper Aleutian forearc. Marine Geology 203, 201-218.

Fütterer, D. K. (1988). The modern upwelling record off Northwest Africa. In "Coastal upwelling: its sediment record, Part B. Sedimentary records of ancient coastal upwelling." (J. Thiede, and E. Suess, Eds.), pp. 105-121. Plenum Press, London.

Gabric, A. J., Garcia, L., Van Camp, L., Nykjaer, L., Eifler, W., and Schrimpf, W. ( 1993). Offshore export of shelf production in the Cape Blanc (Mauritania) giant filament as derived from coastal zone colour scanner imagery. Journal of Geophysical Research 98, 4697-4712.

Grant, J. A., and Schreiber, R. (1990). Modern swathe sounding and sub-bottom profiling technology for research applications: The Atlas Hydrosweep and Parasound Systems. Marine Geophysical Researches 12, 9-19.

Haflidason, H., Sejrup, H. P., Nygard, A., Mienert, J., Bryn, P., Lien, R., Forsberg, C. F., Berg, K., and Masson, D. G. (2004). The Storegga Slide: architecture, geometry and slide development. Marine Geology 213, 201-234.

Hagen, R. A., Bergersen, D. D., Moberly, R., and Colbourn, W. T. (1994). Morphology of a large meandering submarine canyon system on the Peru-Chile forearc. Marine Geology 119, 7-38.

Hampton, M. A., Lee, H. J., and Locat, J. (1996). Submarine lanslides. Rev. Geophys. 34, 33-59.

Hensen, C., Zabel, M., Pfeifer, K., Schwenk, T., Kasten, S., Riedinger, N., Schulz, H. D., and Boetius, A. (2003). Control of sulphate pore-water profiles by sedimentary events and the significance of anaerobic

oxidation of methane for burial of sulfur in marine sediments. Geochimica et Cosmochimica Acta 67, 2631-2647.

Hühnerbach, V., Masson, D. G., and COSTA-Project. (2004). Landslides in the North Atlantic and its adjacent seas: an analysis of their morphology, setting and behaviour. Marine Geology 213, 343-362.

Imbo, Y., De Batist, M., Canals, M., Prieto, M. J., and Baraza, J. (2003). The Gebra Slide: a submarine slide on the Trinity Peninsula Margin, Antarctica. Marine Geology 193, 235-252.

Jacobi, R. D. (1976). Sediment slides on the northwestern continental margin of Africa. Marine Geology 22, 157-173.

Jacobi, R. D., and Hayes, D. E. (1982). Bathymetry, Microphysiography and Reflectivity Characteristics of the West African Margin Between Sierra Leone and Mauritania. In: U. von Rad, K. Hinz, M. Sarnthein, and E. Seibold (Eds.). Geology of the Northwest African Continental Margin. Springer-Verlag, Berlin. pp. 182-212.

Jansa, L. F., and Wiedmann, J. (1982). Mesozoic-Cenozoic development of the Eastern North American and Northwest African Continental Margins: a comparison. In: U. von Rad, K. Hinz, M. Sarnthein, and E. Seibold, (Eds.). Geology of the Northwest African Cantinental Margin. Springer-Verlag, Berlin. pp. 215-269.

Klaucke, I., and Cochonat, p. (1999). Analysis of past seafloor failures on the continental slope off Nice (SE France). Geo Marine Letters 19, 245-253.

Klaucke, I., and Hesse, R. (1996). Fluvial features in the deep sea: new insights from the glacigenic submarine drainage system of the Northwest Atlantic Mid-Ocean Channel in the Labrador Sea. Sedimentary Geology 106, 223-234.

Klaus, A., and Ledbetter, M. T. (1988). Deep-sea sedimentary processes in the Argentine Basin revealed by high resolution-seismic records (3.5 kHz echograms). Deep-Sea Research 35, 899-917.

Knutz, P. C., Jones, E. J. W., Austin, W. E. N., and van Weering, T. C. E. (2002). Glacimarine slope sedimentation, contourite drifts and bottom current pathways on the Barra Fan, UK North Atlantic margin. Marine Geology 188, 129-146.

Koopmann, B. (1981). Sedimentation von Saharastaub im subtropischen Nordatlantik während der letzten 25.000 Jahre. Meteor Forschungsergebnisse 35, 23-59.

Laberg, J. S., and Vorren, T. O. (2000). The Traenadjupet Slide, offshore Norway- morphology, evacuation and triggering mechanisms. Marine Geology 171, 95-114.

Lastras, G., Canals, M., Urgeles, R., De Batist, M., Calafat, A. M., and Casamor, J. L. (2004). Characterisation of the recent BIG'95 debris flow deposit after a variety of seismic reflection data, ebro margin, Western Mediterranean Sea. Marine Geology 213, 235-255.

Laursen, J., and Normark, W. R. (2002). Late Quaternary evolution of the San Antonio Submarine Canyon in the central Chile forearc (~33°S). Marine Geology 188, 365-390.

Lee, H. J., Chough, S. K., and Yoon, S. Y. (1996). Slope stability change from late Pleistocene to Holocene in the Ulleung Basin, East Sea (Japan Sea). Sedimentary Geology 104, 39-51.

Lewis, K. B., and Barnes, P. M. (1999). Kaikora Canyon, New Zealand: active conduit from near-shre sediment zones to trench-axis channel. Marine Geology 162, 39-69.

Lonardi, A. G., and Ewing, M. (1971). Sediment transport and distribution in the Argentine Basin. 4. Bathymetry of the continental margin, Argentine Basin and related provinces. Canyons and sources of

sediments. In: L. H. Ahrens et al. (Eds.), Physics and Chemistry of the Earth.. Pergamon Press, Oxford. pp. 123-251

Lonsdale, P. (1982). Sediment drifts of the Northeast Atlantic and their relationship to the observed abyssal currents. Bull. Inst. Geol. Bassin d'Aquitaine 31, 141-149.

Lykousis, V., Roussakis, G., Alexandri, M., and Pavlakis, P. (2002). Sliding and regional slope stability in active margins: North Aegean Trough (Mediterranean). Marine Geology 186, 281-298.

Martinez, P., Bertrand, P., Shimmield, G. B., Cochrane, K., Jorissen, J., Foster, J., and Dignan, M. (1999). Upwelling intensity and ocean productivity changes off Cape Blanc (northwest Africa) during the last 70,000 years: geochemical and micropalaeontological evidence. Marine Geology 158, 158, 57-74, 57-74.

McAdoo, B. G., Pratson, L. F., and Orange, D. L. (2000). Submarine Landslide geomorphology, US continental slope. Marine Geology 169, 103-136.

McHugh, C. M. G., Ryan, W. B. F., Eittreim, S., and Reed, D. (1998). The influence of San Gregorio fault on the morphology of Monterey Canyon. Marine Geology 146, 63-91.

McHugh, M. G. C., Damuth, J. E., and Mountain, S. G. (2002). Cenozoic mass-transport facies and their correlation with sea level change, New Jersey continental margin. Marine Geology 184, 295-334.

Olson, D. B., Podesta, G. P., Evans, R. H., and Brown, O. B. (1988). Temporal variations in the separation of Brazil and Malvinas Currents. Deep-Sea Research 35, 1971-1990.

Peterson, R. G., Johnson, C. S., Krauss, W., and Davis, R. E. (1996). Langrangian measurements in the Malvinas Current. In "The South Atlantic: present and past circulation." (G. Wefer, W. H. Berger, G. Siedler, and D. J. Webb, Eds.), pp. 239-247. Springer.

Peterson, R. G., and Stramma, L. (1991). Upper-level circulation in the South Atlantic Ocean. Prog. Oceanogr. 26, 1-73.

Piper, D. J. W., and Ingram, S. (2003). Major Quaternary sediment failures on the east Scotian Rise, eastern Canada. Geological Suvey of Canada, Current Research 2003-D1, 7.

Posamentier, H. W. (2003). Depositional elements associated with a basin floor channel-levee system: case study from Gulf of Mexico. Marine and Petroleum Geology 20, 677-690.

Reid, J. L. (1989). On the total geostrophic circulation of the South Atlantic Ocean: flow patterns, tracers and transports. Prog. Oceanogr. 23, 149-244.

Rona, P. (1971). Bathymetry off central northwest Africa. Deep-Sea Research 18, 321-327.

Sarnthein, M., Thiede, J., Pflaumann, U., Erlenkeuser, K., Fütterer, D., Koopmann, B., Lange, H., and Seibold, E. (1982). Atmospheric and Oceanic Circulation Patterns off Northwest Africa During the Past 25 Million Years. In: U. von Rad, K. Hinz, M. Sarnthein, and E. Seibold (Eds.), Geology of the Northwest African Cantinental Margin. Springer-Verlag, Berlin. pp. 545-604.

Seibold, E., and Hinz, K. (1974). Continental slope construction and destruction, West Africa. In: C. A. Burk, and C. L. Drake (Eds.),The geology of continental margins. Springer, New York. pp. 179-196.

Spieß, V. (1993). Digitale Sedimentechograpraphie - Neue Wege zu einer hochauflösenden Akustostratigraphie., Berichte Fachbereich Geowissenschaften. Universität Bremen, Bremen. pp. 1-199.

Spieß, V., and participants, c. (2002). Report and preliminary results of Meteor Cruise M 49/2, Montevideo (Uruguay) - Montevideo, 13.02. - 07.03.2001., Berichte, Fachbereich Geowissenschaften, Universtät Bremen. pp 84.

Stow, D. A. V., and Mayall, M. (2000). Deep-water sedimentary systems: New models for the 21st Century. Marine and Petroleum Geology 17, 125-135.

Thomson, J., and Weaver, P. P. E. (1994). An AMS radio-carbon method to determine the emplacement time of recent of recent deep-sea turbidites. Sedimentary Geology 89, 1-7.

Trifunac, M. D., Hayir, A., and Todorovska, M. I. (2003). A note on tsunami caused by submarine slides and slumps spreading in one dimension with nonuniform displacement amplitudes. Soil dynamics and Earthquake Engineering 23, 41-52.

Van Camp, L., Nykjaer, L., Mittelstaedt, E., and Schlittenhardt, P. (1991). Upwelling and boundary circulation off Northwest Africa as depicted by infrared and visible satellite observations. Prog. Oceanogr. 26, 357-402.

Varnes, D. J. (1958). Landslide types and processes. In "Landslide and Engineering Practice." (E. D. Eckel, Ed.), pp. 20-47. Highway Research Board Special Report.

von Lom-Keil, H., Spiess, V., and Hopfauf, V. (2002). Fine-grained sediment waves on the western flank of the Zapiola Drift, Argentine Basin: evidence for variations in Late Quaternary bottom flow activity. Marine Geology 192, 239-258.

Vörösmarty, C. J., Fekete, B. M., Meybeck, M., and Lammers, R. B. (2002). Global system of rivers: Its role in organizing continental land mass and defining land-to-ocean linkages. Global Biogeochemical Cycles 14, 599-621.

Vorren, T. O., Laberg, J. S., Blaume, F., Dowdeswell, J. A., Kenyon, N. H., Mienert, J., Rumohr, J., and Werner, F. (1998). The Norwegian-Greenland Sea continental margins: morphology and Late Quaternary sedimentary processes and environment. Quaternary Science Review 17, 273-302.

Weaver, P. P. E., Wynn, R. B., Kenyon, N. H., and Evans, J. (2000). Continental margin sedimentation, with special reference to north-east Atlantic margin. Sedimentology 47 (Suppl. 1), 239-256.

Wefer, G., and Fischer, G. (1993). Seasonal patterns of vertical particle flux in equatorial and coastal upwelling areas of the eastern Atlantic. Deep-Sea Research 40, 1613-1645.

Weimer, P. (1991). Seismic facies, characteristics and variations in channel evolution, Mississippi Fan (Plio-Pleistocene), Gulf of Mexico. In "Seismic facies and sedimentary processes of submarine fans and turbidite systems." (P. Weimer, and M. H. Link, Eds.), pp. 323-347. Springer, New York.

Wessel, P., and Smith, W. H. F. (1998). New, improved version of the Generic Mapping Tools Released. EOS, Transactions, AGU 79, 579.

Wilson, C. K., Long, D., and Bulat, J. (2004). The morphology, setting and processes of the Afen Slide. Marine Geology 213, 149-167.

Wissmann, G. (1982). Stratigraphy and Structural Features of the Continental Margin Basin of Senegal and Mauritania. In: U. von Rad, K. Hinz, M. Sarnthein, and E. Seibold (Eds.), Geology of the Northwest African Cantinental Margin. Springer-Verlag, Berlin. pp. 160-181.

Wynn, R. B., Masson, D. G., Stow, D. A. V., and Weaver, P. P. E. (2000). The Northwest African slope apron: a modern analogue for deep water systems with complex seafloor topography. Marine and Petroleum Geology 17, 253-265.

Zühlsdorff, L. (1999). High resolution multi-frequency surveys at the eastern Juan de Fuca Ridge flank and Cascadia Margin - Evidence from thermally and tectonically driven upflow in marine sediments. Berichte Fachbereich Geowissenschaften. Universität Bremen. pp. 118.

# 2 Morphology, seismic characteristics and development of Cap Timiris Canyon, offshore Mauritania: a newly discovered canyon preserved off a major arid climatic region.

Andrew A. Antobreh and Sebastian Krastel

*Marine and Petroleum Geology (in Press, accepted 10 June 2005)*

## 2.1 Abstract

We employ a combined interpretation of Hydrosweep swath bathymetry and high resolution multi-channel seismic reflection data to investigate the development of Cap Timiris Canyon, a newly discovered submarine canyon offshore Mauritania. The dominantly V-shaped and deeply entrenched canyon exhibits many fluvial features including dendritic and meander patterns, cut-off loops and terraces, and is presently incising. Distal meander patterns, confined within a narrow fault-controlled corridor, show several stages of evolution, the latest of which is dominated by a down-system meander-loop migration. Terraces exhibit a variety of internal structures suggesting they originated through different processes including sliding/slumping, uplift-induced incision and lateral accretion. We ascribe canyon origin to an ancient river system in the adjacent presently arid Sahara Desert that breached the shelf during a Plio/Pleistocene sea level lowstand and delivered sediment directly into the slope area. Our data suggest that the initial invading unchannelised sheet of sand-rich turbidity flows initiated canyon formation by gradually mobilizing along linear seafloor depressions and fault-controlled zones of weakness. We propose that the development of canyon morphology and structure was influenced by the stages of active flow of the coupling river system, and hence could act as a proxy for understanding the paleo-climatic evolution of a 'green' Sahara since Plio/Pleistocene times.

Keywords: submarine canyon, meander, terraces

## 2.2 Introduction

The Eastern Atlantic continental margin of Northwest Africa is known to be deeply incised by a number of submarine canyon systems (Jacobi and Hayes, 1982; Wissmann, 1982; Weaver et al., 2000). In addition, the margin, particularly between 15°N and 26°N, is characterised by extensive mass wasting processes, though it receives no significant fluvial input (Weaver et al., 2000; Wynn et al., 2000), as the adjacent land is dominated by the Sahara Desert, a presently major arid climatic zone. A number of upwelling cells, prevalent along the margin, is believed to give rise to high rates of sediment accumulation along the upper slope and shelf edge areas resulting in the large-scale, but infrequent mass sediment movements (Sarnthein et al., 1982; Weaver et al., 2000).

The importance of submarine canyons as preferred pathways for downslope mass sediment transport, notably slides, slumps, debris flows and turbidity currents, from shallow-marine to deep-marine environments, has been recognised in both convergent and divergent continental margin settings (e.g. Lewis and Barnes, 1999; Laursen and Normark, 2002; Babonneau et al., 2002; McHugh et al., 2002), and has been the subject of intense studies in recent years. Apart from constituting an important archive for documenting the sedimentation process history of an area, submarine canyons are also studied as modern analogues for deepwater hydrocarbon reservoirs because of their association with sand-rich turbidites (Clark and Pickering, 1996; Stow and Mayall, 2000; Posamentier, 2003).

The origin of many passive margin submarine canyons, e.g. Amazon Canyon, Monterrey Canyon and Zaire Canyon, has been linked to major terrestrial river systems which were able to erode their way across an emergent shelf during major periods of glacial sea level lowstand in order to deliver their load directly into the slope areas and beyond (Damuth and Kumar 1975; Flood et. al., 1991; McHugh et al., 1998). Such submarine canyons are believed to have been most active during past periods of sea level lowstands, since they were then coupled to the river systems, and hence received direct supplies of terrigenous sediment discharges (Damuth, 1994; Hagen et al., 1994; Babonneau et al., 2002). Detailed studies of such canyons could therefore provide useful information about the stages of active flow of the connecting river system, and hence the paleo-climatic evolution of the adjacent land over a period of time (Bouma, 2001; Krastel et al. 2004). Knowledge of the physical processes governing sediment transport and depositional processes within submarine canyon systems, as well as in their vicinities, has advanced considerably through detailed studies of the morphological characteristics and structural features of canyons. This has largely been achieved through the use of improved bathymetric mapping methods together with modern

high resolution seismic data acquisition and processing techniques (Cirac et al., 2001; Laursen and Normark, 2002; Posamentier and Kolla, 2003).

The development of the canyon systems offshore northwest Africa and the role they have played in the sediment dynamics of the region appear to have received very little attention. Furthermore, to the best of our knowledge, no study has attempted to investigate any links between the development of canyons in the region and the climatic evolution of the adjacent land, which is dominated by the expansive arid Sahara Desert. Except a few of the major canyon systems that have been studied and recognised as important turbidity current pathways (e.g. Jacobi and Hayes, 1982; Weaver et al., 2000; Wynn et al., 2000), only little information is available on most of the canyons in the region. Wissmann (1982) has presented some seismic profiles, with age calibrations, from the upper reaches of the Tioulit Canyon, offshore central Mauritania (Fig. 2.1). However, indentations in bathymetric contours offshore the Mauritanian margin provide indications of the possible existence of several major canyon systems along the margin that remain undocumented (Rona, 1971; Wissmann, 1982). During an expedition to northwest Africa in April 2003 by RV Meteor Cruise M58/1, under the auspices of the Research Center Ocean Margins (RCOM) of the University of Bremen, a large submarine canyon system located off northern Mauritania, and close to the latitude of Cap Timiris, was discovered by a Hydrosweep swath bathymetric system (Krastel et al., 2004). The canyon, named Cap Timiris Canyon by the cruise, was subsequently surveyed with detailed high resolution seismic profiling.

In this study, we employ a combined analysis of swath bathymetric multibeam echosounder data and a high resolution multi-channel seismic reflection (MCS) survey in order to document for the first time the detailed morphology and structural characteristics of Cap Timiris Canyon. This study aims to provide insights into the development of the Cap Timiris Canyon system as it evolved through time, and the role it has played in the sedimentation process history of the high production region of the continental margin offshore Mauritania. Furthermore, the study will investigate any possible link of the canyon to a terrestrial river system, and how the development of the canyon has been influenced by the flow characteristics of the river. By so doing, we hope to provide a new framework for studying the climatic evolution of the adjacent desert region in the last few millions of years.

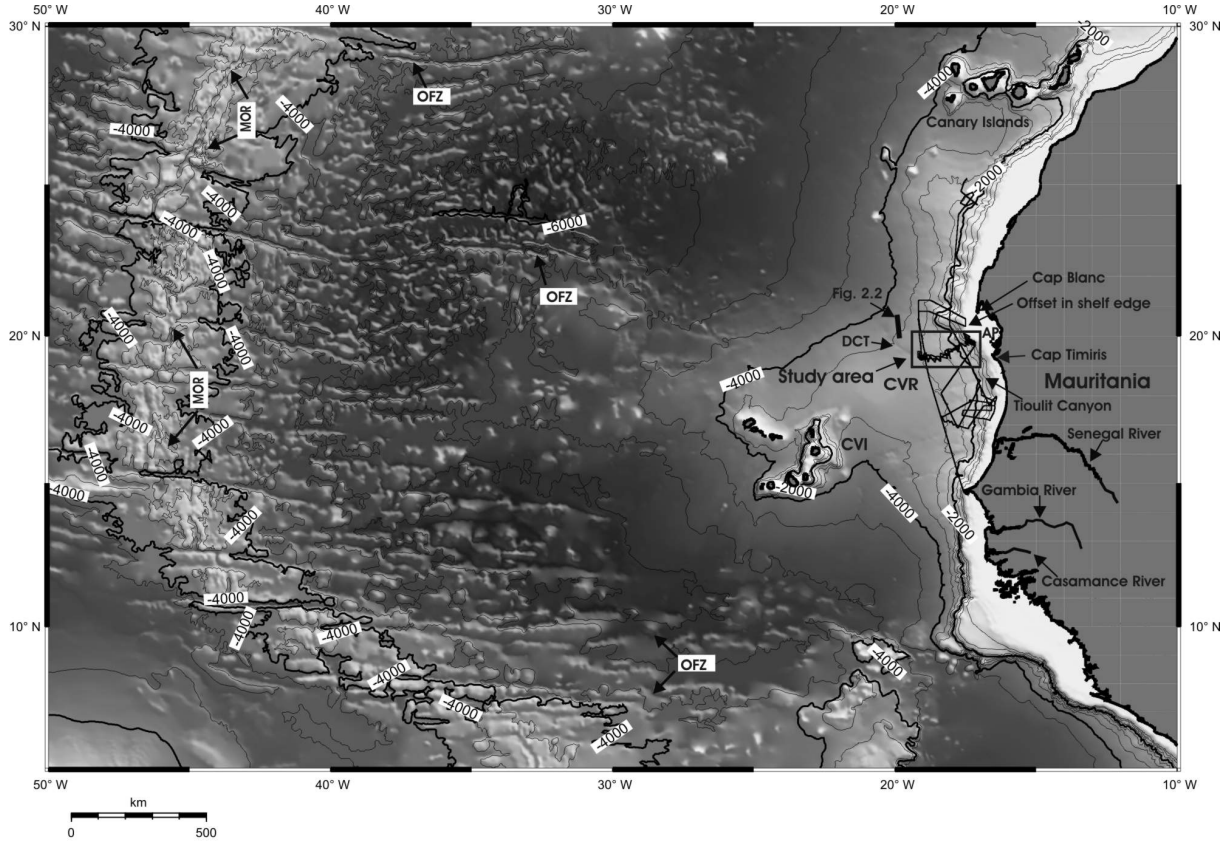


***Figure 2.1:*** *General bathymetry of NW African continental margin (Gebco, 2003) showing the location of Cap Timiris Canyon (study area, in box) in relation to regional structure and bathymetry (contours at 500 m intervals). RV Meteor Cruise M58/1 track lines are shown in solid black lines. The entire margin is deeply incised by submarine canyons, manifested as indentations in, e.g. the 2000 m contours. Cap Timiris Canyon is located close to a prominent seaward offset of the shelf edge. The location of this prominent offset of the shelf break presumably coincides with the continental prolongation of a major oceanic fracture zone. OFZ = oceanic fracture zones, MOR = Mid Oceanic Ridge, CVI = Cape Verde Islands, CVR = Cape Verde Rise, AP = Arguin Platform, DCT = distal Cap Timiris Canyon.*

## 2.3 Geological setting

### *2.3.1 Margin physiography*

Cap Timiris Canyon is located off northern Mauritania, close to the latitude of Cap Timiris, i.e. 19°22’ N (Fig. 2.1). The continental margin off Mauritania, from the south up to off Cap Timiris, in the north, is characterised by a relatively narrow shelf that is 30 - 40 km wide and a moderately steep slope of 2.5 – 3°. The shelf break occurs at a water depth of 50 - 80 m. Just off north of Cap Timiris, a sudden seaward offset in the shelf break leads to a considerable widening of the shelf (up to about 80 - 100 km) expressed by the shallow Arguin Platform, and accompanied by a steepening of the slope up to about 6°. The locations of prominent offsets of the shelf break along the West African continental margin are thought to coincide with the continental prolongations of major oceanic fracture zones (Fig. 2.2; Jacobi and Hayes, 1982; Wissmann, 1982). The shelf and upper slope areas are incised by a number of submarine canyons and gullies which appear to coalesce downslope into major canyon systems.

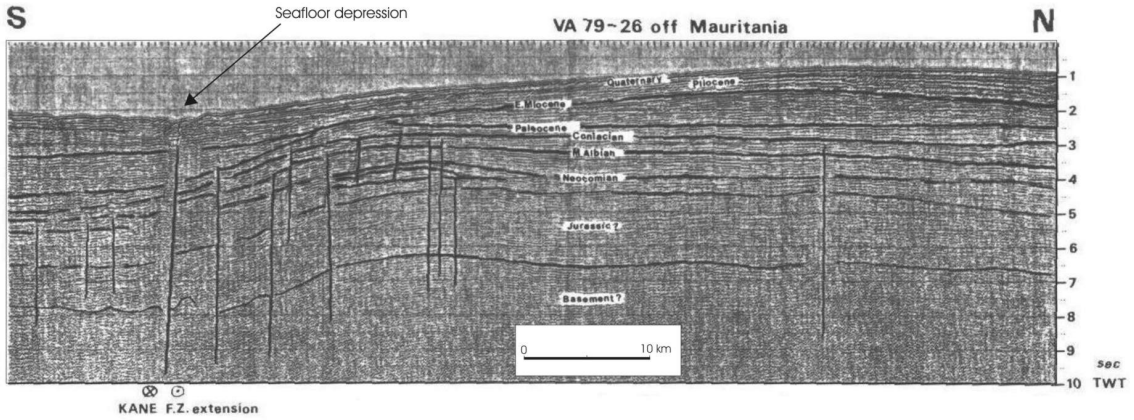


***Figure 2.2:*** *Seismic reflection profile VALDIVIA 79-26 recorded across the continental extension of the Kane Fracture Zone (modified after Wissmann, 1982). The profile strikes N-S, slightly to the east of longitude 18°W, and lies off the margin between Cap Timiris and Cap Blanc (see Fig. 2.1 for location). The profile is cut by several small-offset deep-seated vertical faults which reach across Tertiary sediments. Notice that The Kane Fracture Zone extension lies directly below what appears to be a depressed zone on the seafloor.*

The entire continental rise off Mauritania is very broad, and occurs at water depths of 2500 – 3000 m. Off Cap Timiris, and northwards, the slope and rise areas are characterised by several seamounts and basement highs (Jacobi and Hayes, 1982). The complex seafloor topography arising from the emplacement of the seamounts and fracture zone ridges, is believed to have considerably influenced sedimentation processes on the margin (Jacobi and Hayes, 1982; Wynn et al., 2000). In the south, the rise is dominated by the extensive Cape Verde Rise, a prominent bathymetric swell about 1000 km in diameter and dissected by several WNW-ESE trending fracture zones (e.g. Williams et al., 1986), which gradually elevates into the Cape Verde Islands at its crest (Fig. 2.1). Oceanic fracture zones in the region are known to be dominated by right-lateral transform faults (Garfunkel, 1986).

### *2.3.2 Structural setting and stratigraphy*

Structurally, Cap Timiris Canyon is located within, but close to, the northern boundary of the Mesozoic-Cenozoic Senegal Mauritania Basin which is known to have both onshore and offshore extensions (Wissmann, 1982). The Senegal Mauritania Basin is one of the series of marginal basins emplaced along the Northwest African margin in response to the Mesozoic opening of the Atlantic ocean (Jansa and Wiedmann, 1982; Wissmann, 1982), and it has been divided into several N-S oriented sub-basins by a series of long-lived crustal scale East-West bound faults some of which may be associated with oceanic fracture zones or transform faults (Brown, 2002). The basin is filled by a thick succession of Mesozoic-Cenozoic terrigenous to shallow marine sediments which attain maximum depths of more than 10 km below the lower continental slope off Mauritania (Wissmann, 1982).

Wissmann (1982) has presented the structural development and stratigraphy of the Senegal Mauritania Basin. The oldest units comprise Early Triassic terrigenous clastic rift sediments deposited within local depocenters, and overlain by a thick sequence of late stage syn-rift evaporites deposited in a restricted marine environment. Post-rift sedimentation was dominated by the deposition of a continuous succession of an up to 4 km thick regionally extensive carbonate platform during Jurassic to Cenomanian times. During this period, terrestrial input to the shelf was largely curtailed until Aptian time when a tectonic uplift of the margin led to the development of a series of deltaic wedges that prograded across the shelf and buried the Mesozoic carbonate platform.

By Early Tertiary time, a transgressing epicontinental sea had flooded nearly the entire basin resulting in the deposition of another carbonate platform on the shelf. This was followed again by a regressive interval characterised by another sediment progradation in the Neogene. A tectonic event, especially in Miocene and Early Quaternary times, led to another crustal uplift which culminated in the formation of several small depocenters within the basin. This was accompanied by intense volcanism and the construction of volcanic islands, including the Cape Verde group of islands, and seamounts in the slope and rise areas. Earliest indications of mass wasting processes along the slope are recognised by the presence of slumps and turbidites observed in Early Miocene deposits. After a prevalent tropical climate on the margin during the Middle Eocene, a more arid condition began to emerge during the end of Eocene and within Oligocene time. With the end of the Tertiary humid climate, a long period of arid Quaternary sedimentation emerged known as the ‘Continental terminal’ formation (Jansa and Wiedmann, 1982; Wissmann, 1982).

### *2.3.3 Onshore Quaternary coastal geology and Paleoclimate*

Onshore, near the Mauritanian coast, the ‘Continental terminal’ formation of the Senegal Mauritania Basin is overlain by a succession of marine Quaternary sediments of the Mauritania Quaternary Basin which, in turn, is now buried by widespread aeolian accumulations (Wissman, 1982; Giresse et al., 2000). The Mauritania Quaternary Basin was initiated as a large marine gulf in Early Pleistocene. Until Holocene time, however, the basin underwent a progressive reduction in size as a result of sedimentation dominated by several periods of alternating marine transgression and regression events (Giresse et al., 2000). These intervals were synchronous with severe climatic variations during which two opposite extreme humid and dry climatic conditions rapidly alternated in response to shifts of the Sahara arid zone (Diester-Haass and Chamley, 1982).

During the humid intervals, which occurred under the regime of sea level highstands, the sea invaded the flat coastal lowlands, and extended several tens of kilometres inland as large marine gulfs, creating irregular coastlines and the formation of lakes and sebkhas in interdunal depressions. The humid stages, particularly during the Late Quaternary, recorded the most intense upwelling activity (Diester-Haass and Chamley, 1982). The intervening dry intervals, which generally prevailed during stages of sea level lowstands, were accompanied by periods of sea regression during which aeolian sand was introduced into the shelf environment as sand dunes, mainly by wind sediment transport and coastal redistribution (Diester-Haass and Chamley, 1982; Barusseau et al., 1995). The longest of the dry intervals is thought to have occurred in the Early Pleistocene (Diester-Haass and Chamley, 1982). Since the recent Quaternary, the shoreline of the interdunal depressions has been obstructed by extensive littoral sand barriers that have developed as a result of reworking by the sea during the post-glacial transgressive intervals (Barusseau et al., 1995).

### *2.4 Data and Methods*

The Hydrosweep and MCS data used for this study were simultaneously acquired during R/V Meteor Cruise M58/1 in April 2003. The data were collected as part of a larger marine geophysical survey undertaken by the Research Center Ocean Margins (RCOM) of the University of Bremen to study upwelling and sedimentation processes offshore northwest Africa.

The Hydrosweep swath bathymetric system is a hull-mounted multibeam echosounder which generates 59 pre-formed acoustic beams at a frequency of 15.5 kHz. The beams are transmitted over 90°, thus allowing the system to map a seabed swath of width equal to two times the water depth. Depth information provided by Hydrosweep is based on a patented calibration process designed to minimize depth errors to less than 0.5% of water depth. The public domain softwares Multibeam System (Caress and Chayes, 1996) and Generic Mapping Tools (Wessel and Smith, 1998) were employed for processing and presentation of the bathymetric data.

The seismic source used for acquiring the MCS data was a 1.7 l GI-Gun shot at a distance of ~25 m. The gun operation employed a high air pressure of 150 bar (2150 PSI). The data were received by a 450-m-long Syntron streamer equipped with separately programmable hydrophone subgroups. For recording the seismic data, we used 36 groups of 6.25 m length at a group distance of 12.5 m. The data were digitally recorded at a sampling frequency of 4 kHz over 3 s time intervals. Positioning was based on GPS (Global Positioning

System). Processing of the MCS data was carried out using a combination of 'in-house' and the 'Vista' (Seismic Image Software Ltd) softwares. Standard seismic processing procedures employed included trace editing, setting up geometry, static and delay corrections, velocity analysis, normal moveout corrections, bandpass frequency filtering (frequency content: 55/110 - 600/800 Hz), stack and time migration. A CMP spacing of 10 m was applied throughout.

### *2.5 Morphological characteristics*

A total length of ~290 km of Cap Timiris Canyon along its meandering channel axis, from the shelf edge, at water depths of ~50 m down to the continental rise at a water depth of about 3050 m, was mapped with the Hydrosweep swath bathymetry system. However, it can easily be inferred from the Hydrosweep bathymetric chart (Fig. 2.3) that the canyon continues beyond this most distal surveyed point. The GEBCO data (GEBCO, 2003) also shows that Cap Timiris Canyon extends for hundreds of kilometres into the deep sea (Fig. 2.1). The bathymetry (Fig. 2.3) clearly reveals a meandering submarine canyon system, with an overall sinuosity of 1.4 (locally attaining a maximum of 4.2, but including linear segments), that displays many features similar to a sub-aerial fluvial system including tributaries, meander patterns, a cut-off loop and terraces. Most of the factors that influence the morphological development of sub-aerial fluvial systems, e.g. channel gradient, flow discharge and bedload to suspension load ratio of the flows (Schumm et al., 1987), are known to rightly apply to submarine canyons (Hagen et al., 1994; Klaucke and Hesse, 1996; Pirmez and Imran, 2003).

#### *2.5.1 General Morphology*

The course of Cap Timiris canyon displays two distinct trends. From its head region in the shelf edge and upper slope areas, the canyon shows an initial NE-SW course. However, just on entering the continental rise at about 2850 m water depth, it is sharply diverted to a predominantly E-W direction for the rest of its flow into the deep sea (Fig. 2.3). This abrupt shift in course of the canyon allows us to describe the canyon's morphological features under two main domains: (i) the upper Cap Timiris Canyon, which starts from the shelf edge at about 50 m water depth and ends in the lower slope area at about 2850 m water depth, and (ii) the lower Cap Timiris canyon, which extends from the continental rise seawards to the end of the mapped segment.

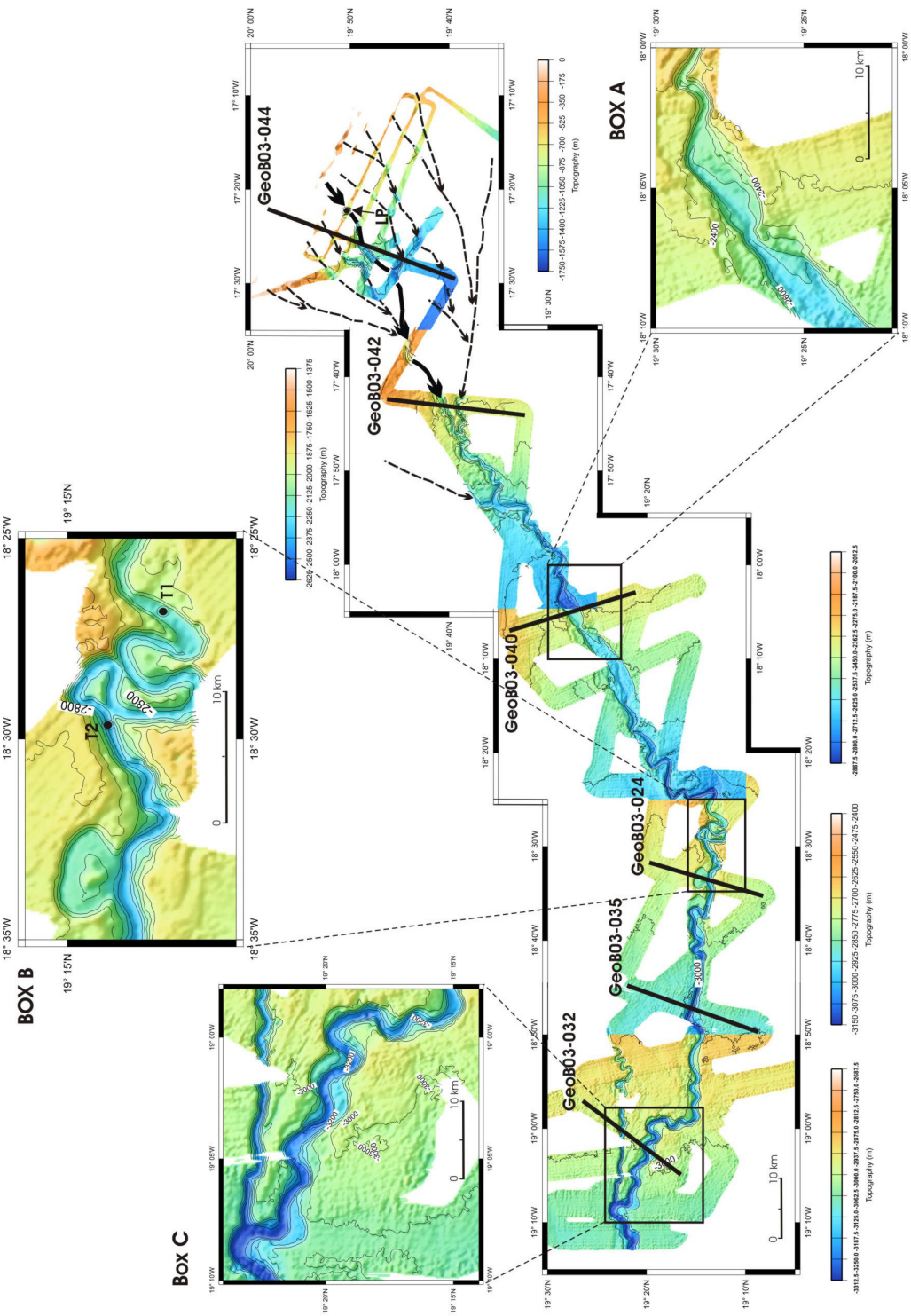


***Figure 2.3:*** *Bathymetric map of Cap Timiris Canyon plotted from the Hydrosweep data of RV Meteor Cruise M58/1 (modified after Krastel et al., 2004). Note the different colour scales for different sections of the map. In the head region, the interpreted main canyon is indicated in arrowed thick solid line, whilst tributary canyons and gullies are indicated in arrowed broken lines. Locations of selected high resolution MCS profiles presented in this study are shown in solid black lines. LP = starting point for plotting longitudinal and relief profiles along the canyon (in Fig. 2.5). T1, T2 (Box B) = reference points used for calculating sinuosity along tortuous meander segment.*

### *2.5.1.1 Upper Cap Timiris Canyon*

The bathymetry (Fig. 2.3) shows that the head region of the Cap Timiris Canyon is defined by several tributary canyons and gullies which deeply incise the shelf edge and upper slope areas in a dendritic pattern. These tributaries feed sediments into two larger canyons which coalesce at an acute angle on the upper slope, at about 2100 m water depth, to constitute the main canyon. About 20 km downslope from this confluence, another tributary canyon, apparently originating from the north-northeast, joins the main canyon at about 2400 m water depth as it heads further downslope towards the continental rise. From the first confluence in the upper slope downstream to about 2500 m water depth, the canyon displays irregular meanders characterised by varying radii of curvature with an average sinuosity of ~1.5.

A series of canyon axial profiles (Fig. 2.4, profiles A to F) generated from the Hydrosweep bathymetry data, clearly reveals the V- as well as U-shaped cross-sectional morphology of this segment of the Upper Canyon which deeply incises the upper slope with relief attaining 460 m and widths from 1.2 to 5.1 km. The canyon walls are generally very steep, and display terraces in varying levels. Downstream to about 2500 m water depth, the meander pattern abruptly gives way to a segment of extensive canyon widening characterised by a series of two small elongated basins, about 10 and 25 km long, and both up to 7.5 km wide, and connected by a narrow constriction of the original canyon width. The distinctive morphological features exhibited by this part of the canyon are more clearly shown by a close-up bathymetry of the basins in Fig. 2.3 (Box A). Profiles across the basins (Fig. 2.4, profiles G, H and I) show an almost U-shaped cross-sectional canyon morphology with broadened floor which, in places, displays multiple thalwegs and terraces. Canyon relief decreases in this segment to an average of 175 m. Further downstream to about 2750 m water depth, the canyon exits from the downslope end of the lower basin by abruptly reverting to its original relatively narrow average width, and once again assumes its irregular meander pattern and V-shaped cross sectional morphology (Fig. 2.4, profiles J, K, and L) as it enters the lower canyon segment.

### *2.5.1.2 Lower Cap Timiris Canyon*

The lower reaches of Cap Timiris Canyon, starting immediately from where it undergoes an abrupt E-W diversion in course down to the most distal surveyed point, is characterised by a highly variable meander pattern. Right after being sharply deflected in the continental rise, i.e. at about 2850 m water depth, the canyon segment assumes a very

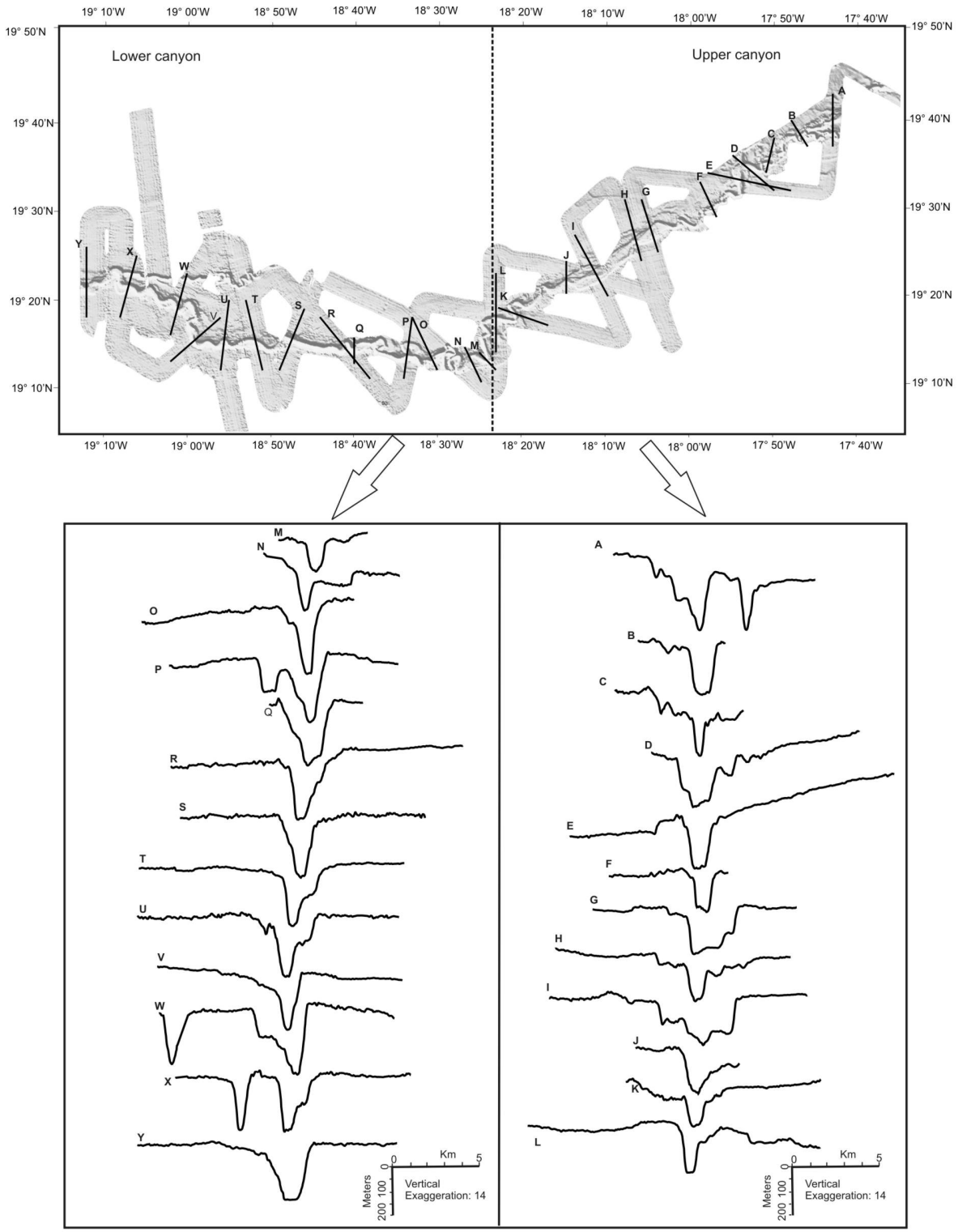


***Figure 2.4:*** *Representative cross-sectional bathymetric profiles across Cap Timiris Canyon generated from Hydrosweep bathymetry data. The profiles are oriented perpendicular to the canyon axis, and their locations are shown in the above box. Profiles from the shelf edge could not be displayed because of inadequate coverage in the steep area by the Hydrosweep system.*

irregular meander pattern, including a distinctive tortuous meander pattern and a cut-off meander loop, over a distance of about 60 km. The tortuous meander is characterised by large and tight irregular loops giving a high sinuosity of 4.2 over a channel length of about 40 km between two points T1 and T2 (Fig. 2.3, Box B), the highest for the entire canyon. Along the irregular meander segment, the canyon remains relatively narrow with widths averaging ~2.2 km, and maintains its general V-shaped cross section (Fig. 2.4, profiles M, N, O and P). Canyon relief is, in places however, drastically reduced to below 100 m, e.g. within the highly sinuous portion. Here, terrace development is generally poor to absent.

Downslope of the cut-off loop, i.e. which is cut by seismic line GeoB03-024 (Fig. 2.3), the canyon flows linearly for about 5 km and then, once again, assumes an irregular meander pattern which progressively reduces in radii of curvature until it enters into another linear stretch for about 12 km. Thereafter, the canyon begins to meander in a quite regular pattern with long wavelengths and very low amplitudes confined within a 3 to 5 km wide band. As it continues further downstream, the canyon finally makes two short sharp bends, first to the north for about 15 km, and then to the WNW-ESE direction for another 25 km, before re-orienting to its dominant E-W direction in the most distal part, just where it is joined by a smaller tributary canyon. The bathymetry shows that this tributary canyon, which apparently originates from the NE-SW direction is, initially, strongly meandering upstream. However, quite like the main canyon, its downstream segment abruptly shifts course to a linear direction sub-parallel to the distinctive E-W segment of the main canyon, including its linear reaches, before reaching the confluence. Axial bathymetric profiles crossing the distal reaches of the main canyon (Fig. 2.4, profiles S to Y) and the smaller tributary canyons (Fig. 2.4, profiles W and X) show that both canyons are characterised by V-shaped as well as trough-like cross sectional morphologies. The main canyon displays widths varying between 1.5 to 5 km, and is characterised by a progressively increasing entrenchment with relief attaining ~300 m in the most distal parts. The tributary canyon is relatively narrower and has widths ranging from 1.2 to 2.5 km, with relief up to 250 m. The walls of the main canyon are here characterised by terraces which, as more clearly shown by a close-up bathymetry of the distal canyon (Fig. 2.3, Box C) and the axial bathymetric profiles (Fig. 2.4, profiles S to X), generally alternate on both sides of the deeply entrenched thalweg.

### *2.5.2 Longitudinal depth profiles and variations in canyon relief*

Several bathymetric profiles generated from the Hydrosweep bathymetry data at axial channel lengths of between 2 to 5 km were used to plot longitudinal depth profiles along Cap

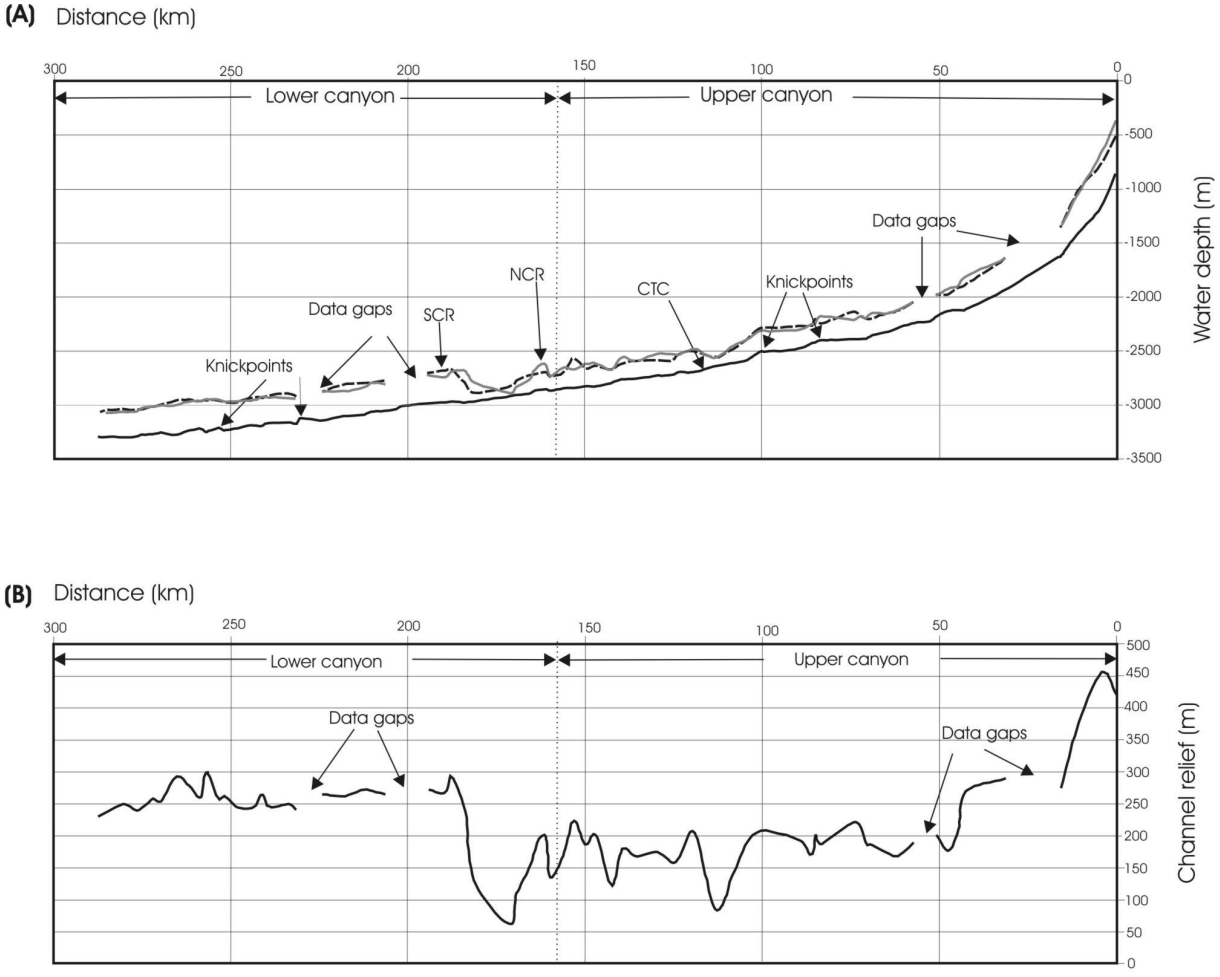


***Figure 2.5:*** *(a) Longitidunal depth profiles along Cap Timiris Canyon. The depth profile along the axis of the thalweg is denoted by CTC (solid black line). Profile NCR (solid grey line) represents the depth profile plotted along the northern canyon rim/levee crests, whilst the profile plotted along the southern canyon rim/levee crests is denoted by SCR (long broken lines). (b) Relief profile of Cap Timiris Canyon plotted along the thalweg of the canyon. The starting point for plotting the profiles in both (a) and (b) was taken at ~6 km upslope from the location of Profile GeoB03-044 along the main canyon (see Fig. 2.3) and is ~10 km seaward from the shelf edge.*

Timiris Canyon thalweg and also the canyon rim/levee crests (Fig. 2.5a). The depth profile, i.e. the longitudinal profile of the thalweg, displays a generally smooth and concave-up curve with very steep gradient, up to 2.8° over a short segment of the upper section of the canyon to the shelf edge, which progressively becomes gentler downstream, over a much longer segment, to <1° in the distal reaches. On a smaller scale, however, the profile is observed to be punctuated by several knickpoints, which appear to be concentrated in two main areas.

The first group is located in the upper canyon domain between 48 and 125 km (Fig. 2.5a), and is made up of two prominent knickpoints with gently sloping flanks, measuring up to 20 km in width. The second group, made up of knickpoints which are densely concentrated between 225 and 270 km in the distal part of the canyon, shows relatively smaller shapes, up to 5 km broad, and more steepness on their flanks. The longitudinal profiles of the northern

and southern canyon rims/levee crests when overlaid on each other (Fig. 2.5a), do not provide any indication to suggest continuously enhanced levee development in any particular direction of canyon bank.

The canyon relief profile (Fig. 2.5b) shows that from a maximum of 460 m near the shelf edge, the relief decreases to about 175 m over 48 km, and oscillates around this as an average value downstream for about 160 km. Just after this point, there is a sudden drop in relief again attaining a minimum of 70 m at 175 km, before the relief starts to increase sharply downstream, attaining a maximum of 300 m around 260 km.

## 2.6 Seismic structure

Our interpretation of the dense grid of seismic data covering the entire surveyed length of the canyon, i.e. from the shelf edge to the most distal part in the continental rise, has afforded us a detailed characterization of the structure of Cap Timiris Canyon. Here, we present a series of six representative seismic strike profiles selected from across the head region down to the distal parts of the canyon, in order to highlight the varying structural features along the canyon system. The locations of the presented profiles are shown in Fig. 2.3.

### *2.6.1 The Upper Cap Timiris Canyon*

Profile GeoB03-044 (Fig. 2.6) was recorded across the upper slope, shelf edge and the outer shelf areas of the continental margin, and cuts obliquely across the canyon system in the head region. The northern canyon clearly reaches into the shelf edge where it is seen to truncate undisturbed outer shelf sediments imaged as parallel, flat-lying low to medium amplitude reflectors. The upper slope area shows a thick wedge of sediments seismically characterised by parallel to sub-parallel, commonly disjointed, very low amplitude reflection packages. The reflectors (marked blue in Fig. 2.6) are truncated in several places by what appear to be sediment glide planes and a system of growth faults.

Downslope, the sediments increase in both thickness and scale of deformation, and are deeply carved by the main canyon and its southern tributary. Here, the sediments exhibit medium to high amplitude reflectors, and are faulted in several places especially in the proximities of the main canyon and its southern tributary. The thalweg of the canyons shows deposits of low amplitude, chaotic reflections, which may be interpreted as slumps derived from the steep, unstable canyon walls. An acoustically transparent and uplifted structure, visible south of Shot Point 1000 and below 2150 ms TWT (top marked as red reflector in the

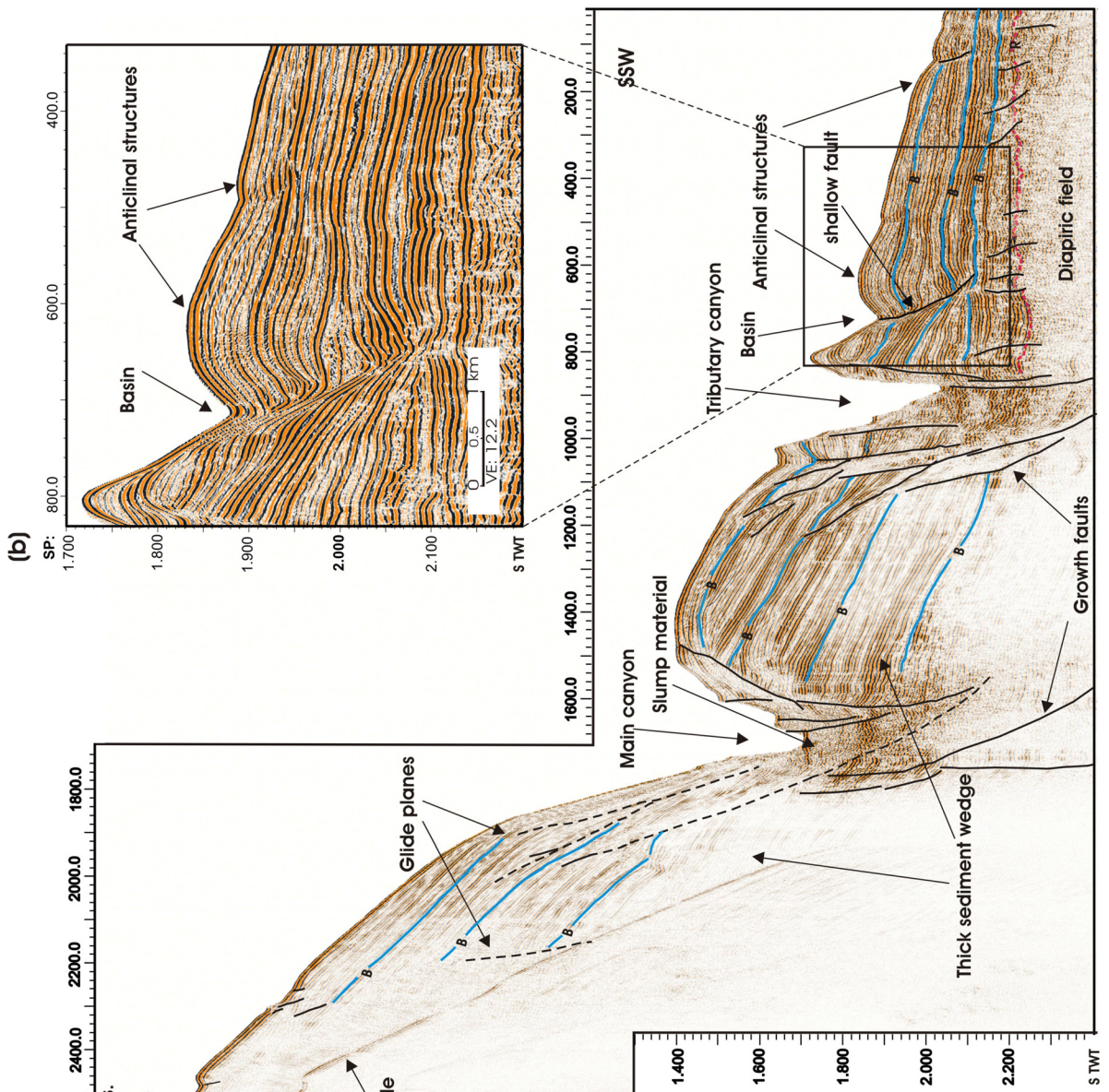


***Figure 2.6:*** *(a) Multi-channel seismic reflection profile GeoB03-044 recorded oblique to Cap Timiris Canyon in the head region. The profile crosses the upper slope, shelf edge and outer shelf areas. Location of the profile is shown in Fig. 2.3. Blue (B) reflectors = main reflectors within thick slope sediments; red (R) reflector = inferred top of sediment undergoing subsurface re-mobilization. Same colour reflectors across the canyons does not necessarily imply same stratigraphic horizons. (b) A close-up showing anticlinal structures and their associated small basins on the seafloor. The initial sediment flows probably mobilised preferentially along such small linear basins to facilitate canyon incision during the formative stages.*

seismic section), is interpreted as an emerging, probably mud, diapiric field. This feature underlies sediments which display small basins and anticlinal structures on the seafloor, particularly, south of Shot Point 800.

In Profile GeoB03-042 (Fig. 2.7), shot further downslope, the main canyon and its southern tributary are observed to cut deeply into the very thick (~400 m) and more intensely deformed and folded sediments of an intra-slope basin. The southern flank of this basin appears to be controlled by an uplifted diapiric field (top marked as red reflector in Fig. 2.7) that underlies the disturbed sediments (main reflectors marked blue in the seismic section). The seafloor, especially in the south, is characterized by topographic irregularities and small elongated depressions created by the growth and upward movement of the diapiric structures. Several faults are interpreted in the vicinity of the canyon walls and at the apices of the diapiric structures. Both canyons are, again, noted to be V-shaped, narrow and terraced. We identify at least two well-developed terraces on the northern wall of the main canyon, which are bounded by faults that cut the very steep canyon wall. The lower terrace is ~0.2 km broad and stands ~60 m above the incised thalweg which the terrace bounds in the north. The upper terrace is much broader, ~ 0.7 km wide, and also stands ~60 m above the lower terrace in the north. The internal structure of the terraces, in their uppermost parts, shows mainly well-layered, low to medium amplitude reflectors which dip gently towards the bounding faults. Their lower parts, however, display intensely deformed high amplitude reflections.

The most striking features of the canyon segment in the middle slope area are the two zones of anomalously widened canyon. The peculiar structural characteristics of this segment is illustrated by Profile GeoB03-040 (Fig. 2.8) which shows a widened main canyon carved into sediments of a relatively shallow intra-slope basin, ~150 m deep, formed in-between two updomed diapiric fields (top marked as red reflector in Fig. 2.8). The basin fill facies overlying the diapirs (i.e. interval between red and uppermost blue reflectors in the seismic section) are seismically characterized by continuous to discontinuous strong amplitude reflection events interspersed with small transparent units. They show erosional truncations in several places, particularly north of the canyon below 3150 ms TWT, and appear to constitute a complex stack of small cut and fill features. South of the canyon, a buried channel with its sediment infill imaged as narrow parallel strong reflectors, is observed near Shot Point 840 and below 3200 ms TWT. The seismic facies that overlie the basin fill sediments are characterized by narrow chaotic, low amplitude to transparent reflection packages separated by very thin, parallel to sub-parallel medium amplitude continuous reflection events. Widespread faults in the northern flank of the canyon, apparently derived from an underlying

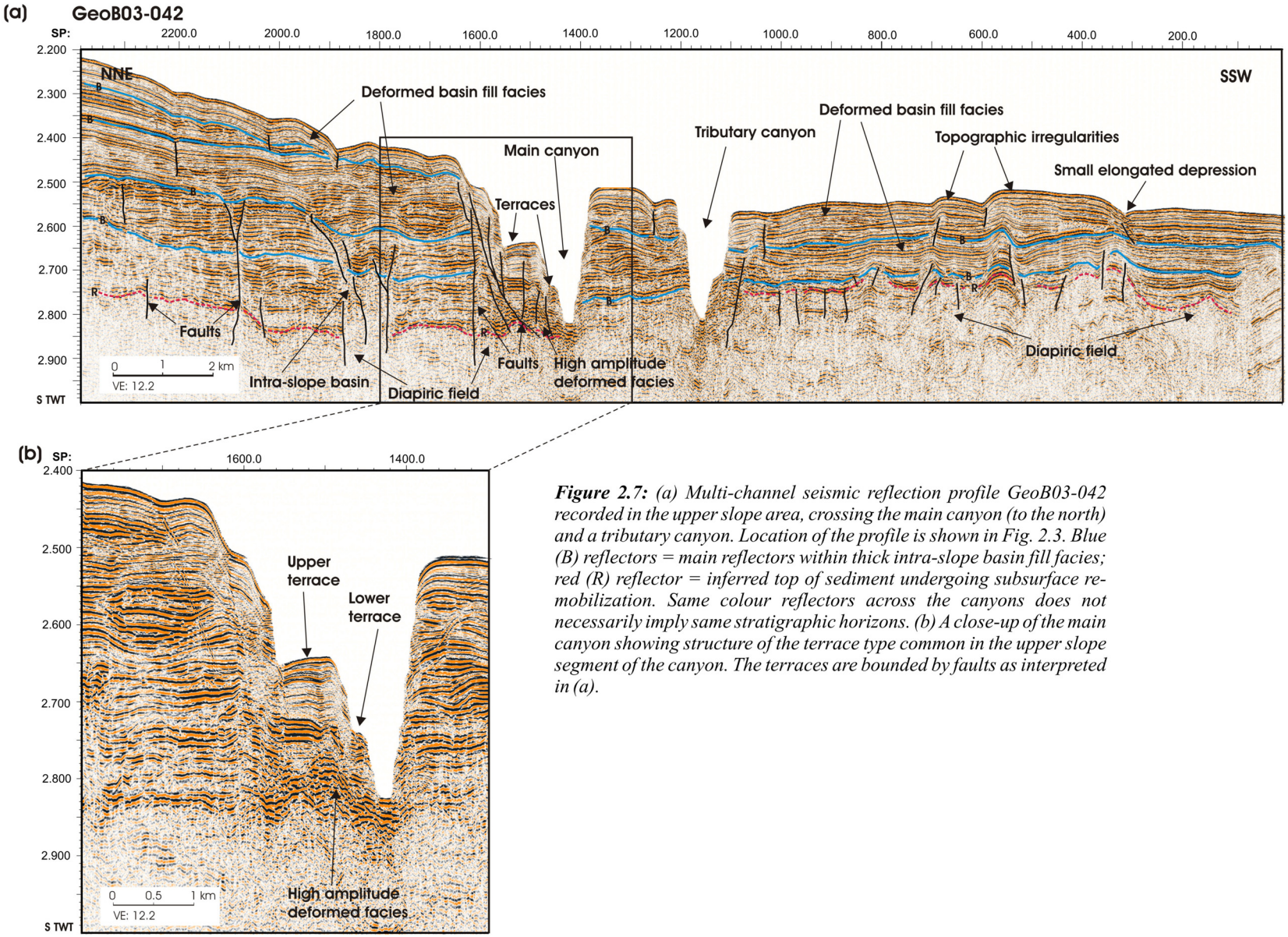


***Figure 2.7:*** *(a) Multi-channel seismic reflection profile GeoB03-042 recorded in the upper slope area, crossing the main canyon (to the north) and a tributary canyon. Location of the profile is shown in Fig. 2.3. Blue (B) reflectors = main reflectors within thick intra-slope basin fill facies; red (R) reflector = inferred top of sediment undergoing subsurface re-mobilization. Same colour reflectors across the canyons does not necessarily imply same stratigraphic horizons. (b) A close-up of the main canyon showing structure of the terrace type common in the upper slope segment of the canyon. The terraces are bounded by faults as interpreted in (a).*

diapiric structure, are observed to bound small acoustically transparent blocks which show slight downward movement on the northern wall. Here, the canyon is U-shaped and shows two well developed terraces on the southern wall, i.e. a broad lower terrace, ~1.2 km wide, confining a northward narrow incised thalweg, and a smaller upper terrace, ~0.5 km wide, in the southern wall. The lower terrace is characterized in its lower part by flat well-layered high amplitude internal reflectors of the basin fill facies, and is draped in its upper part by a thin layer of slightly inclined, medium amplitude reflectors (base marked light green in the section) interpreted as 'inner' levee facies. The lower sediments of the terrace appear to infill a topographic low between two diapiric structures. The upper terrace displays layered to slightly deformed medium amplitude reflectors which appear to rest on a small diapiric structure.

### *2.6.2 The Lower Cap Timiris Canyon*

The occurrence of locally enhanced channel-levee deposition within the high sinuosity proximal segment of the lower canyon, is illustrated by Profile GeoB03-024 (Fig. 2.9) which was shot across the active canyon and an abandoned meander loop in the continental rise area. Here, the active canyon shows very sparse sediment deposition at the thalweg, whereas the abandoned loop is partially infilled with ~300 ms TWT of sediments imaged as parallel, high amplitude reflectors. The levee facies which flank both sides of the canyon (interval between blue and green reflectors in Fig. 2.9) are distinguished by their low to medium amplitude continuous reflections and characteristic lens-shaped geometry overlying a basal unit. The underlying basal unit (interval between magenta and blue reflectors in the seismic section) also appears lens-shaped but is characterized by continuous to semi-continuous, strong amplitude reflectors interspersed with small lenses of acoustically chaotic and transparent reflections. This unit, which is folded in places, appears to locally infill topographic lows associated with underlying deformed sediments (top marked as magenta reflector in the section) and displays a complexity of erosional contacts. The levee facies are draped on the seafloor by a thin sheet, <40 ms TWT, of continuous, low to medium amplitude reflections. A couple of small-offset vertical fault is interpreted beneath the active canyon and also in the south.

In the more distal parts of the canyon, levee development is observed to be relatively poor whilst faulting begins to assume increasing dominance over canyon development, as exemplified by Profile GeoB03-035 (Fig. 2.10) and Profile GeoB03-032 (Fig. 2.11). In Profile GeoB03-035 (Fig. 2.10), which cuts across a linear distal segment of the canyon, the poorly

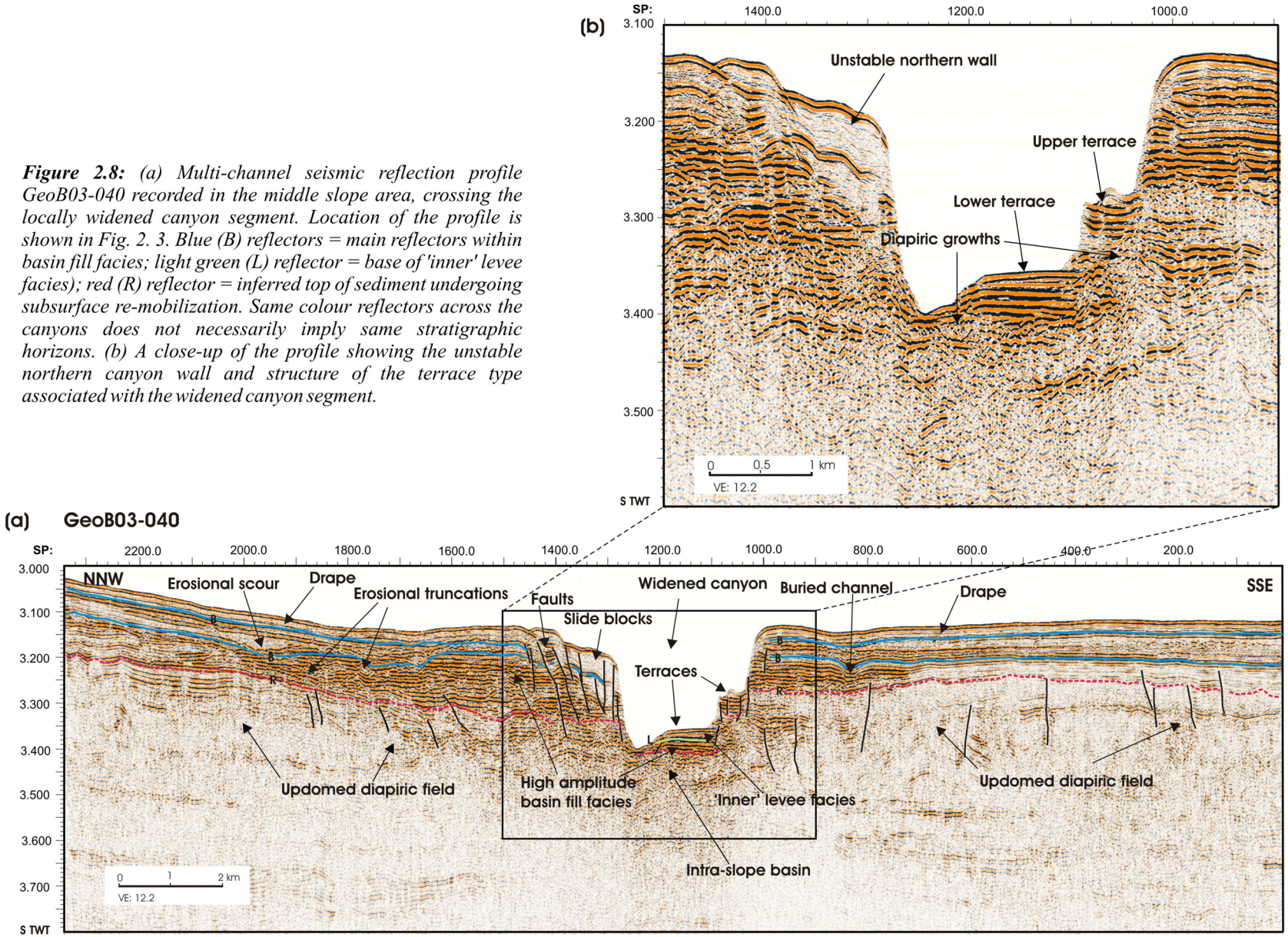


***Figure 2.8:*** *(a) Multi-channel seismic reflection profile GeoB03-040 recorded in the middle slope area, crossing the locally widened canyon segment. Location of the profile is shown in Fig. 2. 3. Blue (B) reflectors = main reflectors within basin fill facies; light green (L) reflector = base of 'inner' levee facies); red (R) reflector = inferred top of sediment undergoing subsurface re-mobilization. Same colour reflectors across the canyons does not necessarily imply same stratigraphic horizons. (b) A close-up of the profile showing the unstable northern canyon wall and structure of the terrace type associated with the widened canyon segment.*

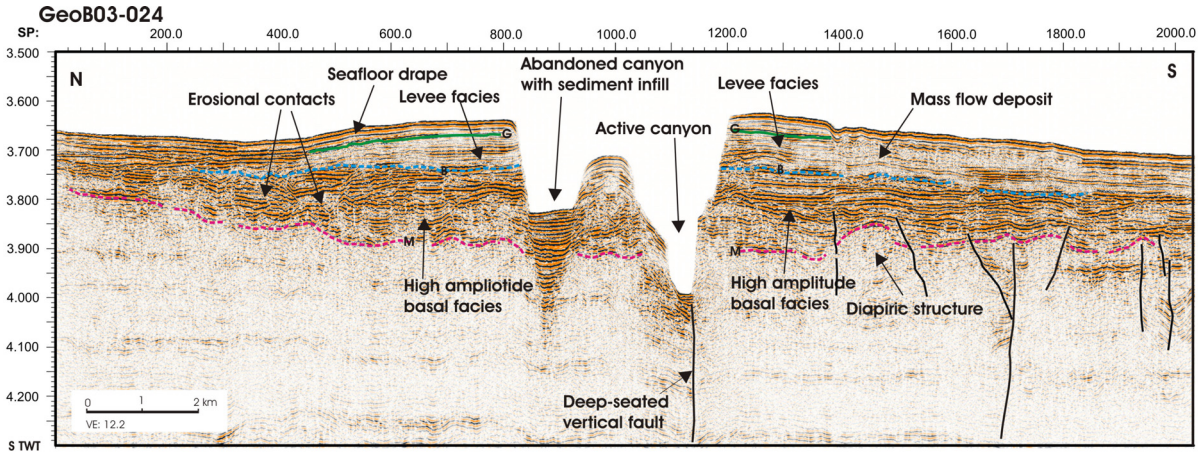


***Figure 2.9:*** *Multi-channel seismic reflection profile GeoB03-024 recorded in the lower canyon domain in the continental rise. The profile crosses a partly infilled abandoned meander loop (to the north) and the active canyon (to the south). Location of the profile is shown in Fig. 2.3. Interval between magenta (M) and blue (B) reflectors = high amplitude basal facies; interval between blue (B) and green (G) reflectors = levee facies.*

developed levees are characterized by sub-parallel low to medium amplitude seismic facies (interval between blue and green reflectors in Fig. 2.10). South of Shot Point 600, a sediment prism, ~100 ms TWT thick and characterized by chaotic low amplitude reflection events, is clearly visible, and may represent a mass flow deposit. Here, the basal unit (interval between magenta and blue reflectors in the seismic section) also shows high amplitude semi-continuous reflections but are sheet-like and progressively thins northwards against a gently updomed area (top marked as magenta reflector in the section). The top of the basal unit, especially in the north, shows what appears to be erosional scours. Profile GeoB03-035 also shows a relatively narrower, i.e. ~2.6 km wide, and deeper, i.e. ~300 m deep, V-shaped canyon with steep walls and poorly developed terraces. Several vertical faults are interpreted directly beneath the canyon floor as well as in the nearby sediments where they generally terminate either within or at the base of the basal unit. To the immediate south of the mass flow deposit, two buried channels have given rise to the development of a seafloor depression. A couple of vertical faults are interpreted directly beneath these buried channels (Fig. 2.10).

Profile GeoB03-032 (Fig. 2.11) which cuts across the main canyon and a smaller tributary canyon to the north also shows poorly developed levees on both sides. Here, the basal unit (interval between magenta and blue reflectors in Fig. 2.11), quite like in the previous profile, thins progressively against a gently uplifting broad area in the north. The basal unit is truncated in the north by an erosional surface which is onlapped by a ~100 ms TWT thick lens of low amplitude chaotic reflections, i.e. 4000 - 4100 ms TWT, inferred to be a mass flow deposit. Parts of this deposit, particularly north of Shot Point 1700, display

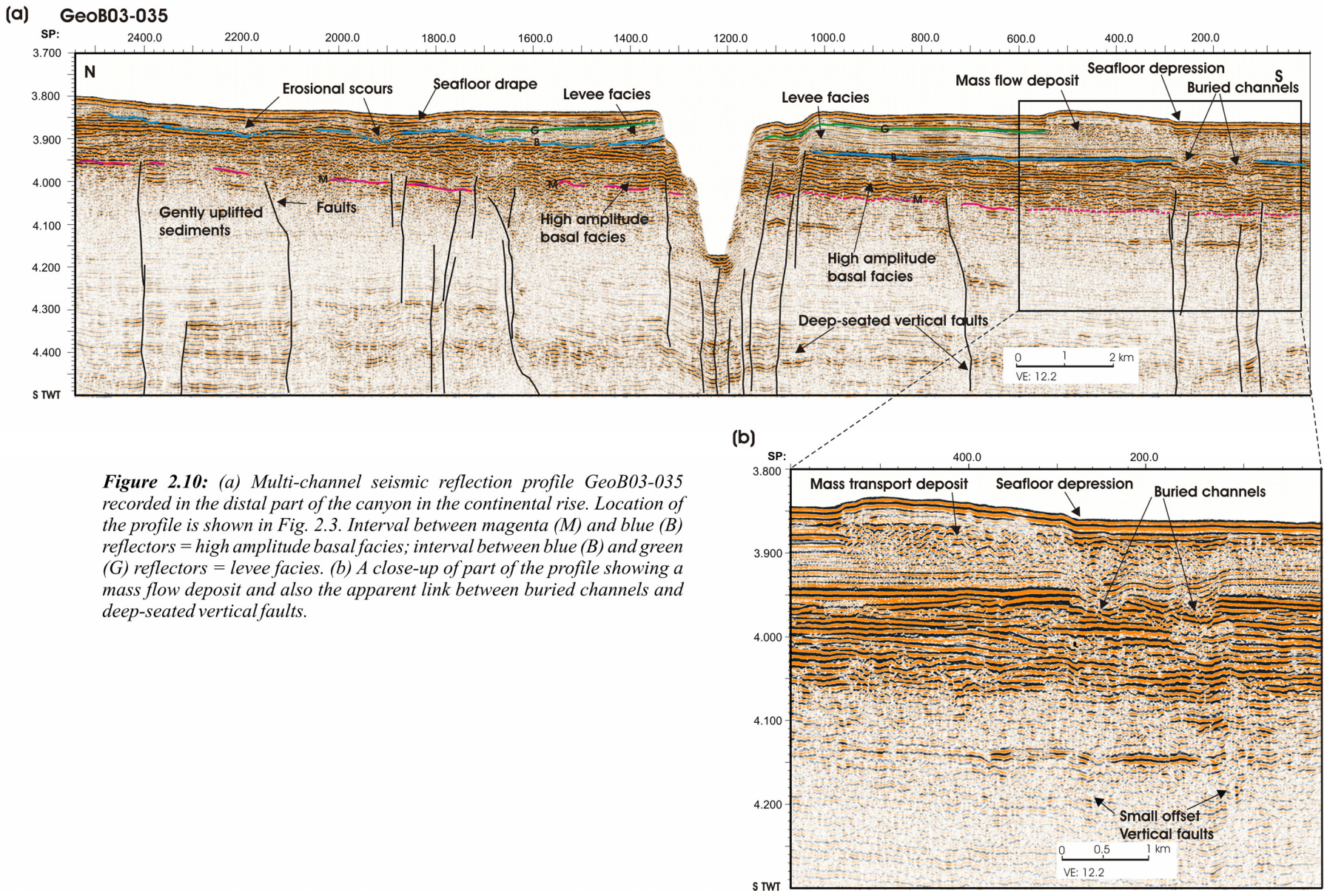


***Figure 2.10:*** *(a) Multi-channel seismic reflection profile GeoB03-035 recorded in the distal part of the canyon in the continental rise. Location of the profile is shown in Fig. 2.3. Interval between magenta (M) and blue (B) reflectors = high amplitude basal facies; interval between blue (B) and green (G) reflectors = levee facies. (b) A close-up of part of the profile showing a mass flow deposit and also the apparent link between buried channels and deep-seated vertical faults.*

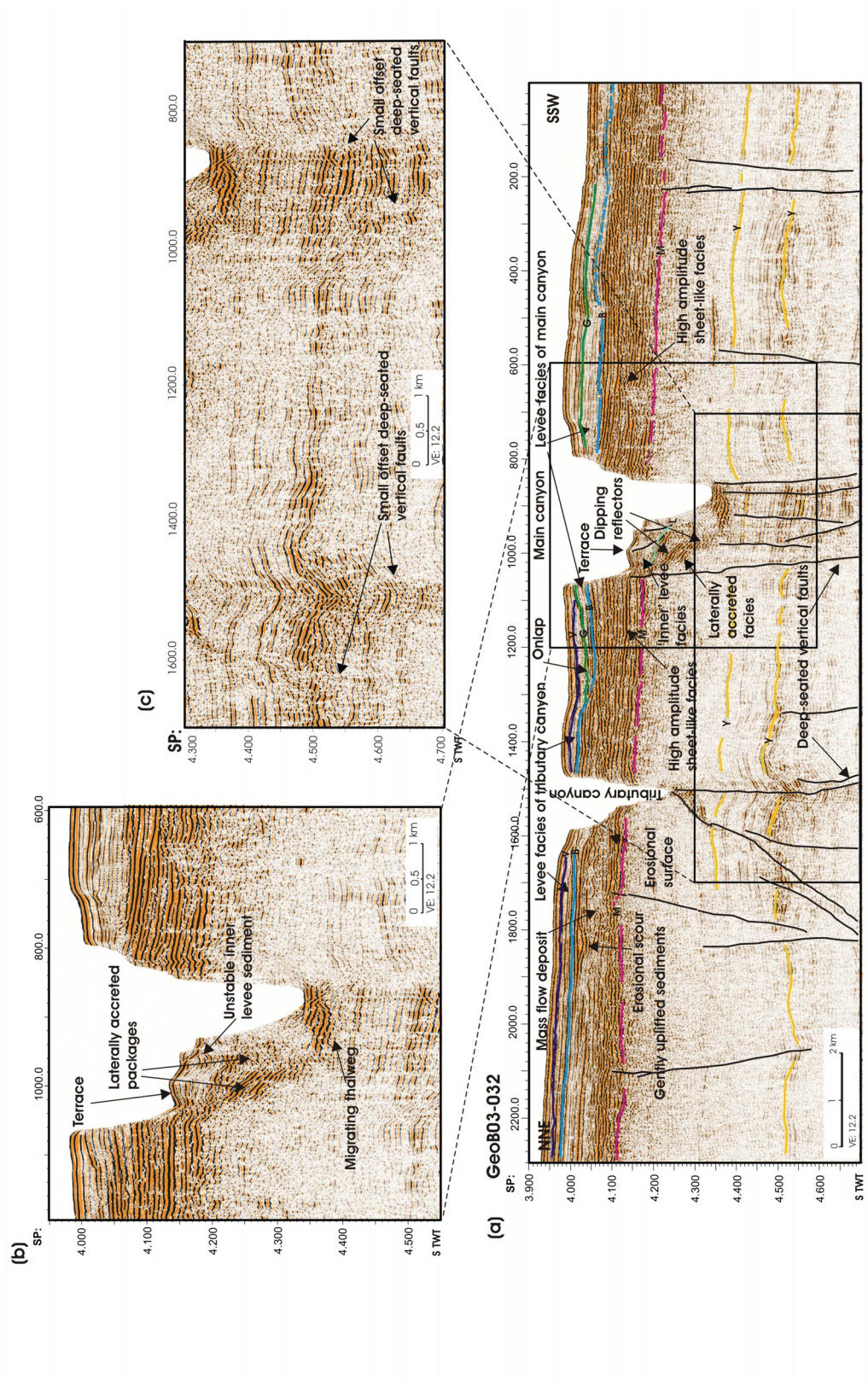


***Figure 2. 11****: (a) Multi-channel seismic reflection profile GeoB03-032 recorded in the distal part of the canyon in the continental rise. The profile crosses the main canyon (to the south) and a distal tributary canyon (to the north). Location of the profile is shown in Fig. 2.3. Interval between magenta (M) and blue (B) reflectors = high amplitude basal facies; interval between blue (B) and green (G) reflectors = levee facies of main canyon; interval between green (G)/blue (B) and violet (V) reflectors = levee facies of tributary canyon; light green (L) reflector = base of 'inner' levee facies; yellow (Y) reflectors = reflectors within sub-surface sediments mainly affected by deep-seated faults. (b) A close-up of the profile showing the characteristic structure of the terrace type associated with the regular meanders in the distal canyon. The terraces formed through progressive lateral accretion in the inner meander bends by deposition of material eroded from the outer bends.*

erosional scours. The mass transport deposit is cut by a tributary canyon. Levee sediments of the smaller canyon (interval between green/blue and violet reflectors in the seismic section) are observed to onlap the levee units of the main canyon at Shot Points 1100 - 1300 and below 4000 s TWT (interval between blue and green reflectors in the section). Whereas the southern wall of the main canyon is nearly vertical, the northern wall shows a well developed terrace which may be separated into two parts based on their very different internal seismic structure. The lower stack of terrace sediments displays at least three laterally accreted sediment packages characterized by steeply inclined medium amplitude prograding internal reflectors which dip towards the canyon. At the canyon floor, the base of these packages shows pockets of disorganized high amplitude reflections associated with a progressive southward migration of the thalweg. The upper stack of terrace sediments (with base marked as a light green reflector in the section), on the other hand, is characterized by thin layers of sub-parallel, medium amplitude reflectors cut by a couple of minor shallow discontinuities. The zone beneath the two canyons and their vicinities (i.e. with main reflectors marked yellow in Fig. 2.11), quite like in the previous upstream profile, is intensely cut by several deep-seated vertical faults which also generally terminate within or at the base of the basal unit.

## *2.7* Discussions

### *2.7.1 Structural controls on canyon development*

We have demonstrated from our bathymetry that the course of Cap Timiris Canyon is characterised by a major abrupt shift in direction, i.e. from an initial NE-SW oriented upper canyon segment to a predominantly E-W oriented lower canyon segment. This provides an initial indication that tectonic structure may have exerted a first order control on canyon location, particularly in the distal reaches.

The course of the upper canyon, as well as that of the several tributaries which feed into it in the head region, was initially likely chartered by small elongated depressions formed in association with topographic irregularities created through diapiric growths or sub-surface sediment remobilization (Figs. 2.6 and 2.7). These small basins may have guided the earliest turbidity current pathways, and thereby facilitated canyon incision. In the Niger Delta, for example, similar topographic irregularities on the seafloor are believed to have promoted seafloor erosion and, subsequently, canyon formation (Damuth, 1994). Widespread faulting in the vicinity of the upper canyon walls may also have enhanced sediment instability and, consequently, given rise to canyon widening by mass wasting of the canyon walls. This is

especially the case in the middle slope area where the walls of the anomalously widened canyon are observed to display fault-bounded acoustically transparent blocks (Fig. 2.8).

In its distal parts, the course of the lower canyon is characterised by sharp turns, including a right-angled bend, fairly long linear segments and long wavelength, low amplitude meanders contained within a narrow corridor (Fig. 2.3). The tributary canyon also displays a linear segment aligned sub-parallel to a long linear segment of the main canyon. Fault-controlled canyons are known to commonly display linear segments and abrupt changes in direction (Hagen et al., 1994; McHugh et al., 1998). Our distal seismic profiles (Figs. 2.10 and 11) have confirmed the presence of several faults cutting vertically beneath the thalwegs of the lower canyon. We also note that some of these faults lie directly beneath a number of buried channels (Figs. 2.2 and 10) suggesting that the location of the channels may be related to the faults. We believe that fault-controlled zones of weakness pre-determined the location of the distal canyon and also facilitated erosional downcutting during its formative stages. Our interpretation is consistent with the structural setting of Cap Timiris Canyon which, being located close to a prominent offset of the shelf break, potentially coincides with the continental extension of a major fracture zone (Figs. 2.1 and 2.2).

### *2.7.2 Style and patterns of meander development*

Our data interpretation suggests that a combination of a number of factors, including the nature of underlying rock material, seafloor gradient, frequency and type of sediment load as well as tectonics, may have significantly influenced the development of the variety of meander and flow patterns exhibited by Cap Timiris Canyon. In the head region where very low sinuosity of ~1.2 is recorded, the very deep entrenchment of the canyon system within a thickly sedimented intra-slope basin must have prevented any significant meander formation. As deformation of the wedge of sediments becomes more prominent downstream, i.e. from the upper slope to the middle slope, the pathways of the canyon are locally chartered by topographical lows and depressions developed irregularly on the seafloor, thereby inducing an irregular meander pattern. In the middle slope area, however, the locally widened U-shaped canyon morphology, characterised by terraces and unstable walls, and an incised main thalweg, which in places splits into two or more thalwegs (Fig. 2.3, profile I), suggest a pre-existing widened canyon now being overprinted by a meander pattern. The abrupt transition from a meander pattern to a widened segment, and then back to a meander pattern downstream, may be a direct reflection of the sudden changes in the nature of the underlying rock.

The locally tortuous meander pattern appears to be the initial direct response of the flow to the subtle updoming effect by the Cape Verde Rise. As the flow encountered the rise, the canyon increased its sinuosity in the steeper part of the updomed area. Several examples where submarine canyon/channel systems have increased their sinuosities locally in response to increased slopes, have been documented elsewhere, e.g. the Amazon Fan channels (Flood and Damuth, 1987) and the canyon system on the Peru-Chile forearc (Hagen et al., 1994). Another reason for the anomalously high sinuosity in the area may be explained by the restrictions to meander migration imposed by the deeply incised linear segment immediately downstream of the highly sinuous segment. An apparently similar situation where increased sinuosity is observed upstream of a linear segment, is exemplified by the style of meandering of the distal tributary canyon before it joined the main canyon (Fig. 2.3). Anomalously high sinuosities are known to result upstream of canyon segments which are incised into bedrock or other resistant units so as to impede downstream channel meander migration (Holdbrook and Schumm, 1999; Schumm et al. 1994). The interaction between tectonics and meander evolution becomes increasingly evident in the more distal part of the canyon. Here, the lateral migration of the canyon meander is restricted by faulting, as confirmed by our seismic data, to a narrow corridor, giving rise to the development of long wavelength, low amplitude regular meander patterns. If we consider the course of the distal canyon as being pre-determined by regional structural lineations, then it is most likely that the initial incision was characterised by several straight segments before developing subsequently into meander patterns during different stages of evolution. A youthful stage of the distal canyon appears to be replicated by the younger distal tributary canyon, whose linear segment is apparently in its infant stage of meander development.

A detailed examination of the bathymetric map (Fig. 2.3, Box C) suggests that the distal canyon, since its initial formation, has experienced at least three different stages of meander evolution (Fig. 2.12). The earliest stage of meander development (Stage 1), i.e. after the infant linear stage, was characterised by a low sinuosity ( ~1.2) pattern. This was followed by a second stage (Stage 2) of a low to moderate sinuosity (~1.3) pattern which laterally migrated slightly to the south. These two stages were then overprinted by the latest stage (Stage 3) presently characterised by a centrally more deeply incised canyon with a slightly higher sinuosity (~1.45) and a dominant downstream meander loop migration pattern. Whereas these observations show that the meander patterns have evolved through time by progressive increases in sinuosity, lateral meander migrations have been effectively contained within the narrow fault-controlled corridor. Variations in sinuosity associated with different

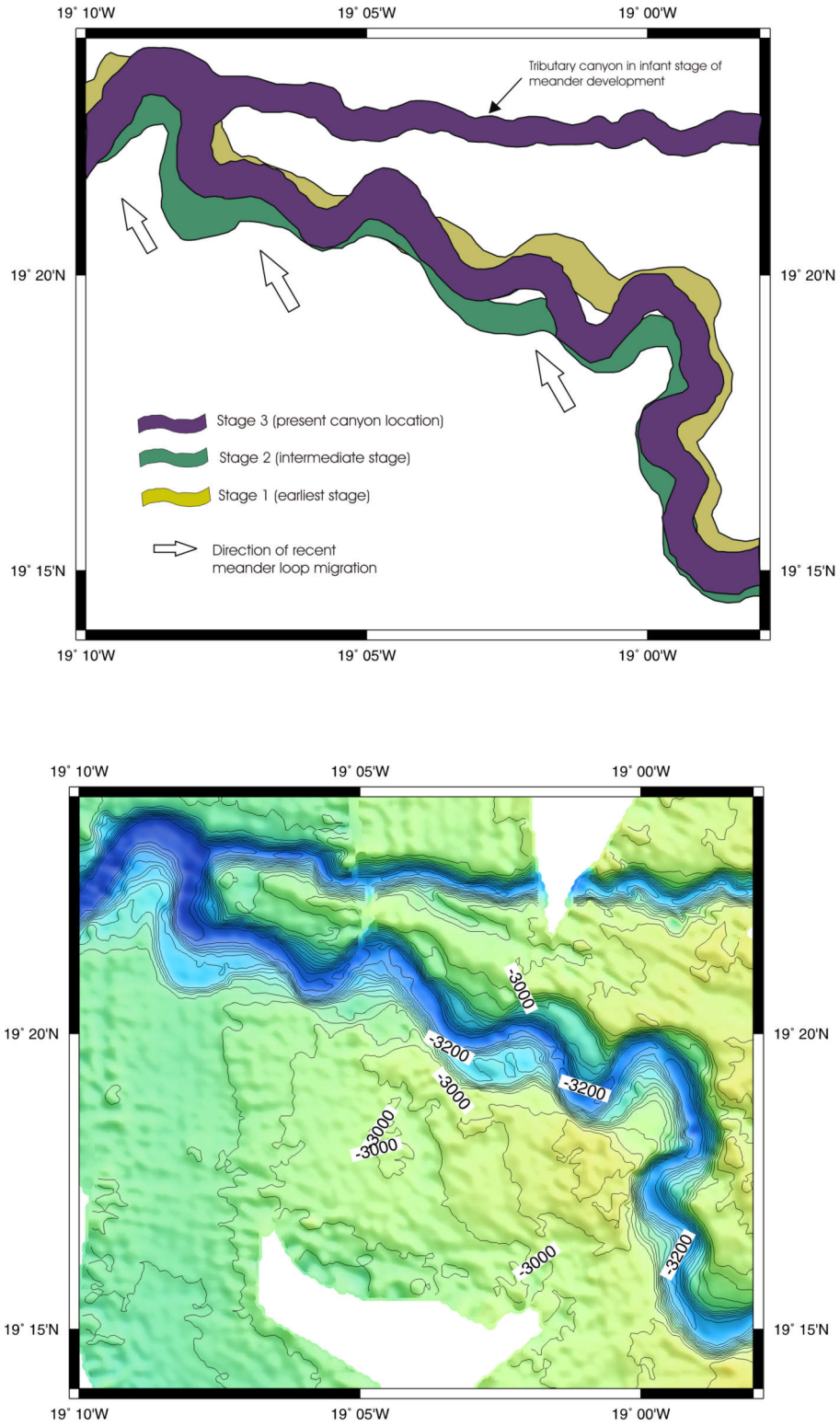


***Figure 2.12:*** *Schematic representation of the stages of meander evolution in the distal part of Cap Timiris Canyon based on our interpretation of Hydrosweep bathymetry data of the canyon segment shown below (location of the segment corresponds to Fig. 2.3, Box C). Development of the meanders has been confined within a narrow fault- controlled corridor, giving rise to regular meander patterns characterised by long wavelengths and low amplitudes. The confinement has precluded any significant lateral meander loop migration, allowing recent migration to largely proceed down-system. The model assumes that canyon width has remained largely unchanged during meander development.*

stages of meander development may result from major changes in the flow regime and type of sediment load (Posamentier and Kolla, 2003). It appears that because of the structural controls imposed on free lateral meander migration, the latest stage meander evolution has tended to accommodate subsequent increases in flow discharges, not only through increased sinuosity, but by pronounced downstream migration as well (Fig. 2.12).

### *2.7.3 Canyon incision*

We infer from the canyon relief profile (Fig. 2.5b) that the morphology of Cap Timiris Canyon is dominated by deep incisions along most of its course, attaining relief maxima of 460 m and 300 m in the upper slope and distal segments respectively. Incision has been shown to be only locally limited in the highly sinuous middle segment which is characterised by enhanced levee development.

In the upper slope area, the very deep incision was probably achieved through intense erosional downcutting by the canyon into the ~400 m thick poorly consolidated and deformed sediments of the deep intra-slope basin (Fig. 2.7). However, in the middle slope area, pronounced upward mud diapiric growths have resulted in rather shallow intra-slope basins, <150 m thick (Fig. 2.8). The progress of vertical incision must have been retarded for some time now probably because of the presence of relatively higher erosion-resistant sediment materials at the thalweg. In this case, any surge in flow would have been locally accommodated by canyon widening through increased lateral erosion and mass wasting of the relatively less erosion-resistant and faulted sediments that form the canyon walls. This setting probably favoured the development of the anomalously widened segments of the canyon.

The generally smooth and concave-up longitudinal profile of the canyon thalweg (Fig. 2.5a) is typical for most sub-aerial fluvial systems whose flow discharge has established long term equilibrium with the underlying substrate (Pirmez and Flood, 1995, Pirmez and Imran, 2003). However, the presence of the knickpoints in the upper and lower canyon segments, suggests continued localized active erosional downcutting by the canyon in those localities as the flow strives to achieve a finely smoothened out profile in order to re-establish equilibrium (Pirmez and Flood, 1995, Pirmez and Imran, 2003). By comparing the longitudinal depth profile with the bathymetry, we note that the location of the widened canyon segments roughly coincides with the broadly shaped upper canyon knickpoints (Fig. 2.5a). We therefore ascribe the origin of these broadly shaped knickpoints to the episodic localised uplift of the beds of resistant sediment which must still be undergoing active downcutting by the canyon. The pronounced canyon downcutting may have given rise to a slight upslope knickpoint

migration. We note that the distal canyon is deeply entrenched in a narrow fault-controlled corridor set within a gently tectonically uplifted zone (Figs. 2.10 and 2.11). The dominant steep and narrow V-shaped cross-sectional morphology which characterizes this distal segment of the canyon, is suggestive of enhanced incision into an erosion resistant bedrock. The initial incision process was certainly facilitated by widespread faulting which created elongated zones of weakness to focus the energy of the erosive turbidity currents.

The group of distal knickpoints (Fig. 2.5a), has been shown to be characterized by relatively smaller shapes and more steepness downstream. A comparison of the longitudinal profile with the bathymetry links these knickpoints with the deeply entrenched distal segment where confined long wavelength, short amplitude regular meander courses with abrupt short changes in direction have been described (Fig. 2.3). The origin of these distal knickpoints may therefore be the result of incisions into a faulted zone, which includes several minor offsetting faults. Accordingly, we reason that the distal canyon, just like the upstream segment which has been associated with the upper canyon knickpoints, must also be undergoing active incision to re-establish a smoothened out equilibrium profile.

### *2.7.4 Terrace formation*

Terraces are known to be common features in fluvial environments, and several types of different genetic origin have also been described in submarine canyon or channel settings. The formation of terraces in submarine canyons are believed to document the history of canyon incisions and meander evolution (Hagen et al., 1994; Deptuck et al., 2003). Slide- or slump-related terraces which usually show disturbed seismic facies at the base, are believed to result from slope failures of the canyon walls (Friedmann, 2000; Deptuck et al., 2003; Pichevin et al., 2003), and may be located anywhere along a linear canyon or its meander bend (Pichevin et al., 2003). Terraces may also originate in a fashion similar to ‘point bar’ development observed in meandering sub-aerial fluvial systems (Abreu et al., 2003). Such terraces form from the erosion of the outer meander bends and simultaneous lateral accretion of the eroded material in the inner meander bends, giving rise to an internal seismic structure recognised by prograding foresets which dip steeply towards the thalweg (Abreu et al., 2003). Again, some terraces are thought to have originated as ‘inner’ levees or ‘confined’ levees (Hubscher et. al., 1997; von Rad and Tahir, 1997; Pichevin et. al., 2003; Babonneau et. al., 2004). ‘Inner’ levee terraces have been variously described as ‘depositional’ terraces (von Rad and Tahir, 1997). They are commonly identified by their wedge shaped or layered internal seismic facies (Deptuck et al., 2003, Pichevin et. al., 2003; Babonneau et. al., 2004).

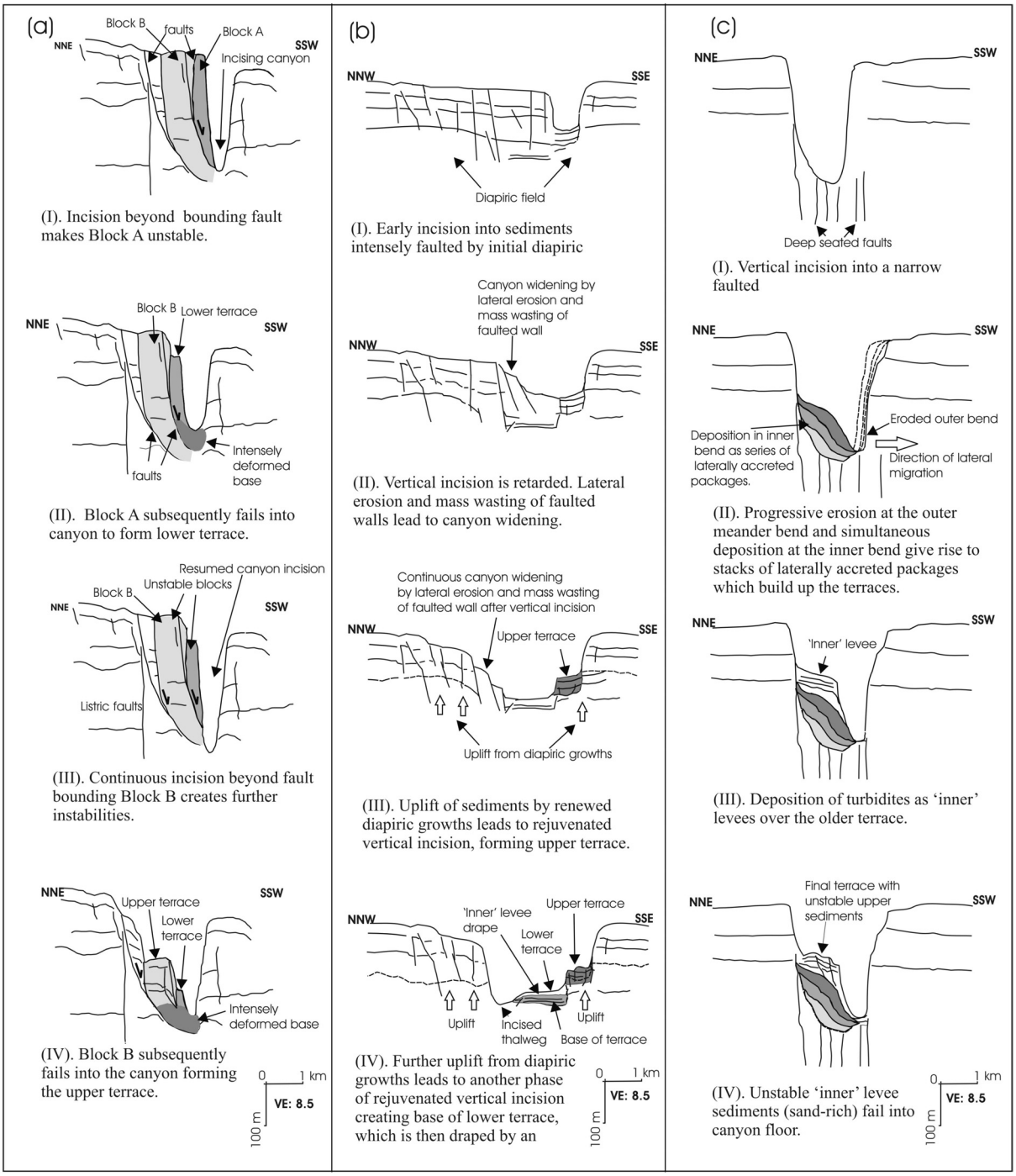


***Figure 2.13:*** *Schematic illustrations of the various processes and stages of terrace development along Cap Timiris Canyon. (a) Terrace development in the upper slope segment (see Fig. 2.7b for seismic section). (b) Terrace development within the widened canyon segment in the middle slope area (see Fig. 2.8b for seismic section). (c) Terraces formed through meander processes in the distal parts of the canyon (see Fig. 2.11b for seismic section).*

Our data interpretation shows the presence of several terrace-like morphological features spanning the length of Cap Timiris Canyon. The variety of internal seismic structural characteristics exhibited by these terraces, suggests that they may have originated through a number of different processes, and should therefore likely store important records about the evolutionary history of the canyon.

In the upper slope, the presence of disturbed sediments at the base of the terraces (Profile GeoB03-042, Fig. 2.7) suggests that the formation of the terraces was initiated through sediment failure along the bounding faults. We propose that these terraces, which may appropriately be described as 'slump' or 'slide' terraces, probably formed in response to at least two major successive phases of incision depicted by the following stages (Fig. 2.13a):

(i) As the canyon walls were continuously oversteepened by the progress of downcutting during the first phase of incision, widespread compaction and growth faults promoted instabilities in the vicinities of the northern wall;

(ii) This subsequently gave rise to failure of the northern wall once the intersecting fault planes, which bound the terrace-forming Block A, were breached, consequently forming the lower terrace.

(iii) During a second major phase of incision, resumed and intensified downcutting breached deeper intersecting faults, which bound the terrace-forming Block B, leading to further instabilities.

(iv) Block B subsequently failed into the canyon forming the upper terrace, at the same time dragging along the lower terrace further down and causing more intense deformation of lower parts of the blocks.

We suppose that the development of these terraces should record the history of canyon incisions in the upper slope area, and hence may be related to periods of glacial sea level lowstand during which gravity-induced flows were potentially most erosive.

In the middle slope area, the unique setting of the anomalously widened canyon has given rise to the development of other types of terraces. With their well-layered internal structure, the middle slope terraces may appear to have originated as an 'inner' levee through deposition of turbidity currents trapped within the canyon. However, there is no clear indication to support an 'inner' levee origin. Rather, the base of the terrace sediments are observed to either rest above diapiric structures, i.e. the upper terrace, or infill a topographic low, i.e. the lower terrace, and hence should constitute part of the surrounding high amplitude reflection intra-slope basin facies.

Consequently, we envisage that these terraces have originated through phases of uplift-induced vertical incisions which may be represented by the following stages (Fig. 2.13b):

(i) Initial canyon incision facilitated by small faults near the apices of shallow diapiric structures;

(ii) Canyon widening through increased lateral erosion and mass wasting of the canyon walls to compensate for retarded downcutting;

(iii) Renewed mud diapiric growths, mostly at the northern flank, resulted in faulting and uplifts of the area, followed by extensive mass wasting of the intensively faulted northern wall, and rejuvenated canyon incision as a result of a locally lowered base level. The upper terrace was then created in the southern wall as a remnant of the abandoned thalweg. The new canyon is now much wider and U-shaped;

(iv) Further diapiric growths led to more faulting and uplifts giving rise to slope failures and extensive mass wasting, particularly, of the northern wall. The renewed uplift, once again lowered the base level to rejuvenate the canyon to deeply incise a new thalweg in the north, as the old thalweg was abandoned to form the lower terrace. The slight change in seismic character at the top of the lower terrace suggests that the terrace is draped by deposits from confined low energy turbidity currents.

If we suppose that the intermittent diapiric growths have largely been induced by rapid sediment accumulations, then understanding the sources and triggers for the sporadic sediment inputs into the slope areas should provide useful indications about controls of sediment influx on canyon evolution.

The distal part of the canyon, whose development is strongly influenced by deep seated faults, gives rise to the formation of another genetically different type of terraces. Here, we note that though meander development is restricted to the narrow fault-controlled corridor, the inner bends of the low amplitude meanders are associated with well developed terraces. These terraces, which are mostly arcuate in plan (Fig. 2.4, Box C) and whose internal seismic structures have been shown to be dominated in the lower part by steeply dipping foresets (Fig. 2.11), may be ascribed to a ‘point bar’ origin. The internal seismic configuration of the terrace suggests several phases of terrace construction which may be represented by the following stages (Fig. 2.13c):

(i) Earliest stage of canyon formation dominated by vertical incision into a faulted linear zone;

(ii) Start of meander development enhanced by increasing lateral erosion led to initial terrace growth. The gradual terrace build-up was achieved through progressive erosion at the outer meander bend and simultaneous deposition of the eroded material at the inner bends. These processes must have taken place in at least three phases which we associate with the three laterally accreted sediment packages, each with its own migrating thalweg.

(iii) Following a relatively calm phase, the upper part of the terrace began developing over the lower accreted packages as an 'inner' levee. During this period the flow became less energised, and allowed limited overspill of turbidity currents over the older terrace element to form the 'inner' levee sediments, recognised in the seismic data by their well-layered, near-horizontal internal reflections.

(iv) The latest stage was characterised by instabilities of the 'inner' levee sediments giving rise to failure of the upper part of the terrace into the canyon floor.

Irrespective of the different genetic origins associated with the Cap Timiris Canyon terraces, their modes of formation have, in all cases, been connected with erosional downcutting of the thalweg and/or lateral erosion of the canyon walls. This re-echoes the highly erosive character that has dominated most of the evolutionary history of the canyon.

### *2.7.5 Origin and age of Cap Timiris Canyon*

Several indications seem to link the origin of Cap Timiris Canyon to a major river system in the adjacent land. We note from its geological setting, that the head region of Cap Timiris Canyon traces directly into the adjacent coastal area known to have hosted a receded large marine gulf, which was initiated during the Early Pleistocene marine transgression to form the onshore Mauritania Quaternary Basin (Wissmann, 1982; Giresse et al., 2000). We again note that Flicoteax et al. (1975), as cited by Wissmann (1982), elsewhere in the region deduced a link between similar receding marine gulfs and the Casamance and Gambia rivers, through paleo-geographic reconstruction of coastlines off Senegal dating from the Paleocene. By analogy, we may speculate that the Quaternary marine gulf adjacent to Cap Timiris may have constituted the estuary of a major fluvial system. This assertion appears to be in agreement with findings of Vörösmarty et. al. (2002) who, from their study of potential paleo-drainage patterns of NW Africa, postulated that the Cap Timiris area possibly served as the estuary of a major river system, named Tamanrasset. During previous marine incursions at

interglacial sea level highstands, this estuary would have trapped and stored huge quantities of fluvial terrigenous sediments supplied by the flowing river, together with marine and re-worked terrigenous sediments.

In seismic Profile GeoB03-044 (Fig. 2.6), we have demonstrated that the northern canyon deeply incises the shelf edge, and therefore may likely reach across the outer shelf. Very high resolution seismic profiling of the shelf in the Cap Timiris area confirms the presence of buried shallow incised valleys on the outer shelf (Krastel et al., 2004), lending credence to our assertion that the shelf was drained by a terrestrial river during periods of lowered sea level, and hence establishing a link between a major fluvial system and the location and origin of the canyon. We have shown by our data that the lower canyon is deeply incised into the Cape Verde Rise. Had the canyon been formed either before or during the uplift and growth of the rise, we would have expected the lower canyon to respond to the uplift through consistent and pronounced northward lateral migrations of that segment. Since we do not observe these in the canyon morphology (Figs. 2.3 and 2.12), but rather a diversion of the course of the lower canyon by the rise coupled with a local anomalous increase in sinuosity at the topographically elevated bend, we infer that Cap Timiris Canyon must be younger than the Cape Verde Rise. Hence, the uplift of the Cape Verde Rise, believed to have occurred in Miocene time (Lancelot and Seibold, 1978; Wissmann, 1982), may be employed to constrain the maximum age for the canyon. In addition, Krastel et al (2004) have proposed ~170 ka as the minimum age for the canyon, constrained by a dated major slide that onlaps very distal levees of the canyon. We are, therefore, inclined to believe that Cap Timiris Canyon began forming around Plio/Pleistocene times during one of the major glacial stages of sea level lowstands when the head region established direct connection with a major sub-aerial river system from the adjacent land, and allowed large volumes of clastic terrigenous sediments to move across the shelf environment into the slope area. This assertion is in agreement with Jacobi and Hayes (1982), who also postulated that many canyons along the margin began forming during Plio/Pleistocene times.

In several of our profiles, (Figs. 2.8 – 2.11), we have described the presence of an extensive seismic facies, characterised by sheets of high amplitude reflectors with patches of transparent to chaotic zones, which locally infill topographic lows. We have also shown that the facies, which is deeply incised by the canyon, extends several tens of kilometres in width, and progressively thins away from the canyon flanks as well as against underlying gently uplifted zones. We interpret this facies as representing the initial unchannelised but broad elongate sheet of sand-rich turbidity currents, that must have flooded the margin during the

resulting major sea level lowstand. That the facies is characterised by several truncations, cut and fill structures, small infilled channels and erosional scours, is clear evidence of the highly erosive nature of the turbidity currents. The presence of widespread seismically transparent and chaotic reflection zones within the facies suggests that the turbidity currents entrapped a significant amount of debris flows and other slide- or slump-generated materials sourced mainly from the upper slope area as they flowed downslope. This shows that the margin had been prone to widespread instabilities prior to the formation of the canyon, and that fractures, folding and elongated seafloor depressions created by these instabilities, subsequently facilitate erosional downcutting along the slope during the formative stages of the canyon.

The invading clastic terrigenous sediments must have generated powerful erosive turbidity currents which initially covered a large area on the margin, but gradually mobilized preferentially along the linear pathways, and thereby allowed a more focused flow energy to persistently cut several discrete channels which eventually merged downstream to constitute the main canyon. The well developed dendritic canyon pattern in the head region, is a clear manifestation of the intense sub-aerial erosional activity that culminated in the formation of the many pathways, and which allowed the canyon head to funnel sediments from a much wider area, >5000 km², into the mainstream. Since being carved, the canyon has undergone significant modifications largely through the combined action of turbidity current flows, mass wasting of canyon walls, deformation and mud diapiric growths.

### *2.7.6 Sediment transport processes and canyon preservation*

That the different stages identified with meander development (Fig. 2.12), canyon incisions and terrace formation (Fig. 2.13) can be attributed to major surges in flow discharges, suggests that the evolution of Cap Timiris Canyon, has been characterised by large episodic sediment inputs. We associate such large intermittent sediment supplies into the canyon with periods of glacial sea level lowstands. During these periods the canyon remained coupled to the river system, and hence was likely to have been most active. A fall in sea level would have given rise to an increase in river gradient (Babonneau et. al., 2002), hence rejuvenating the river to transport huge quantities of sediments directly into the canyon head for onward transfer into the deep sea. The stages of development of the terraces and meander patterns must have, therefore, been strongly influenced by the flow characteristics of the river. Consequently, we propose that a proper age constraint of the evolutionary history of canyon morphological features like the terraces, meanders patterns, incisions and levees could provide a temporal framework for studying the stages of flow of this now extinct river system,

and hence serve as a useful proxy for understanding the climatic evolution of the Sahara region since Plio/Pleistocene times.

The inundation of the shelf areas by the oceans during the recent sea level highstand has disconnected many submarine canyons from their terrestrial point sources, making them currently inactive. A few of them, e.g. Zaire Canyon (Babonneau et. al., 2002) and San Antonio Canyon (Hagen et al., 1995) have, however, remained active largely because of sediment inputs through their continued connection to onshore river sources. Now, though Cap Timiris Canyon currently receives no fluvial inputs, its dominantly V-shaped and deeply entrenched thalweg morphology, which is only sparsely sedimented in places, points to a still active canyon. The presence of knickpoints along the canyon profile means that the canyon is continuously incising. In addition, sediments recovered from coring the canyon thalweg have shown no stratification at the top, suggesting recent activity within Cap Timiris Canyon. Some of the sediments revealed a succession of more than thirty turbidites of different genetic origins, with the turbidite fraction reaching up to 50% of the sediment (Holz,2005). The succession of several turbidites is ascribed to the frequent turbidity current flows associated with the canyon (Schulz et al., 2003; Holz, 2005). A still active and open Cap Timiris Canyon is quite intriguing, considering the fact that this huge submarine canyon is located off the Sahara Desert, a major arid climatic zone, and at the moment is not connected to any active river system. In our effort to understand the processes that have acted to preserve this canyon under the present inter-glacial regime, we examine recent potential sources for sediment inputs into the canyon.

The low seismic energy returns recorded from some of the upper slope sediments, e.g. Profile GeoB03-044 (Fig. 2.6), may be a reflection of the disrupted internal structure of the layered sediments as a result of the decreased cohesion and shear strength caused by the slow movement or creeping of the rapidly deposited sediments. This, in addition to the widespread sediment glide planes and growth faults associated with the different sediment layers in the upper slope area, suggests that the upper slope area has been prone to sediment instabilities for quite some time now. This interpretation is consistent with earlier observations by, e.g. Weaver et al. (2000) and Wynn et al. (2000), that the margin is dominated by intense mass wasting processes, which have largely been attributed to high rates of sediment accumulation through upwelling-induced primary production (Sarnthein et al., 1982). Predominant faulting and sliding in the vicinity of the steep canyon walls, as well as slump deposits observed along the canyon thalweg, also provide indications of active mass wasting in the head region of the canyon. Again, large amounts of sediments are generated from the middle slope area where

intense lateral erosion and mass wasting of the canyon walls have resulted in canyon widening. The slump and other mass flow materials derived from all these gravity-driven processes must have been integrated into the sediment flow processes, as a very significant component, and transported downstream.

Since the last glacial maximum, the landscape of the western Sahara Desert in Mauritania down to the coast has been dominated by huge expanses of mostly NE-SW trending linear sand dunes formed during three generations, i.e. 25 – 15 ka, 10 – 13 ka, and after 5 ka (Lancaster et al., 2002). Huge quantities of this aeolian sand are believed to have been transported into the deep sea mainly by offshore blowing Harmattan winds (Sarnthein et. al., 1982, Wefer and Fischer, 1993). The alignment and close proximity of the head region of Cap Timiris Canyon to huge littoral sand bodies, places the canyon in a strategic location to receive large amounts of the sand. In addition, a lot of the aeolian inputs into the margin north of the canyon is swept southwards by the strong nearshore currents (Sarnthein et. al., 1982; Weaver et al., 2000) hence allowing the canyon and its tributaries to further intercept huge quantities of the sand for onward transport into the deep sea.

The different sediment sources are incorporated into the flow discharge within the canyon and transported downslope. As the flow enters the lower canyon domain, the sharp diversion in its course gives rise to a reduction in flow energy and flow overspill, locally resulting in significant sediment deposition as expressed by the enhanced levee development in the highly sinuous segment. Towards the distal parts, however, a sudden deepening of the entrenched canyon within the uplifted Cape Verde Rise may have allowed only limited intermittent overspill of turbidity currents, hence explaining the poor nature of levee formation in these parts. Since most of the flows remain largely confined, they are able to maintain most of their high energy, thereby allowing the distal canyon to transport sediments for several hundreds of kilometres further seaward into the abyssal plains. As a similar example, the ability of Zaire Channel to transport sediments to very distal fans has been attributed to its deeply entrenched morphology (Babonneau et al. 2002). The foregoing lines of evidence provide clear indications that Cap Timiris Canyon has continuously received and transported huge amounts of sediments downslope for a relatively long time.

## 2.8 Conclusions

Based on a combined analysis of hydrosweep swath bathymetry and high resolution multi-channel seismic reflection data, we document for the first time the detailed morphology and structural characteristics of Cap Timiris Canyon, a newly discovered submarine canyon

system offshore Mauritania. Our data interpretation has allowed us to investigate the development of the canyon and the role it has played in the sedimentation process history of the region.

- The dominantly V-shaped canyon displays several fluvial features including tributaries, meander patterns, a cut-off loop, and terraces. The head region is composed of a series of dendritic canyons and gullies that funnel sediments from a large area, >5000 km², along the Mauritanian margin into the main canyon.
- The course of the canyon is characterized by abrupt shifts in direction and linear segments, particularly in the distal reaches, suggesting strong structural control on canyon location and development.
- The development of irregular meander patterns in the proximal canyon is a direct reflection of topographic irregularities induced by the underlying geology which has been affected by diapiric growths. Meandering in the distal canyon is characterized by long wavelength and low amplitude regular meander patterns confined within a narrow fault-controlled corridor. These meander patterns show several stages of evolution, the latest of which is dominated by a down-system meander loop migration
- Terraces identified by the study show a variety of internal seismic structures suggesting that they have originated through different processes including: (i) sliding and slumping in the upper slope segment as a result of progressive vertical incision of faulted zones; (ii) uplift-induced incision in the widened canyon segment of the middle slope; and (iii) 'point-bar' development in the meandering distal segment.
- We ascribe canyon origin to an ancient river system in the adjacent presently arid Sahara Desert that breached the shelf during a major Plio/Pleistocene sea level lowstand and delivered sediment directly into the slope area. Our data suggest that the invading initially unchannelised sheet of sand-rich turbidity flows, initiated canyon formation by gradually mobilizing along linear seafloor depressions and fault-controlled zones of weakness.
- We propose that the development of canyon morphology and structure was influenced by the stages of active flow of the coupling river system, and hence proper age control of the evolutionary history of canyon features like meander patterns, terraces and levees would act as a useful proxy for understanding the paleo-climatic evolution of a 'green' Sahara since Plio/Pleistocene times.
- Under the present regime of sea level highstand (and also being located off a major arid climatic region) Cap Timiris Canyon presently does not receive any significant

fluvial sediment inputs but has remained preserved through supplies from sources including: (i) upwelling-induced sedimentation, (ii) sediment transport by longshore currents, (iii) offshore wind-blown sediments and (iv) mass wasting.

- The deep canyon entrenchment in the distal parts is able to keep most of the sediment flows confined, and hence energized, thereby allowing the canyon to actively transport sediments over several hundreds of kilometers further seaward into the abyssal plains.

## 2.9 Acknowledgements

We gratefully acknowledge the team spirit and support of the captain and crew members as well as all the cruise participants of RV Meteor Cruise M58/1. This study is part of an on-going research of 'Upwelling and sedimentation off NW Africa' by RCOM. The manuscript benefited greatly from reviews by two anonymous referees. This is publication RCOM0295 of the DFG-Research Center 'Ocean Margins' (University of Bremen).

## References

Abreu, V., Sullivan, M., Mohrig, D. & Pirmez, C. (2003). Lateral accretion packages (LAPS): an important reservoir element in deep water sinuous channels. Marine and Petroleum Geology, 20, 631-648.

Babonneau, N., Savoye, B., Cremer, M. & Bez, M. (2004). Multiple terraces within the deep incised Zaire Valley (ZaiAngo Project): are they confined levees? In S.A. Lomas & P. Joseph (Eds.), Confined Turbidite Systems. Geological Society, London, Special Publications, 222, 91-114.

Babonneau, N., Savoye, B., Cremer, M. & Klein, B. (2002). Morphology and architecture of the present canyon and channel system of the Zaire deep-sea fan. Marine and Petroleum Geology, 19, 445-467.

Barusseau, J.P. et al. (1995). Coastal evolution in Senegal and Mauritania at $10^3$, $10^2$ and 10-year scales: Natural and human records. Quaternary International, 29/30, 61-73.

Bouma, A.H. (2001). Fine-grained submarine fans as possible recorders of long- and short-term climatic changes. Global and Planetary Change, 28, 85-91.

Brown, L. (2002). Petroleum prospectivity of the MSGBC Basin Northwest africa; an emerging deepwater petroleum province? AAPG Annual Meeting, Houston, Texas.

Caress, D.W. & Chayes, D.N. (1996). Improved Processing of Hydrosweep Multibeam Data on the R/V Maurice Ewing. Marine Geophysical Researches, 18, 631-650.

Cirac, P. et al. (2001). Canyon of Capbreton: new morphostructural and morphosedimentary approaches. First results of the ITSAS cruise. Earth and Planetary Sciences, 332, 447-455.

Clark, J.D. & Pickering, K.T. (1996). Submarine channels; Processes and Architecture (p. 231). London: Vallis Press.

GEBCO (2003) IHO-UNESCO, General Bathymetric Chart of the Oceans, Digital Edition, 2003, www.ngdc.noaa.gov/mgg/gebco.

Damuth, J.E. (1994). Neogene gravity tectonics and depositional processes on the deep Niger Delta continental margin. Marine and Petroleum Geology, 11, 320-346.

Damuth, J.E. & Kumar, N. (1975). Amazon cone: Morphology, sediments, age and growth pattern. Geological Society of America Bulletin, 86, 873-878.

Deptuck, M.E., Steffens, G.S., Barton, M. & Pirmez, C. (2003). Architecture and evolution of upper fan channel-belts on the Niger Delta slope and in the Arabian Sea. Marine and Petroleum Geology, 20, 649-676.

Diester-Haass, L. & Chamley, H. (1982). Oligocene and Post-Oligocene History of Sedimentation and Climate off Northwest Africa (DSDP Site 369). In: U. von Rad, K. Hinz, M. Sarnthein & E. Seibold (Eds.), Geology of the Northwest African Continental Margin (pp. 529-544). Berlin: Springer-Verlag.

Flicoteaux, R., Lappartient, J.-R. & Trenous, J.-Y. (1975). Contribution a l'etude du Tertiare du bassin senegalo-mauritanien (au sud de la vallee du Senegal). Evolution paleogeographique et structurale. 3e Reunion and Sci. Terre., Montpellier, p. 150.

Flood, R.D. & Damuth, J.E. (1987). Quantitative characteristics of sinuous distributary channels on the Amazon deep-sea fan. Geological Society of America Bulletin, 98, 728-738.

Flood, R.D., Manley, P.L., Kowsmann, R.O., Appi, C.A. & Pirmez, C. (1991). Seismic facies and Late Quaternary growth of Amazon submarine fan. In: P. Weimer, M.H. Link (Eds.) Seismic Facies and Sedimentary Processes of Modern and Ancient Submarine Fans (pp. 415-433). New York: Springer-Verlag.

Friedmann, S.J. (2000). Recent advances in deep-water sedimentology and stratigraphy using conventional and high resolution 3-D seismic data., GeoCanada 2000, Calgary, Alberta.

Giresse, P., Barusseau, J.P., Causse, C. & Diouf, B., (2000). Successions of sea-level changes during the Pleistocene in Mauritania and Senegal distinguished by sedimentary facies study and U/Th dating. Marine Geology, 170, 123-139.

Garfunkel, Z. (1986). Review of oceanic transform activity and development. Journal of the Geological Society, London, 143, 775-784.

Hagen, R.A., Bergersen, D.D., Moberly, R. & Colbourn, W.T. (1994). Morphology of a large meandering submarine canyon system on the Peru-Chile forearc. Marine Geology, 119, 7-38.

Hagen, R.A., Vergara, H. & Naar, D.F. (1996). Morphology of San Antonio submarine canyon on the central Chile forearc. Marine Geology, 129, 197-205.

Holdbrook, J. & Schumm, S.A. (1999). Geomorphic and sedimentary response to tectonic deformation: a brief review and critique of a tool for recognizing subtle epeirogenic deformation in modern and ancient settings. Tectonophysics, 305, 287-306.

Holz, C (2005). Climate-induced variability of fluvial and aeolian sediment supply and gravity-driven sediment transport off Northwest Africa. PhD Dissertation. Dept. of Geosciences, University of Bremen (pp. 116). http://elib.suub.uni-bremen.de/publications/dissertations/E-Diss1205_Diss_Holz.pdf

Hübscher, C., Spieß, V., Breitzke, M. & Weber, M.E. (1997). The youngest channel-levee system of the Bengal fan: results from digital sediment echosounder data. Marine Geology, 141, 125-145.

Jacobi, R.D. & Hayes, D.E. (1982). Bathymetry, Microphysiography and Reflectivity Characteristics of the West African Margin Between Sierra Leone and Mauritania. In: U. von Rad, K. Hinz, M. Sarnthein & E. Seibold (Eds.), Geology of the Northwest African Continental Margin (pp.182-212). Berlin: Springer-Verlag.

Jansa, L.F. & Wiedmann, J. (1982). Mesozoic-Cenozoic development of the Eastern North American and Northwest African Continental Margins: a comparison. In: U. von Rad, K. Hinz, M. Sarnthein & E. Seibold (Eds.), Geology of the Northwest African Continental Margin (pp. 215-269). Berlin: Springer-Verlag.

Klaucke, I. & Hesse, R. (1996). Fluvial features in the deep sea: new insights from the glacigenic submarine drainage system of the Northwest Atlantic Mid-Ocean Channel in the Labrador Sea. Sedimentary Geology, 106, 223-234.

Krastel, S. et al. (2004). Cap Timiris Canyon: A newly discovered channel-system off Mauritania. EOS, Transactions, 45/42, (pp. 417, 423).

Lancaster, N. et al. (2002). Late Pleistocene and Holocene dune activity and wind regimes in the western Sahara Desert of Mauritania. Geological Society of America Bulletin, 30(11), 991-994.

Lancelot, Y. & Seibold, E. (1978). The evolution of the central Northeastern Atlantic - Summary of results of DSDP Leg 41. Initial Reports of the Deep Sea Drilling Project. Vol 41, (pp. 1215-1245). Washington, DC: US Government Printing Office.

Laursen, J. & Normark, W.R. (2002). Late Quaternary evolution of the San Antonio Submarine Canyon in the central Chile forearc (~33°S). Marine Geology, 188, 365-390.

Lewis, K.B. & Barnes, P.M. (1999). Kaikora Canyon, New Zealand: active conduit from near-shore sediment zones to trench-axis channel. Marine Geology, 162, 39-69.

McHugh, C.M.G., Ryan, W.B.F., Eittreim, S. & Reed, D. (1998). The influence of San Gregorio fault on the morphology of Monterey Canyon. Marine Geology, 146, 63-91.

McHugh, C.M.G., Damuth, J.E. & Mountain, G.S. (2002). Cenozoic mass-transport facies and their correlation with relative sea-level change, New Jersey continental margin. Marine Geology, 184, 295-334.

Pichevin, L. et al. (2003). The Golo submarine turbidite system (east Corsica margin): morphology and processes of terrace formation from high-resolution seismic reflection profiles. Geo Marine Letters, 23,117-174.

Pirmez, C., & Flood, R. D. (1995). Morphology and structure of Amazon Channel. In R.D. Flood, D.J.W. Piper & A. Klaus (Eds.), Proceedings of Ocean Drilling Program. Initial reports. Vol. 155 (pp. 23-45).

Pirmez, C., & Imran, J. (2003). Reconstruction of turbidity currents in Amazon Channel. Marine and Petroleum Geology, 20, 823-849.

Posamentier, H.W. (2003). Depositional elements associated with a basin floor channel-levee system: case study from Gulf of Mexico. Marine and Petroleum Geology, 20, 677-690.

Posamentier, H.W. & Kolla, V. (2003). Seismic geomorphology and stratigraphy of depositional elements in deep-water settings. Marine and Petroleum Geology, 20, 677-690.

Rona, P. (1971). Bathymetry off central northwest Africa. Deep-Sea Research, 18, 321-327.

Sarnthein, M. et al. (1982). Atmospheric and Oceanic Circulation Patterns off Northwest Africa During the Past 25 Million Years. In: U. von Rad, K. Hinz, M. Sarnthein & E. Seibold (Eds.), Geology of the Northwest African Continental Margin (pp. 545-604). Berlin: Springer-Verlag.

Schulz, H.D. & participants, C. (2003). Report and preliminary results of METEOR Cruise M 58/1, Dakar-Las Palmas, 15.04.2003-12.05.2003. 215, Universität Bremen, Bremen, p. 186.

Schumm, S.A., Mosley, M.P. & Weaver, W.E. (1987). Experimental Fluvial Geomorphology (p. 413). New York: Wiley and Sons.

Schumm, S.A., Rutherfurd, I.D. & Brooks, J. (1994). Pre-cutoff morphology of the lower Mississippi River. The Variability of Large Alluvial Rivers (pp.13-44). New York: American Society of Civil Engineers Press.

Stow, D.A.V. & Mayall, M. (2000). Deep-water sedimentary systems: New models for the 21st Century. Marine and Petroleum Geology, 17, 125-135.

von Rad, U. & Tahir, M. (1997). Late Quaternary sedimentation on the outer Indus shelf and slope (Pakistan): evidence from high resolution seismic data and coring. Marine Geology, 138, 193-236.

Vörösmarty, C.J., Fekete, B.M., Meybeck, M. & Lammers, R.B. (2002). Global system of rivers: Its role in organizing continental land mass and defining land-to-ocean linkages. Global Biogeochemical Cycles, 14(2), 599-621.

Weaver, P.P.E., Wynn, R.B., Kenyon, N.H. & Evans, J. (2000). Continental margin sedimentation, with special reference to north-east Atlantic margin. Sedimentology, 47 (Suppl. 1), 239-256.

Wefer, G. & Fischer, G. (1993). Seasonal patterns of vertical particle flux in equatorial and coastal upwelling areas of the eastern Atlantic. Deep-Sea Research, 40(8), 1613-1645.

Wessel, P. & Smith, W.H.F. (1998). New, improved version of the Generic Mapping Tools Released. EOS, Transactions, AGU, 79, (p. 579).

Williams, C.A., Hill, I.A., Young, R. & White, R.S. (1990). Fracture zones across the Cape Verde Rise, NE Atlantic. Journal of the Geological Society Geology, London, 147, 851-857.

Wissmann, G. (1982). Stratigraphy and Structural Features of the Continental Margin Basin of Senegal and Mauritania. In:

U. von Rad, K. Hinz, M. Sarnthein & E. Seibold (Eds.), Geology of the Northwest African Continental Margin (pp. 160-181). Berlin: Springer-Verlag.

Wynn, R.B., Masson, D.G., Stow, D.A.V. & Weaver, P.P.E. (2000). The Northwest African slope apron: a modern analogue for deep water systems with complex seafloor topography. Marine and Petroleum Geology, 17, 253-265.

# 3 Mauritania Slide Complex: Morphology, seismic characterisation and processes of formation

Andrew A. Antobreh and Sebastian Krastel

*To be submitted to International Journal of Earth Sciences.*

## 3.1 Abstract

Recently acquired Parasound sediment echosounder data and high resolution multi-channel seismic reflection profiling have afforded a more detailed investigation of the Mauritania Slide Complex. The slide is more complex than previously reported, and has affected an area in the order of 34,000 km² between ~600 m - >3500 m water depths. The ovate-shaped slide displays a long run-out distance >300 km. Higher sediment flow mobility may have been induced in the northern parts of the slide by the bounding Cape Verde Rise and canyon systems. In addition widespread diapiric growths have enhanced disintegration of overlying contouritic sediments. Slide formation was pre-conditioned mainly by uninterrupted deposition of upwelling-induced organic-rich sediments in an open slope environment which gave rise to rapid accumulation of poorly consolidated bedded sediments intercalated with thin weak layers.

Our data interpretation suggests that the stages of slide development were characterised by multiple failure events. The sediment failures probably occurred mainly as retrogressive sliding which exploited widespread weak layers as glide planes. The study suggests that excess pore pressures, resulting from decayed organic matter and/or sea level fluctuations, could be the most important trigger mechanism for slide formation. However, seismic shaking associated with the Cape Verde Islands may have played a mostly complementary or, at one time or the other, a leading role in triggering the sediment failures. Diapiric growths have locally triggered minor instability events which resulted in remobilizing of pre-existing debris flows as well as translational sliding. The combined activities of all these triggering factors are the most like cause of the complex morphology of the Mauritania Slide Complex.

Keywords: submarine slide, diapiric growths, contourites, retrogressive sliding, weak layers, excess pore pressure, trigger mechanism.

### 3.2 Introduction

Over the last couple of decades, sustained research efforts, driven by improved geophysical mapping methods, are gradually establishing that submarine slides occur globally and affect all types of continental margins including passive, e.g. the eastern Scotian margin (Piper and Ingram, 2003), the New Jersey continental margin (McHugh et al., 2002) and the Norwegian-Greenland Sea continental margins (Bugge, 1983; Vorren et al., 1998) as well as active margins, e.g. NE Mediterranean Sea (Lykousis et al., 2002) and Japan Sea (Lee et al., 1996). Along the eastern Atlantic continental margins, submarine slides have been recognised in various dimensions ranging from relatively smaller slides <1000 km², e.g. the Afen Slide off northwest of Shetlands Islands (Wilson et al., 2004) and the Gebra Slide off the Trinity Peninsula margin, Antarctica (Imbo et al., 2003) to giant slides affecting areas > 10 000 km², e.g. the Canary Slide (Canals et al., 2004) and the Storegga Slide off western Norway (Bugge, 1983; Haflidason et al., 2004, Canals et al., 2004).

Submarine slides constitute one of the most important mechanisms for mass sediment movement from shallow- to deep-water marine environments and also for shaping continental margins (Hampton et al., 1996; McAdoo, 2000; Casas et al., 2003). Because of their widespread and often episodic nature, mass sediment movement events are perceived as being important components of the modern stratigraphic record, and have been studied in connection with global climatic cycles, including sea level changes (e.g. McHugh et al., 2002). In recent years, the importance of submarine slides has become very crucial in geo-hazard assessment studies for engineering and environmental projects connected with offshore economic resource exploitation and installations, especially as interest of the oil industry moves further into the deep sea (Baraza et al., 1999, Piper and Ingram, 2003). In addition, the oil industry finds further motivation in studying submarine slides because slides are capable of modifying the architectural and, hence, sedimentological characteristics of submarine channel systems and channel-levee complexes which are often connected with potential deep sea hydrocarbon reservoirs. Furthermore, being large-scale mass sediment failure events, submarine slides are capable of displacing large volumes of water and hence have, in recent years, been studied towards evaluating their tsunami generation risks to coastal communities (e.g., Dawson, 1999; Fryer et al., 2003; Trifunac et al., 2003; Fine et al., 2004).

Several studies have suggested that continental margins which receive high rates of sediment accumulation are especially prone to mass sediment failures, e.g. the Uruguayan continental margin (Klaus and Ledbetter, 1988). The rapid sediment build-up gives rise to huge volumes of undercompacted sediment packages which may be rendered highly unstable

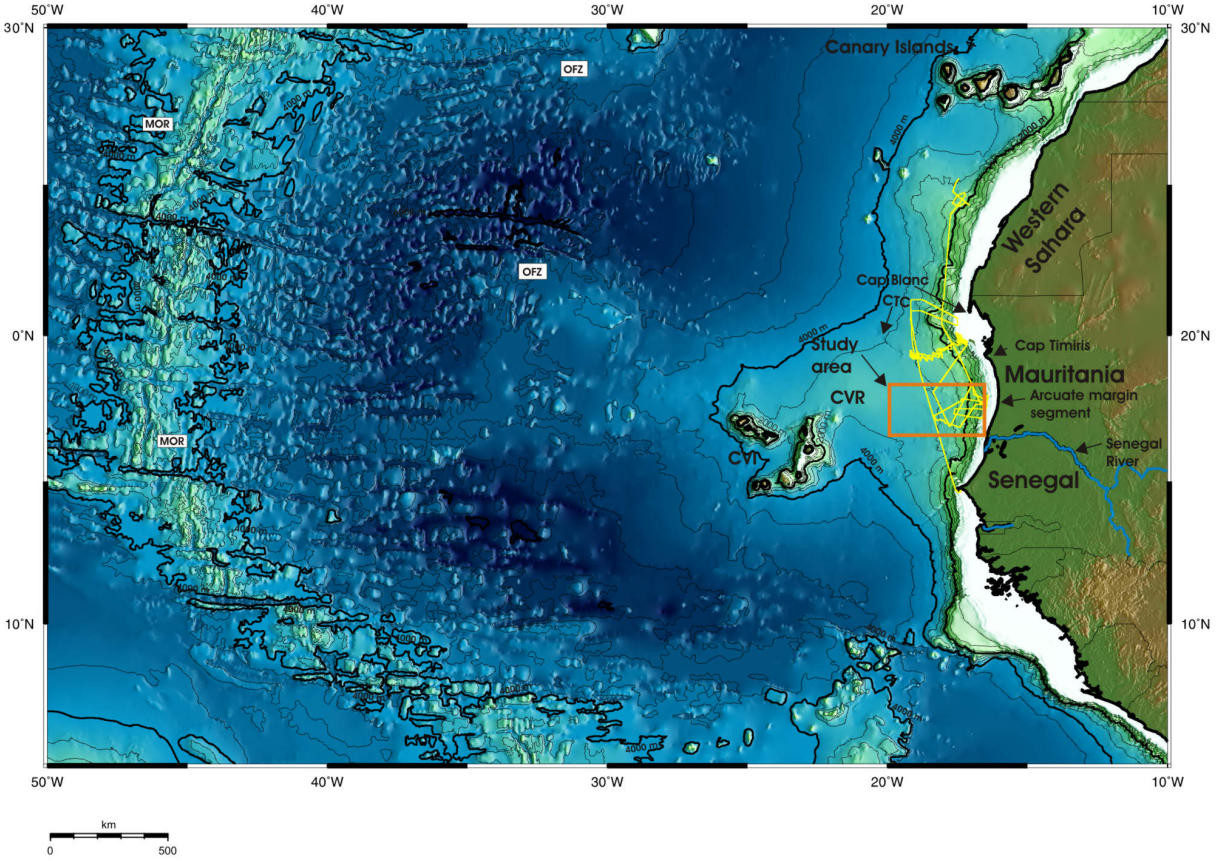


***Figure 3.1:*** *General bathymetry of NW African continental margin (Gebco, 2003) showing the location of the study area (in box) in relation to regional structure and bathymetry (contours at 500 m intervals). RV Meteor Cruise M58/1 track lines are shown in yellow lines. The study area is located off a giant arcuate segment of the Mauritanian margin. OFZ = oceanic fracture zones, MOR = Mid Oceanic Ridge, CVI = Cape Verde Islands, CVR = Cape Verde Rise, CTC = Cap Timiris Canyon.*

by the presence of increased pore pressure from entrapped water and/or shallow gas generated from decaying buried organic matter. In addition, changes in sedimentation rates and types of sediment resulting from climatic controls may lead to the formation of lithologically weak sediment layers which facilitate sediment failure by serving as glide planes e.g. as reported in the Barents Sea (Laberg and Vorren, 1996) and the Aegean Sea (Lykousis et al., 2002). Furthermore, the often resulting slope oversteepening may also contribute to sediment instability (Hampton et al., 1996; Canals et al., 2004) though submarine slide events, quite unlike aerial slides, are known to occur along slope gradients as low as <1° (Hampton et al., 1996). In addition to excess pore pressures and slope oversteepening, other factors commonly cited as the immediate trigger mechanism for the mass sediment failure events include earthquakes, decay of gas hydrates, diapirism and tectonic movements, or a combination of two or more of them (e.g. Bugge, 1983; Laberg and Vorren, 1996; Haflidason et al., 2004; Canals et al., 2004).

A number of large mass sediment movement events have been documented along the continental margin off NW Africa (e.g. Jacobi and Hayes, 1982; Gee et al., 2001; Wynn et al., 2000). However, only a few of them, notably, the Sahara Debris Flow (Gee et al., 1999) and the numerous slides on the flanks of the Canary Islands (Krastel et al., 2001; Masson et al., 1998) have been mapped and studied in detail. The Mauritania Slide Complex was previously mapped and described by Jacobi (1976) following its discovery offshore Mauritania by Seibold and Hinz (1974). Based primarily on 3.5 kHz profiles, Jacobi (1976) estimated that the Mauritania Slide Complex covered an area of ~34,300 km². This areal dimension of the Mauritania Slide Complex places it as one of the largest submarine failure events ever mapped along the NE Atlantic margin, perhaps next in size only to the Storegga Slide, 95,000 km² (Bugge, 1983; Haflidason et al., 2004), the Saharan Debris Flow, 48,000 km² (Jacobi and Hayes, 1982) and the Canary Slide, 40,000 km² (Masson et al., 1998). Jacobi and Hayes (1982) provided a general overview of seafloor reflectivity characteristics of the margin between 3° and 23°N, which included the area offshore Mauritania. Since these previous studies of the Mauritania Slide Complex were based on sparsely distributed data, and in connection with more regionally-based investigations, important questions regarding, among others, the internal architecture of the slide, slide dynamics and trigger mechanisms as well as origin and age of slide formation have not been properly resolved.

The main objective of RV Meteor Cruise M 58/1 expedition in April/May 2003 (Fig. 3.1) was to study upwelling and sedimentation processes off NW Africa (Schulz et al., 2003). During the cruise, new and more extensive Parasound echo-sounder profiling as well as high resolution multi-channel seismic reflection (MCS) data were collected over the Mauritania Slide Complex to provide a better framework for studying the slide. In this study, we employ primarily the newly acquired Parasound and MCS data to describe and analyse in detail the main morphological components of the slide. In addition, the study intends to evaluate the scale of destabilization caused by the slide and also identify or suggest possible slide release mechanisms. The study will also investigate the relationships between slide development and regional sedimentation processes as well as influence from structural features in the margin, including the Cape Verde Rise, canyon systems and diapirism.

## 3.3 Geological setting and oceanography

### *3.3.1 Margin physiography*

The Mauritania Slide Complex lies between latitudes 16° 40’ - 18° 20’ N, and is centrally located off the giant arcuate segment of the Mauritanian coastline which extends

from Cap Timiris in the north to offshore northern Senegal in the south (Fig.3.1). The shelf break in this segment occurs at a water depth of 50 - 80 m. The shelf is relatively narrow within the arcuate segment, typically between ~25 - 40 km wide, but widens up to ~100 km just off north of Cap Timiris following an abrupt seaward offset in the shelf break. The continental slope displays gradients which vary between 1° - 3°. The shelf and slope areas to the immediate north of the Mauritania Slide Complex are deeply incised by a system of canyons and gullies including the Tiolit Canyon (Wissmann, 1982) and farther to the north, the Cap Timiris Canyon, a prominent canyon system recently discovered off the latitude of Cap Timiris (Schulz et al., 2003; Krastel et al., 2004). The entire continental rise off Mauritania is very broad, and occurs at water depths of between 2000 – 2500 m where slope angles are typically <1°. Off the arcuate segment, however, the rise is dominated by the extensive Cape Verde Rise which gradually elevates into the Cape Verde Islands further seawards. The northern and southern boundaries of this group of volcanic islands possibly trace directly into major fracture zone extensions (Jacobi and Hayes, 1982).

### *3.3.2 Structural setting*

Structurally, the Mauritania Slide Complex is located within the depocenter of the large Senegal Mauritania Basin, one of the series of marginal basins emplaced along the NW African margin in response to the Mesozoic opening of the Atlantic ocean (Jansa and Wiedemann, 1982; Wissmann, 1982). Initial opening of the basin was accompanied by evaporite deposition within a narrow elongate zone between 16° N and 19° N. The basin is filled by a thick succession of Mesozoic-Cenozoic terrigenous to shallow marine sediments which are known to attain maximum depths of more than 10 km below the lower continental slope off Mauritania (Wissmann, 1982). Earliest indications of mass wasting processes along the slope are provided by the presence of slumps and turbidites observed in Early Miocene deposits. After a prevalent tropical climate along the margin during the Middle Eocene, a more arid condition began to emerge during the end of Eocene and within Oligocene time. Following the end of a Tertiary humid climate, a long period of arid Quaternary sedimentation known as the ‘Continental terminal’ formation emerged (Jansa and Wiedemann, 1982; Wissmann, 1982).

### *3.3.3 Sources of sediment supply to the margin*

During the last 20 000 years, the margin has been fed huge quantities of offshore wind-blown sediment from the adjacent Sahara Desert (Sarnthein et al., 1982). Currently,

offshore wind-transported sediment remains the main source of terrigenous sediment input into the margin, and is estimated to supply about 50 x $10^6$ tons of eolian sediment per year over a 1000 km broad zone (Koopman, 1981). In addition, the margin is the site of rapid sediment accumulation resulting from upwelling-induced high productivity.

Though the margin receives no significant fluvial sediment supply at present, a study of potential paleo-drainage patterns off NW Africa by Vörösmarty et al. (2002) indicates that the Cap Timiris area once constituted the estuary of a major ancient river system which is now extinct, hence suggesting that part of the margin may have previously received significant fluvial sediment supplies. Furthermore, the Senegal River is believed to have entered the coast near 18° 30'N during Miocene/Pliocene time, thereby supplying large quantities of sediment which are thought to have triggered salt halokinesis in the area (Wissmann, 1982). The area of salt diapirs lies between 16° - 19° N (Wissman, 1982) and includes the location of the Mauritania Slide Complex (Figs. 3.2 and 3.3). Currently, the Senegal River enters the coast in the south near latitude 16° 05'N, i.e. slightly to the south of the slide area, and its sediment discharges are swept southwards by nearshore currents (Seibold and Hinz, 1974). Hence, the river is at present unlikely to contribute any significant sediment inputs into the slide area.

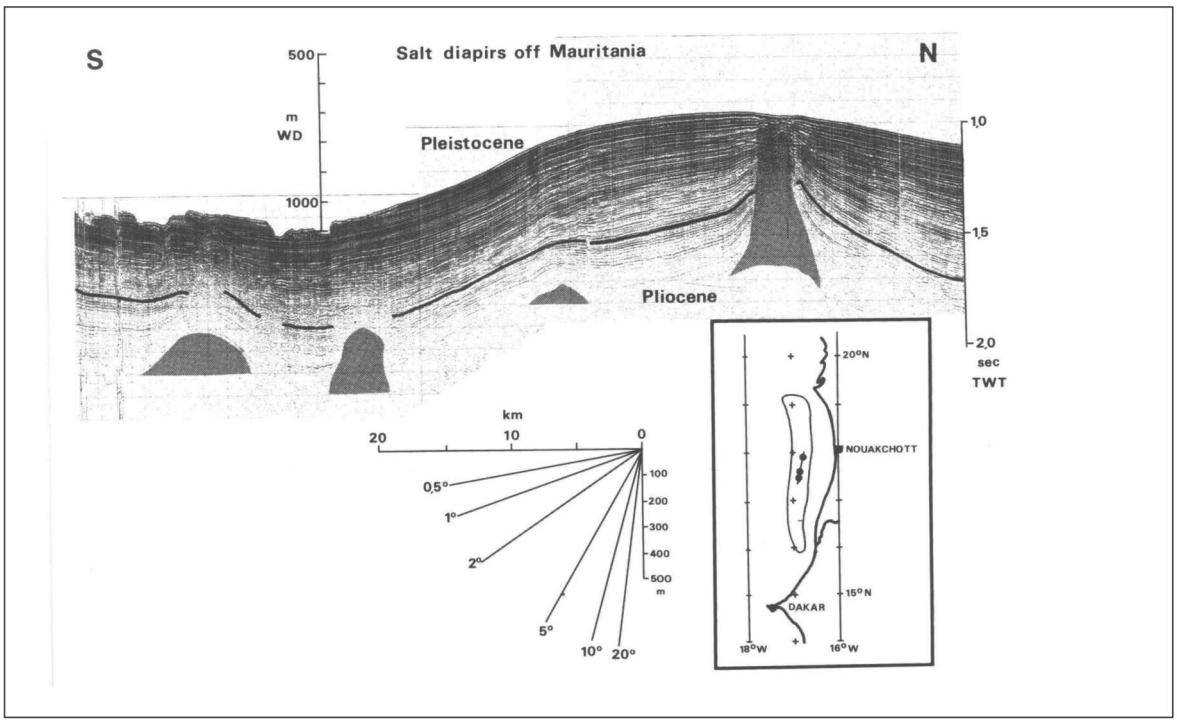


***Figure 3.2:*** *Seismic reflection profile METEOR 25-E 2 in the elongate zone of salt diapirs off Mauritania. Thickened reflector is interpreted to separate Pliocene from Pleistocene sediments (after Wissman, 1982). Location of profile is indicated in Fig. 3.3 as well.*

### *3.3.4 Oceanography*

Along the outer shelf and slope areas of the Mauritanian margin, i.e. <200 m water depth, the current regime is controlled by the southward-flowing Canary Current which splits up into two on reaching Cap Blanc. From here, the dominant fraction is diverted away from the coast to the southwest, whilst the minor fraction continues further southwards where it is transformed into the Guinea Current (Sarnthein et al., 1982). Below the Canary Current, i.e. between ~150 – 400 m, the current regime is controlled by the northward-flowing South Atlantic Central Water (SACW) which in turn is underlain by the southward-flowing North Atlantic Central Water (NACW) operating down to ~600 – 700 m water depths. The deeper waters are dominated by the southward-flowing North Atlantic Deep Water (NADW), which operates down to ~3500 – 4000 m water depths, and the underlying northward-flowing Antarctic Bottom Water (AABW). Present current velocities of the deep waters are thought to be generally weak, i.e. <5 cm/s, but this may increase significantly up to ~20 cm/s in areas where the current circulation is focussed by seafloor morphology (Lonsdale, 1982).

## 3.4 Data and methods

The Parasound and MCS data used for this study were simultaneously acquired during R/V Meteor Cruise M58/1 in April 2003 as part of a larger marine geophysical survey (Fig. 3.1) undertaken by the Research Center Ocean Margins (RCOM) of the University of Bremen in order to study upwelling and sedimentation processes offshore northwest Africa. Data coverage over the Mauritania Slide Complex analysed for this study include more than 1200 km of Parasound profiles and ~900 km of MCS profiles. The areas covered comprised the outer shelf and the headwall region in the slope areas down to the continental rise and ranged from 200 m to >3500 m water depths.

### *3.4.1 The Parasound system*

The Parasound system (Grant and Schreiber, 1990) is a hull-mounted high frequency sediment echosounder that utilizes the so-called parametric effect to generate an operational signal of 4 kHz which is focused within a cone of opening angle of 4°. This results in a footprint diameter of ~7% of the water depth, which affords better horizontal resolution than conventional 3.5 kHz systems. In addition, the broader signal bandwith gives a better vertical resolution, which is in the order of a few decimeters. Depending on the type of sediment and attenuation, depth penetration may vary between 0 - 200 m. The ParaDigMA system (Spiess,

1993) was used to digitally record and store the data in a compressed SEGY format. A band pass frequency filter of 2.0 – 6.0 kHz was applied before display.

### *3.4.2 The high resolution MCS system*

The MCS data were acquired using a 1.7 l GI-Gun seismic source shot at a distance of ~30 m. The gun was operated with a high pressure air of 150 bar (2150 PSI). A 450-m-long Syntron streamer, equipped with separately programmable hydrophone subgroups, was employed to receive the data, whilst for data recording 36 groups of 6.25 m length at a group distance of 12.5 m were used. Digital recording of the data was carried out at a sampling frequency of 4 kHz over 3 s. Positioning was based on GPS (Global Positioning System). The MCS data were processed using a combination of 'in-house' and the 'Vista' (Seismic Image Software Ltd) softwares, and standard procedures including trace editing, setting up geometry, static and delay corrections, velocity analysis, normal moveout corrections, bandpass frequency filtering (frequency content: 55/110 – 600/800), stack and time-migration were employed. A CMP spacing of 10 m was applied throughout.

## 3.5 Echosounder characteristics and seafloor morphology of the Mauritania Slide Complex

### *3.5.1 Echosounder characteristics*

The Parasound data allow us to describe the main architectural elements of the slide under two major morphological divisions based primarily on a major change in seafloor slope gradient accompanied by a downslope variation in seafloor acoustic characteristics. The divisions are: (i) the headwall and the proximal slide areas, and (ii) the main debris flow depositional area.

#### *3.5.1.1 The headwall and proximal depositional areas*

Parasound dip-profiles (e.g. Figs. 3.4 and 3.5) which reach out from the outer shelf and upper slope areas downslope into the main slide area, show that sediments shallower than 600 m have generally not been affected by sliding. The unaffected sediments are acoustically characterised by sharp prolonged flat, but locally undulating, seafloor reflections. The dip profiles (e.g. Figs. 3.4 and 3.5) display a feature acoustically imaged as a sharp rise in seafloor relief to narrow isolated transparent peaks, up to 75 m high occurring between 450 – 550 m water depths. These peaks have been confirmed by gravity coring to consist of carbonate

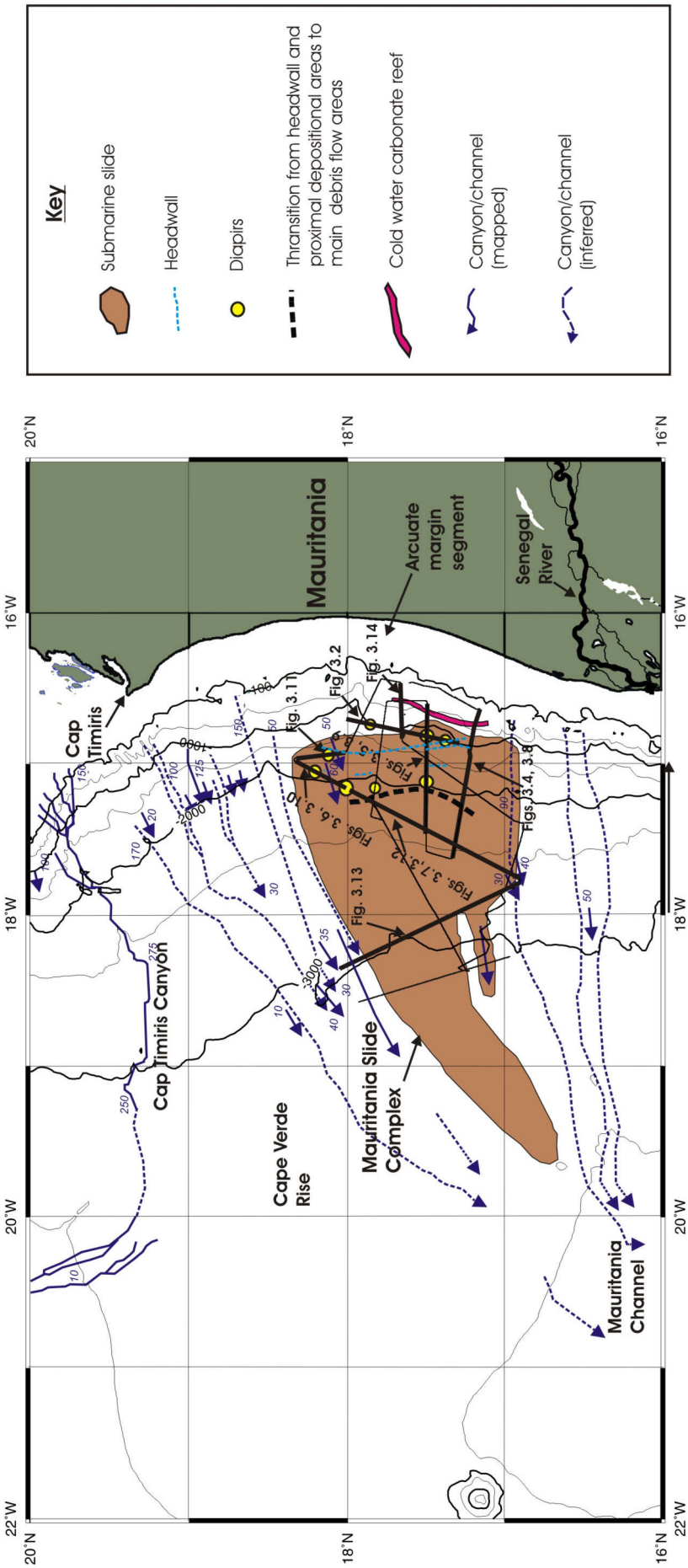


***Figure 3.3:*** *Detailed bathymetry of the Mauritanian margin (Gebco, 2003) showing the seafloor map of the Mauritania Slide Complex derived mainly from Parasound data from RV Meteor Cruise M58/1. Map of features outside the Parasound data coverage area was compiled from published data (i.e. Jacobi, 1976; Jacobi and Hayes, 1982). Parasound and MCS survey lines analysed for the study are shown in solid black straight lines. Locations of Parasound and MCS profiles presented in the study are shown in thick solid black lines.*

mounds inhabited by fresh water corals (Schulz et al., 2003; Colman et al., 2004). No sliding activity is observed upslope of the feature.

In most parts of the slide, headwall scars are imaged as a series of distinct steps in morphology with heights ranging from <25 m to 100 m above the seafloor. This is especially the case in the southern parts (e.g. Fig. 3.4), where the scars occur between 800 m - 1150 m water depths. However, in the middle part of the slide, the uppermost headwalls appear to be associated with a number of detached blocks, up to 40 m thick and some with widths >4 km, between 600 - 1400 m water depths (Fig. 3.5). The seafloor reflections of these blocks are acoustically characterised by very sharp prolonged returns, with very faint or no clear sub-bottom reflectors. The lower headwall scars are step-like, and occur between 1200 - 1400 m water depths (Fig. 3.5).

In the northern parts of the slide, especially towards its northeastern boundary, the headwall area is dominated by several canyons and gullies which have given rise to a number of isolated sediment blocks (Fig. 3.6). Some of these blocks show layered internal structure while others are acoustically transparent. The largest of the canyons attain depths up to 100 m or more and widths up to 3 km (Fig. 3.6). In general, the canyon floors do not show any significant debris flow infill. In the uppermost slope area, towards the northern end of Parasound Profile GeoB03-046a (Fig. 3.6), a sidewall scar, ~40 m high which is associated upslope with undisturbed sediments, is seen near 1775 m water depth. The profile also shows a distal scar occurring near 2100 m water depth close to the southern end, but this clearly cuts across a pre-existing debris flow deposit which is ~40 m thick.

In most of the profiles (e.g. Figs. 3.4 – 3.6) the deposits occurring immediately beneath the headwall scars show highly blocky structure, and are acoustically characterised by irregular hyperbolae of weak to strong surface reflections with vertices often attaining relief up to 30 m high (Fig. 3.4b). These proximal debris flows are commonly underlain by clearly visible prolonged strong to weak sub-bottom reflectors (Fig. 3.6). The thickness of these deposits is usually <25 m but may gradually increase downslope up to ~ 40 m or more. The headwalls commonly occur between 600 – 1400 m water depths where slope gradients are typically up to ~2.5° (Figs. 3.4 and 3.5). However, the headwall scars themselves may attain gradients up to ~8°. The proximal depositional areas extend downslope to between ~2100 - 2150 m water depths (Figs. 3.4 and 3.6), so that the overall average slope gradient for the headwall and proximal depositional areas, is typically ~1.9°.

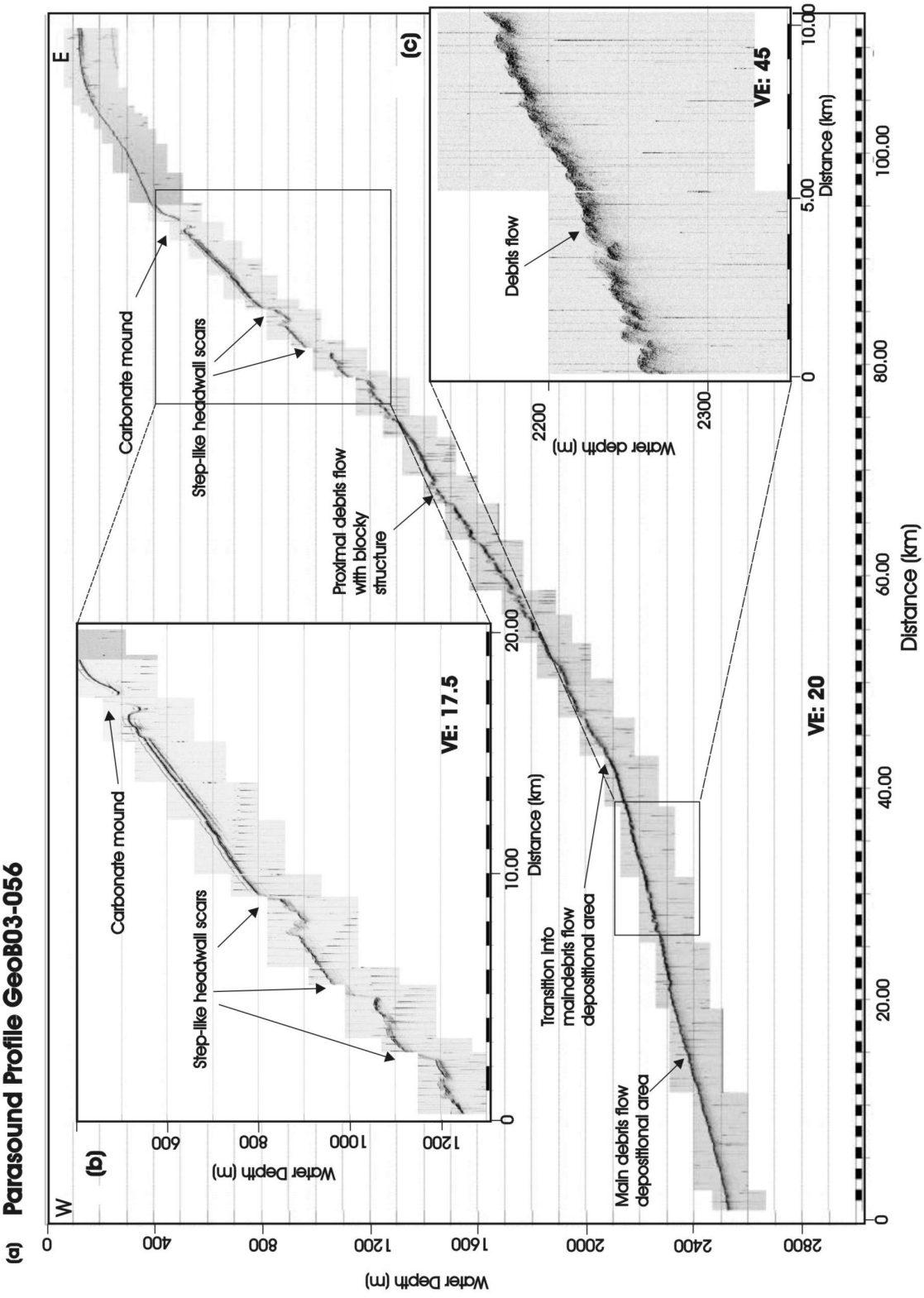


***Figure 3.4:*** *(a) Parasound dip profile GeoB03-056 recorded across the southern part of Mauritania Slide Complex. The profile cuts across the headwall and proximal depositional areas as well as the transition into the main debris flow depositional area. Location of the profile is shown in Fig. 3.3. (b) Close-up of slope area showing headwall scars and immediate vicinity. (c) Close-up showing debris flow in main depositional area.*

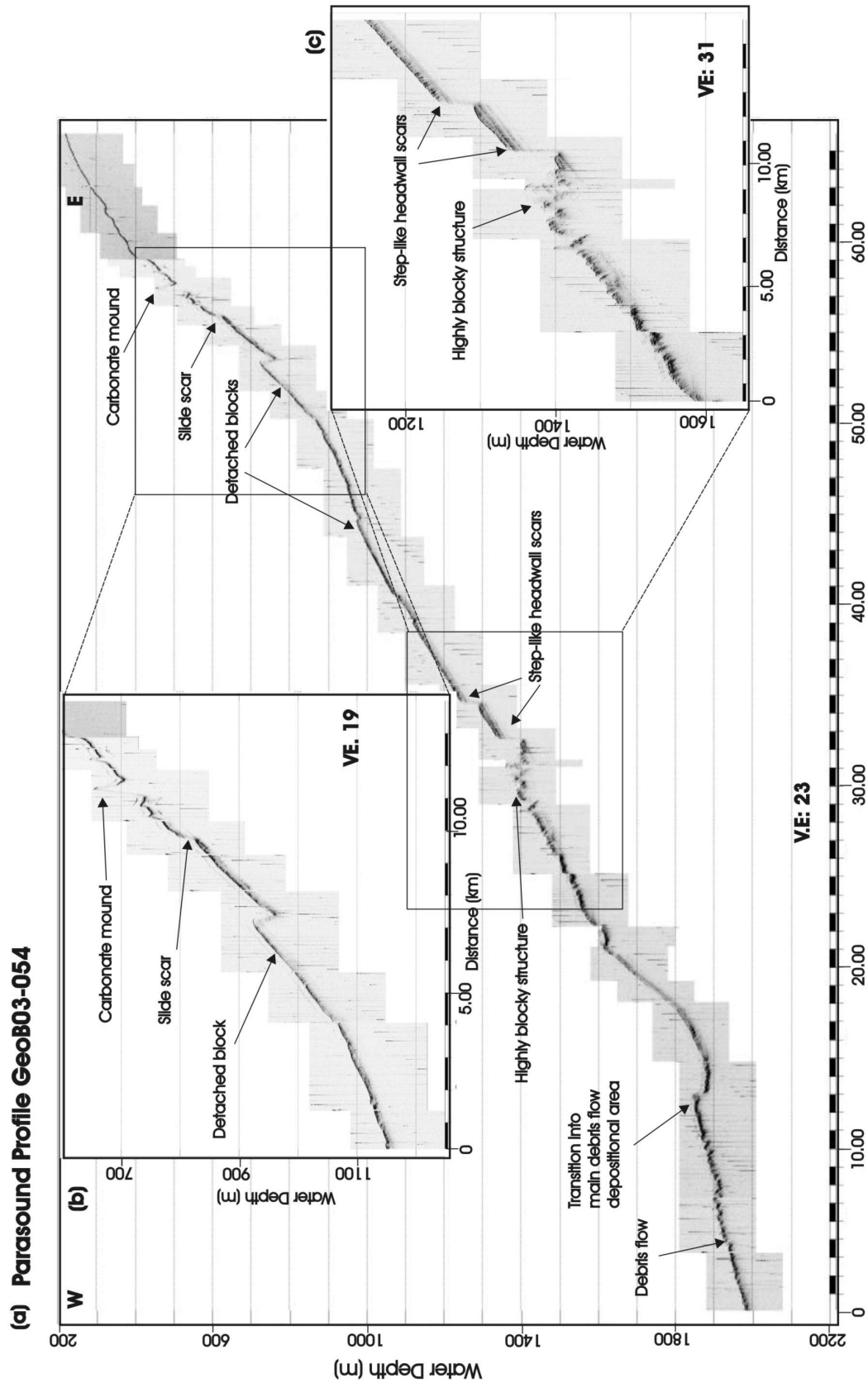


***Figure 3.5:*** *(a) Parasound dip profile GeoB03-054 recorded across the middle part of Mauritania Slide Complex. The profile cuts across the headwall and proximal depositional areas as well as the transition into the main debris flow depositional area. Detached blocks are seen in the upper and middle slope areas. Location of the profile is shown in Fig. 3.3. (b) Close-up of the upper slope area showing slide scar and detached block. (c) Close-up showing headwall scars.*

### *3.5.1.2 Main debris flow depositional area*

Downslope ~2100 - 2150 m water depths, the slope gradient is drastically reduced from the average of ~1.9° observed in the headwall and depositional proximal areas, to <1°. No scars are seen deeper than this depth but rather debris flow deposition becomes laterally extensive (Figs. 3.4 – 3.7). The deposits are characterised mostly by prolonged seafloor reflections which may, however, locally appear blocky (Fig. 3.7). This major reduction in slope gradient, which is accompanied by a change in acoustic character, marks the transition into a dominantly debris flow depositional regime which characterises the main depositional area of the slide in most of our profiles (e.g. Figs. 3.4 – 3.7).

Profile GeoB03-046b (Fig. 3.7) which cuts across the main depositional area in the NE - SW direction, shows that debris flow deposition extends from the northeast more than 120 km across the length of the profile, and is only delimited in the southwestern end by a small channel-levee system. In places, the debris flow deposits are underlain by prolonged sub-bottom reflectors which grow weaker downslope and eventually fade out. The debris flow deposits display widths from <25 m up to ~45 m. They appear to be composed of several units which lie side by side and commonly onlap one another, especially within the northeastern half of the profile (Fig. 3.7). Towards the distal parts of the slide, the seafloor reflections become more prolonged, and no sub-bottom reflectors are clearly visible, except in the vicinity of the channel-levee system that bounds the debris flows in the southwestern end of the profile. The presence of debris flow facies at the floor of the channel indicates that some of the slide material has travelled down the channel. However, the particularly well-stratified southern levee facies show that slide material has not moved further southward beyond the channel-levee system.

### *3.5.2 Seafloor morphology of the Mauritania Slide Complex*

We present a newly compiled map of the seafloor morphology of the Mauritania Slide Complex (Fig. 3.3), based on the mapping of slide features identified in the Parasound data. However, the most distal part of the slide that was not covered by our Parasound profiling, has been incorporated from published data by Jacobi (1976) and Jacob and Hayes (1982) into the map. The map shows that the slide has affected an area in the order of 34,000 km², which is generally in agreement with that previously reported by Jacobi (1976). The affected area includes the upper slope area, from water depths ~600 m, down to the rise at water depths >3500 m.

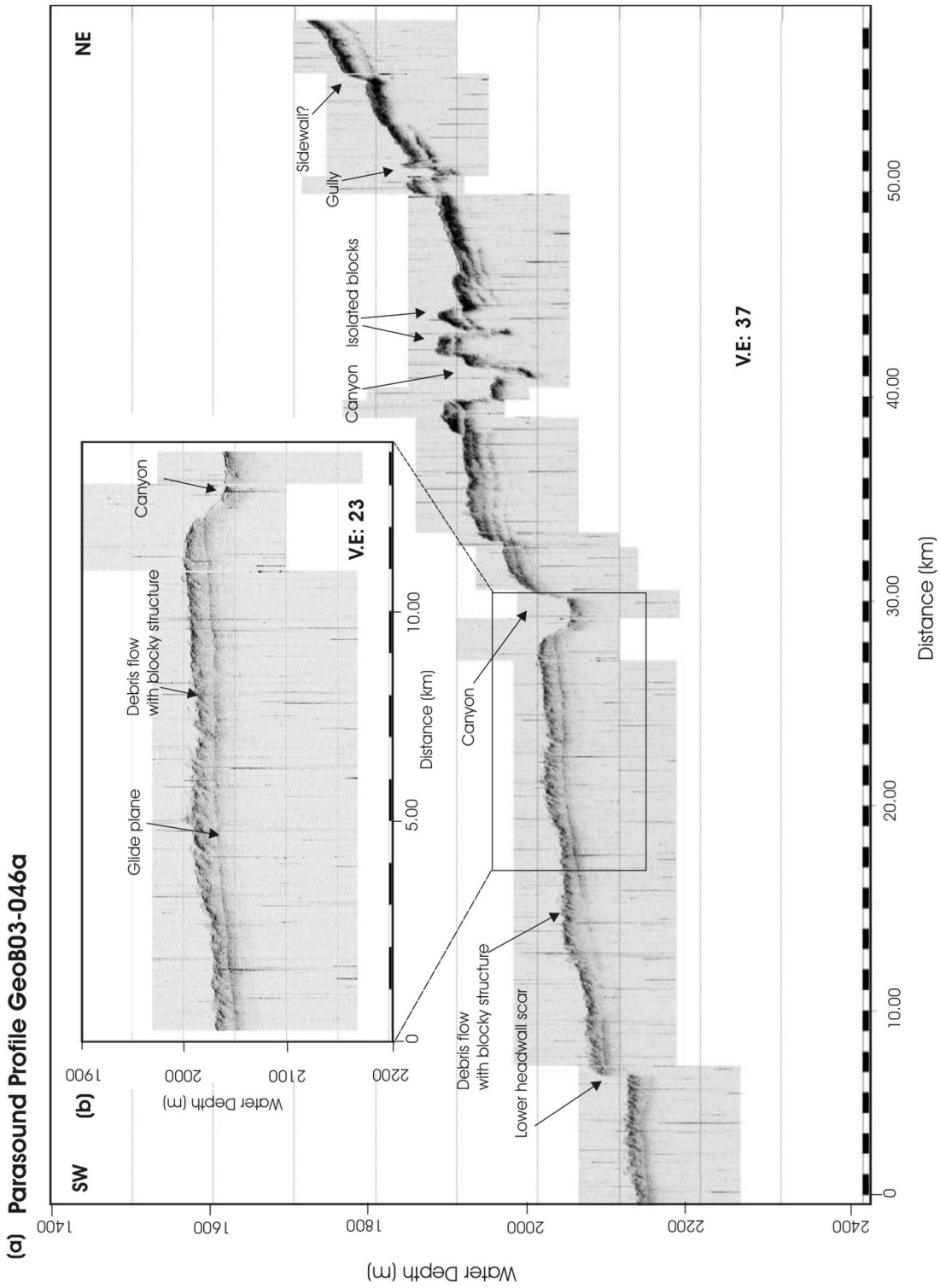


***Figure 3.6:*** *(a) Parasound profile GeoB03-046a recorded in the NE-SW direction across the northern headwall region of Mauritania Slide Complex which is dominated by canyon and gully incisions. Location of the profile is shown in Fig. 3.3. (b) Close-up showing glide plane and blocky debris flow structure.*

The seafloor map shows that the slide is delimited in the upper slope area by a slightly arched to sub-linear headwall boundary, ~150 km long and located below 600 m water depth, which trends sub-parallel to the shelf edge bathymetric contour (i.e. 100 m contour) and opens seaward to the west. Immediately west of this headwall boundary, the failed sediments assume a general westward flow direction forming a complex, more or less, ovate-shaped body which extends seawards into the continental rise. From 2750 m water depth, however, the northern part of the sediment flow suddenly emerges into an elongated distal body whose flow direction is gradually diverted to the southwest by a system of canyons and the Cape Verde Rise which bound the slide in the north and northwestern parts. The distal slide body eventually tapers off further seawards near 3500 m water depth. The total run-out distance of the slide from the uppermost headwall boundary to the most distal slide tongue is >300 km. In the southern part of the slide, a relatively much smaller sediment flow also emerges from ~2750 m water depth from where it flows within a westward flowing channel. The southern slide boundary is effectively delimited by a system of westward flowing canyons. Just beyond the apex of the most distal part of the slide, i.e. near 3500 m water depth, the southwest and westward flowing bounding canyon systems appear to coalesce to constitute a single major canyon system. In the upper slope area, the cold water carbonate mound reef is mapped as a linear topographic feature located immediately between the headwall boundary and the shelf edge.

## *3.6* Seismic characteristics

Our MCS profiles have generally afforded a very good resolution of sedimentary features within the upper 600 m (800 ms TWT) of the seafloor cover, and hence provide additional valuable information about the Mauritania Slide Complex which is otherwise lacking in the Parasound echosounder data. Consequently, the seismic profiles have allowed a detailed visualisation of the internal structure of the Mauritania Slide Complex as well as its basal sliding surfaces and headwall features. Quite as in the case with the Parasound profiles, we distinguish between the source region and the main depositional area of the slide based primarily on changes in the seafloor reflection characteristics and slope gradient.

### *3.6.1 Headwall and proximal depositional areas*

The seismic data (e.g. Figs. 3.8 – 3.11) reveal that the headwall areas of the Mauritania Slide Complex are strongly characterised by a complexity of seafloor morphologies comprising of slide scars, detached slide blocks as well as, locally, canyons and erosional

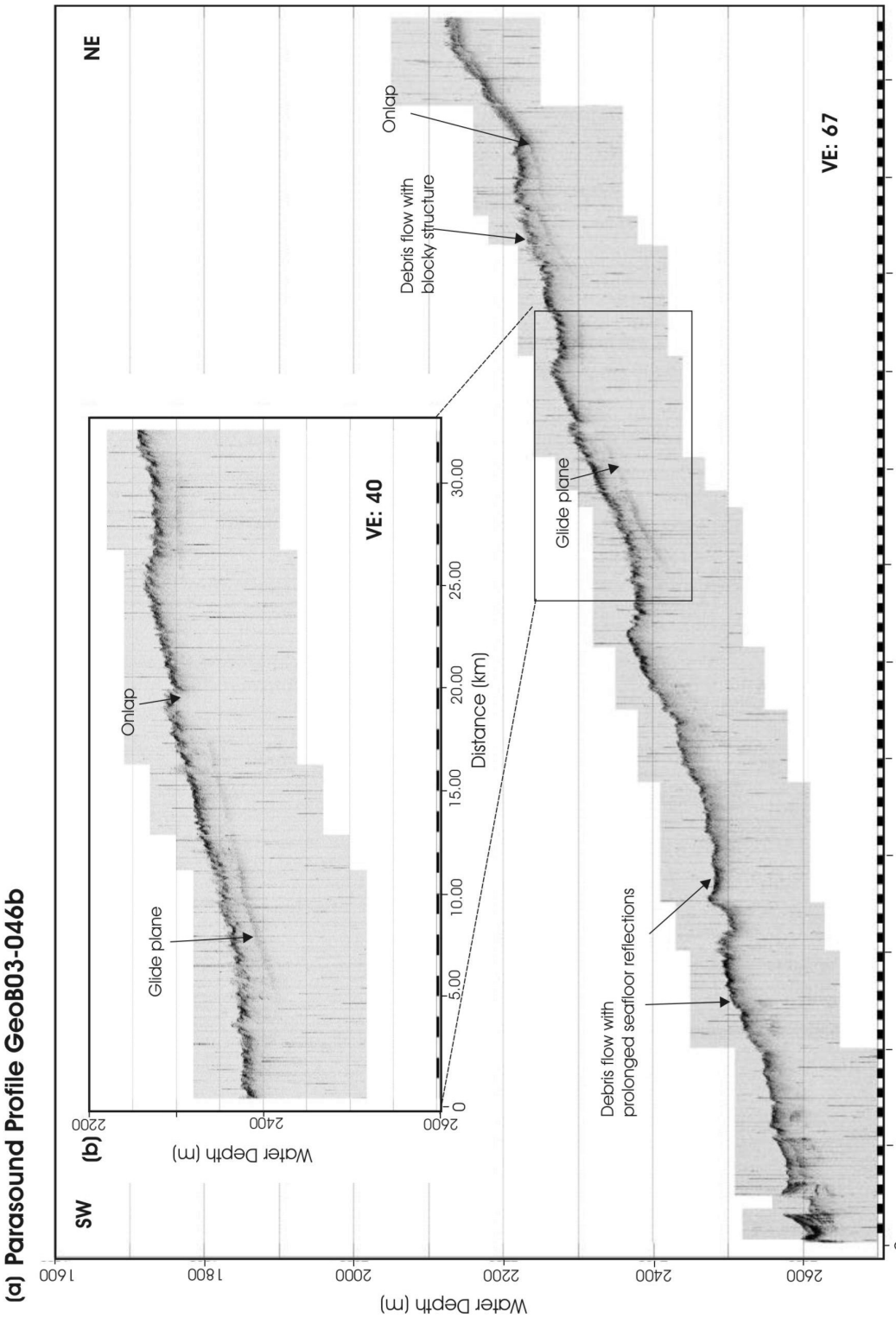


***Figure 3.7:*** *(a) Parasound profile GeoB03-046b which is the SW continuation of Parasound Profile GeoB03-046a, extending across the main debris flow depositional area to the southern boundary of Mauritania Slide Complex. The profile shows extensive debris flow deposition. Location of the profile is shown in Fig. 3.3. (b) Close-up showing glide plane and debris flow onlap.*

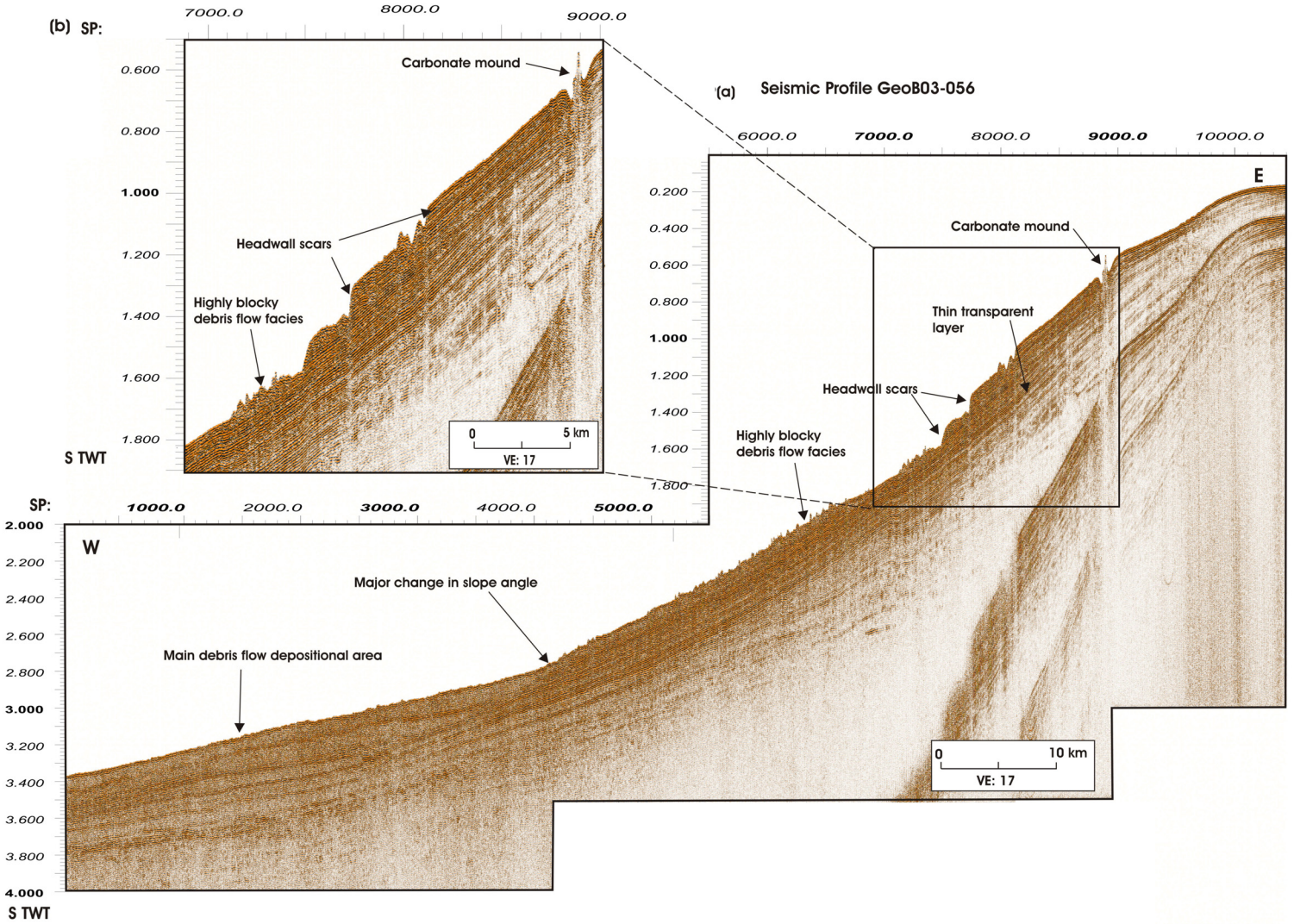


***Figure 3.8:*** *(a) Seismic dip profile GeoB03-056 recorded across the southern part of Mauritania Slide Complex. The profile cuts across the headwall and proximal depositional areas as well as the transition to the main debris flow depositional area. Location of the profile is shown in Fig. 3.3. (b) Close-up of slope area showing headwall scars and immediate vicinity.*

gullies and their associated isolated blocks. In addition the debris flow deposits occurring on the seafloor immediately beneath the headwall scars display highly blocky and strongly hyperbolic seismic reflections.

Seismic dip-oriented profile, Profile GeoB03-056 (Fig. 3.8) which crosses the southern part of the Mauritania Slide Complex from the upper slope to the rise, shows a headwall area characterised by a series of step-like slide scars which truncate well-layered reflectors on the seafloor between 800 – 1150m water depths. Upslope the uppermost headwall, i.e. at Shot Point 8900, the profile displays an isolated sharp peak ~50 m high characterised by chaotic to transparent seismic signature which we ascribe to the presence of the cold water carbonate mound (observed earlier in the Parasound data)

Within the middle parts of the slide, the seismic data show that the upper slope headwall area is characterised by large detached blocks measuring up to 4 km wide, and some with thickness exceeding 40 ms TWT (Fig. 3.9). The blocks show preserved mostly well-layered internal reflectors, and rest conformably over undisturbed generally continuous and well-stratified reflectors parallel to the general slope stratigraphy. In places, the base of the blocks appears to be associated with very thin transparent layers which are intercalated within the well-layered sediment packages. Between 1250 – 1350 m water depths, the lower parts of the blocks are truncated by seaward facing scars which define the lower headwalls. The sediment packages in the slope area have been gently updomed by two underlying diapiric structures occurring near Shot Points 2250 and 4250. A large section of the blocky debris flow deposit located near the downslope flank of the lower updomed seafloor appears to be missing. The presence of the carbonate mounds in the middle parts of the slide, is again observed as a chaotic to transparent piercement structure with a sharp rise in seafloor relief up to 50 m high.

Most of the headwall area in the northern parts of the slide is dominated by intense erosion and gully incision of well-layered sediment packages giving rise to a number of canyons and several isolated sediment blocks on the seafloor (Figs. 3.10 and 3.11). The well-layered sediment packages are intercalated with thin acoustically transparent layers, commonly <20 ms TWT, which may locally pass into lens-shaped debris flow bodies. The overlying sediments have in places been deformed and updomed by sub-surface sediment remobilization (Fig. 3.10) and upward diapiric growths (Fig. 3.11). In Profile GeoB03-046b (Fig. 3.10), located close to the northern boundary, an isolated headwall scar ~ 40 m high is seen to truncate the seafloor debris flow layer near Shot Point 1280. The seafloor topography towards the northeast is highly irregular, and several gullies and a number of canyons, up to

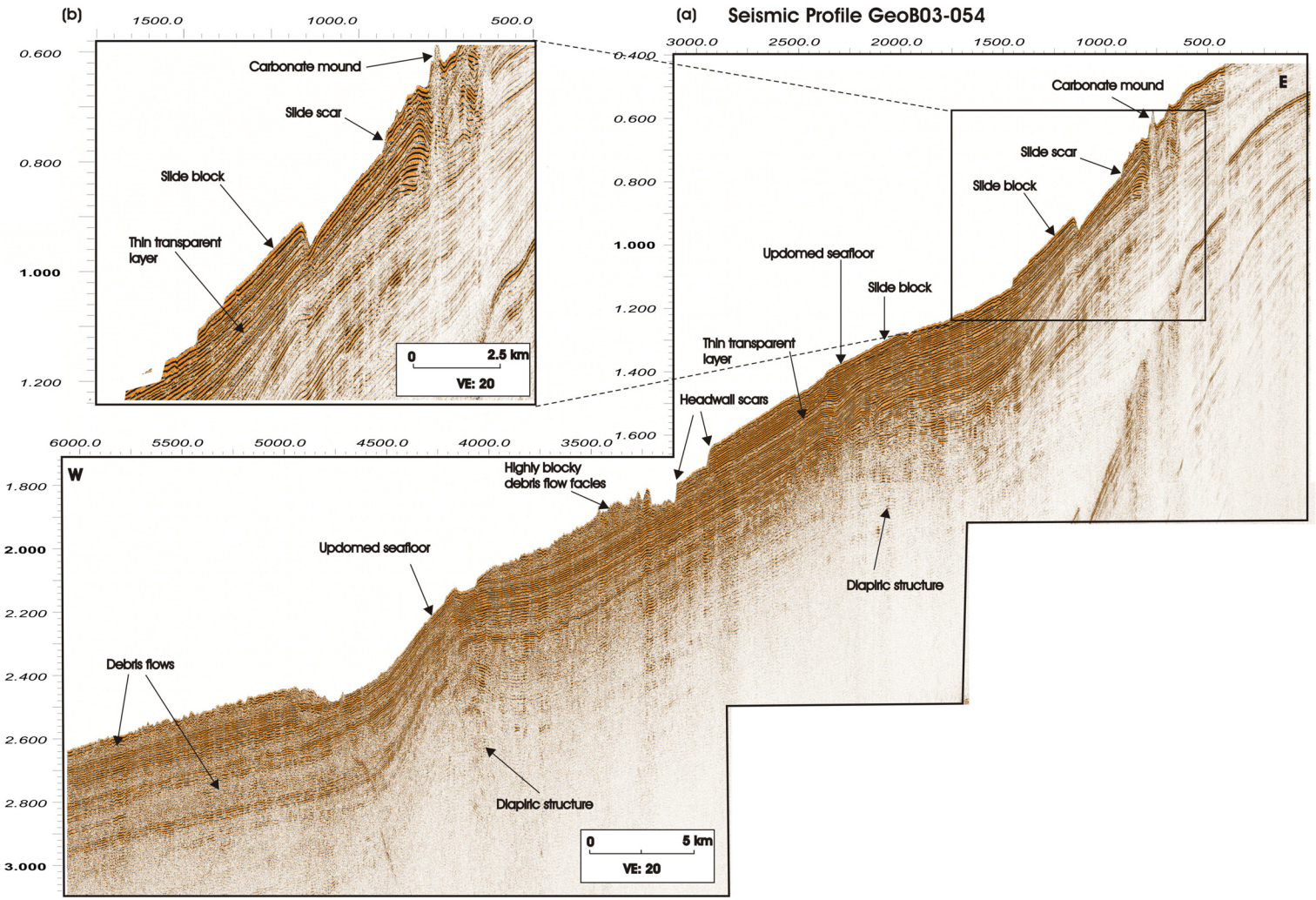


***Figure 3.9:*** *(a) Seismic dip profile GeoB03-054 recorded across the middle part of Mauritania Slide Complex. The profile cuts across the headwall and proximal depositional areas as well as the transition to the main debris flow depositional area. Discrete slide blocks are seen in the upper and middle slope areas. Also, the seafloor is updomed in two places by underlying diapiric structures. Location of the profile is shown in Fig. 3.3. (b) Close-up of the upper slope area showing slide scar and slide block.*

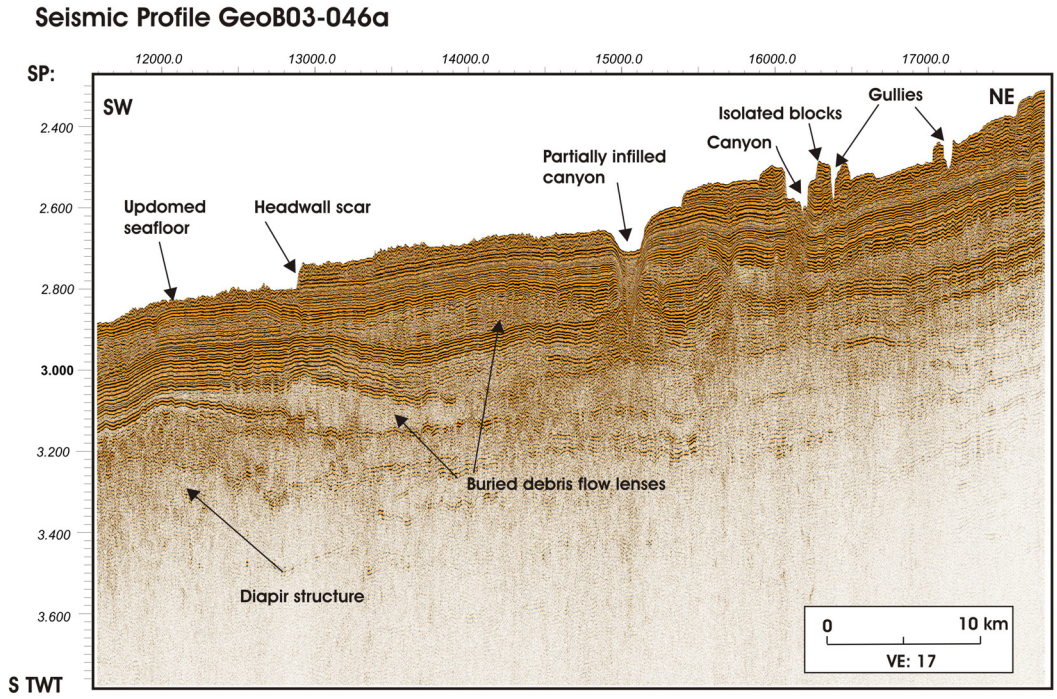


***Figure 3.10:*** *Seismic profile GeoB03-046a recorded in the NE-SW direction across the northern headwall region of Mauritania Slide Complex. The headwall area in the northern part of the profile is dominated by canyon and gully incisions. The seafloor at the southern end of the profile appears to be gently updomed by diapiric structure. Location of the profile is shown in Fig. 3.3.*

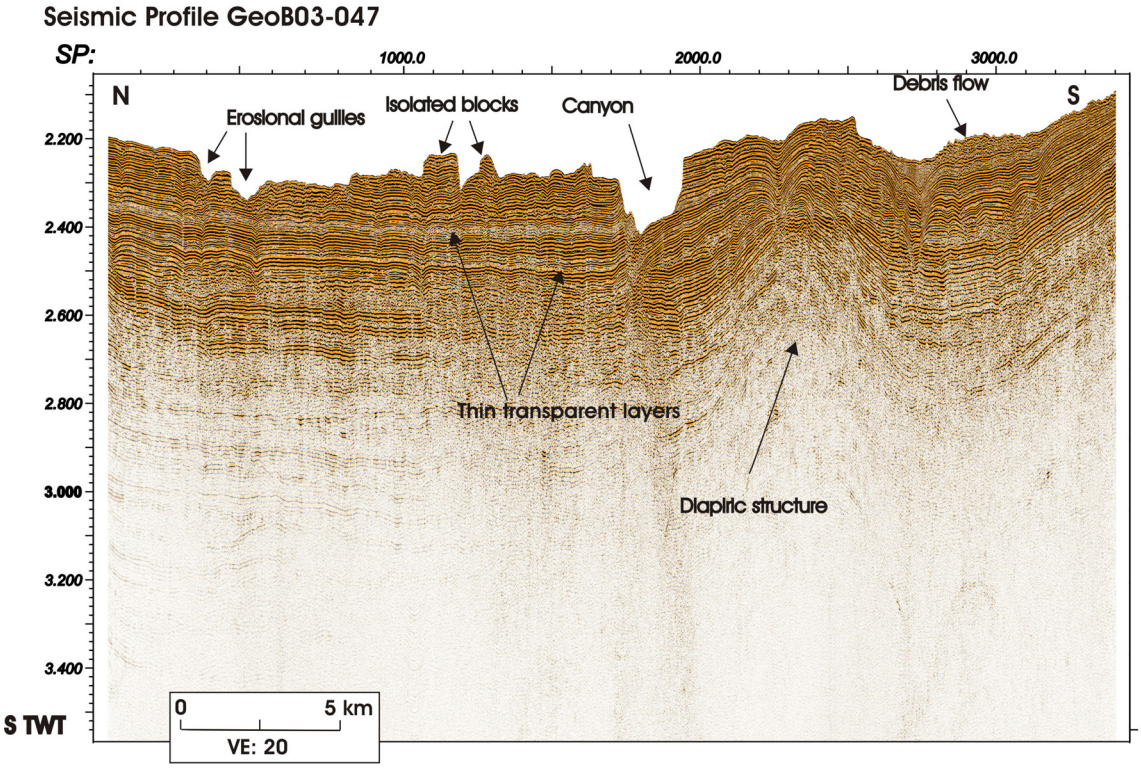


***Figure 3.11:*** *Seismic profile GeoB03-047 recorded in the N-S direction across the northern headwall region of Mauritania Slide Complex. Again, the headwall area is dominated by canyon and gully incisions. The seafloor towards the northern end of the profile is updomed by diapiric structure. Location of the profile is shown in Fig. 3.3.*

4 km wide and 100 m deep, are observed to incise within the surrounding topographic low areas of this intensely wasted headwall area. The isolated blocks display mostly blocky structure with well-layered to chaotic internal reflections (Figs. 3.10 and 3.11).

### *3.6.2 Main debris flow depositional area*

Downslope-oriented seismic profiles (e.g. Figs. 3.8 and 3.9) show that the transition from the headwall area to the main body of the slide is generally characterised by a major change in seafloor gradient from ~1.9° to <1° as already observed in corresponding Parasound profiles. These seismic profiles, together with others which cut obliquely across the main body of the Mauritania Slide Complex (e.g. Fig. 3.12), reveal that the main depositional area of the slide occurs immediately downslope of the major slope gradient transition. In the main slide depositional area, the slide is dominated by a complex stack of sheet-like and lens-shaped debris flow deposits, seismically imaged as laterally extensive zones of transparent to chaotic reflections, separated by well-stratified, generally continuous strong amplitude reflection packages (Figs. 3.12 and 13). In general, the uppermost debris flow deposits within the main depositional area show less blocky seismic facies on the seafloor, and towards the distal parts of the slide they commonly display a more or less smooth surface.

In Profile GeoB03-045 (Fig. 3.13), a large buried debris flow deposit >90 km wide and up to 80 ms TWT thick is seen to lie below 4.200 s TWT and extends from Shot Point 9000 to the northwestern end of the profile. The overlying sediment body between Shot Points 2500 – 8000, which also infills the erosional depression, is characterised by well-layered strong amplitude reflection packages intercalated by thin, i.e. <20 ms TWT thick, acoustically transparent layers. This sediment body is up to 150 ms TWT thick and has a mound-shaped geometry. Towards the southwest the well-layered interval is seen to locally display smaller mound-shaped forms. At the northwestern part of the profile, i.e. between Shot Points 1000 – 5200, the overlying debris flow deposit, is about 80 ms TWT thick and shows mound forms on the seafloor. At its northwestern end, this debris flow deposit locally displays very blocky facies, though it appears less blocky in most parts. At Shot Point 5200, the deposit is sharply bounded by two relatively thin, generally <50 ms TWT, vertically stacked debris flow sheets which extend up to the southwestern end of the profile. In Profile GeoB03-046b (Fig. 3.12), the well-layered sediment intervals show mound-shaped forms in places, especially where they infill pre-existing topographic lows, e.g. between Shot Point 5000 – 8000 and below 3.500 s TWT. Quite like in the previous profile, the uppermost debris flow layer at the northeastern part of the profile is seen to sharply bound two vertically stacked debris flow

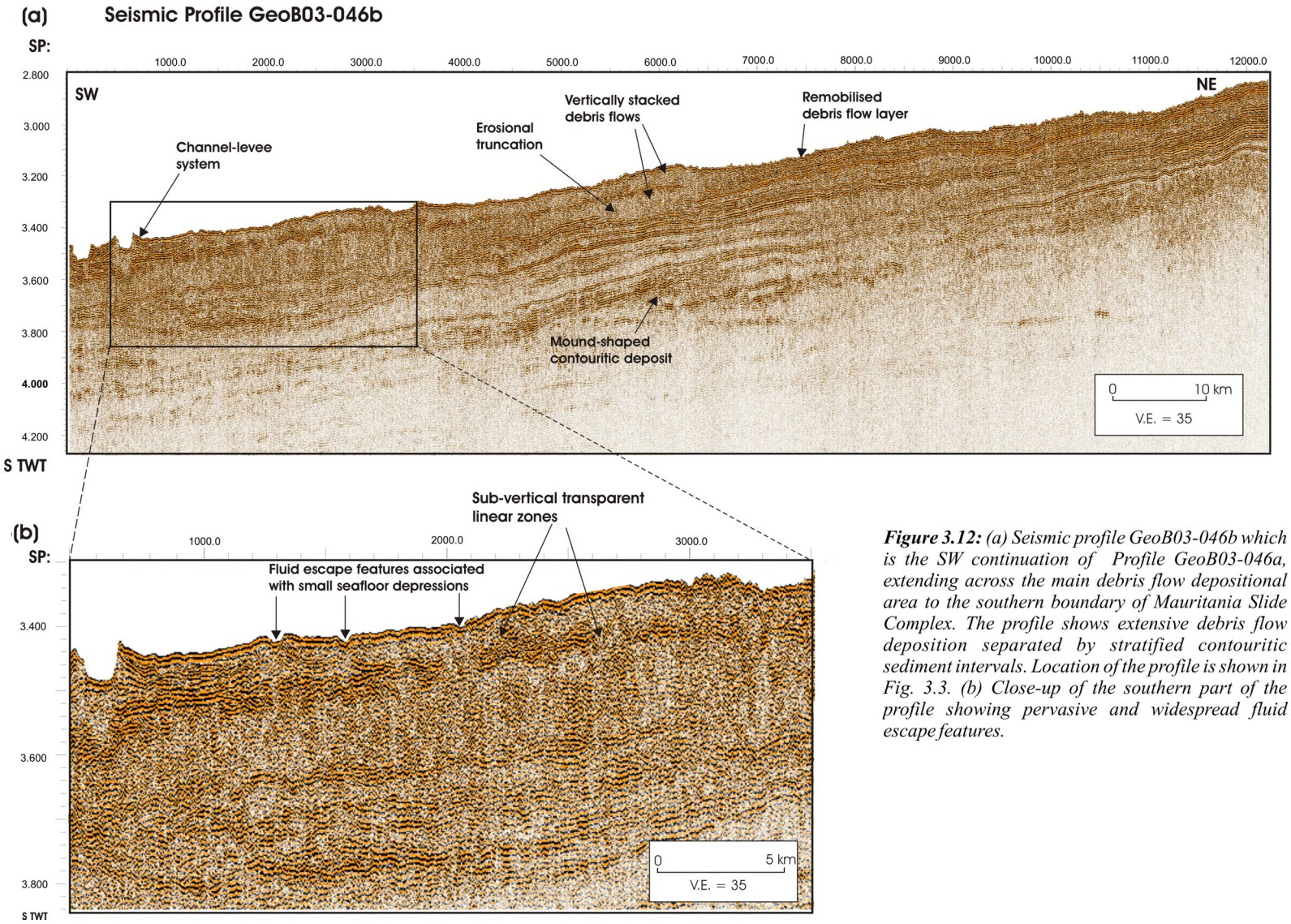


***Figure 3.12:*** *(a) Seismic profile GeoB03-046b which is the SW continuation of Profile GeoB03-046a, extending across the main debris flow depositional area to the southern boundary of Mauritania Slide Complex. The profile shows extensive debris flow deposition separated by stratified contouritic sediment intervals. Location of the profile is shown in Fig. 3.3. (b) Close-up of the southern part of the profile showing pervasive and widespread fluid escape features.*

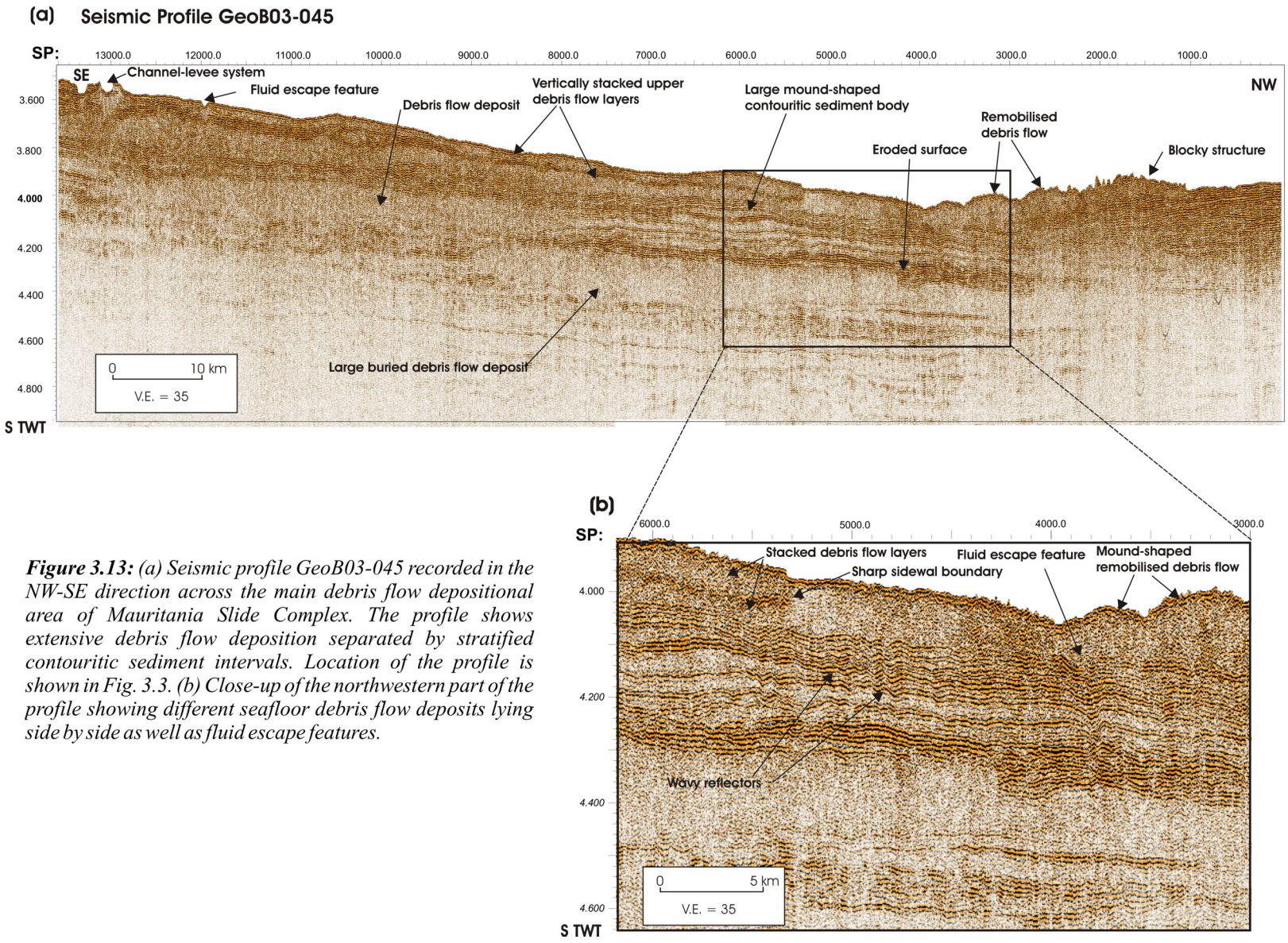


***Figure 3.13:*** *(a) Seismic profile GeoB03-045 recorded in the NW-SE direction across the main debris flow depositional area of Mauritania Slide Complex. The profile shows extensive debris flow deposition separated by stratified contouritic sediment intervals. Location of the profile is shown in Fig. 3.3. (b) Close-up of the northwestern part of the profile showing different seafloor debris flow deposits lying side by side as well as fluid escape features.*

layers near Shot Point 7500. The channel-levee system seen in the previous profile, is again observed to bound the uppermost debris flow layers at the southwest end of the profile. Large sections of both profiles, show very pervasive acoustically transparent sub-vertical linear zones originating from the sub-surface which cut upwards through both overlying debris flow layers and the well-layered sediment intervals. In some parts, these sub-vertical features give rise to wavy and often disjointed reflectors within the well-layered intervals, and where they emerge on the seafloor, especially towards the southern parts of the profiles, the features are associated with small depressions (Figs. 3.12 and 3.13).

## 3.7 Discussions

### 3.7.*1* *Controls on slide geometry and mobility*

We note from the seafloor map of the Mauritania Slide Complex (Fig. 3.3) that whereas the morphology of the main depositional area displays an ovate-like shape, its distal part is exceptionally elongated, giving the slide complex a long run-out distance of more than 300 km. Our data interpretation suggests that several factors may have contributed in determining this peculiar geometry of the Mauritania Slide Complex. These factors include controls exerted by the Cape Verde Rise and the bounding canyon systems, the rheology of slide material and the presence of diapiric structures.

The Cape Verde Rise acts as a major topographic diversion for downslope mass sediment movements along the Mauritanian margin (e.g. Wynn et al., 2000). Our seafloor map of the Mauritanian Slide Complex shows that the southwestern flow direction of the northern part of the slide has clearly been induced by the flow direction of the system of canyons that controls the northwestern boundary of the slide complex. The general course of these canyons may have been pre-determined by the Cape Verde Rise, as noted for the flow direction of the north-lying distal Cap Timiris Canyon (Antobreh and Krastel, in press).

By acting as a topographic diversion for the canyons and debris flows in the northern parts of the slide, the Cape Verde Rise may have contributed in focussing the mass sediment flows. In addition, the predominance of canyons and gullies within headwall areas north of the slide would have focused flow energy so as to facilitate more rapid downslope evacuation of the failed sediments. Consequently, flows close to the northern boundary are likely to remain more fluidised and energised than those in the southern parts, and hence should have greater ability to travel much longer distance. As a similar example, the development of an erosional channel within the central scar of the Storegga slide is thought to have enabled

channelized flow and increased velocity of the debris flows in that part of the slide (Bryn et al., 2005b).

Our seismic profiles (Figs. 3.10 and 3.11) suggest that in the head region of the northern parts of the slide most of the upper sediments have been destabilized by underlying diapiric uplifts and sub-surface sediment remobilization. The resulting sediment destabilization has led to the remobilization of pre-existing debris flows and also the disintegration of overlying sediment, thus providing more mobility to the slide material for further downslope transport.

The seismic data (e.g. Figs. 3.12 and 3.13) show the presence of mound-shaped sediment units with well-layered internal reflectors which we interpret as contouritic deposits. Contourite drifts in large slide environments have been found to be more sensitive and brittle than surrounding coarse grained sediments, e.g. as observed for the Storegga Slide (Bryn et. al., 2005a) and the Traenadjupet Slide (Laberg and Vorren, 2000). In a similar vein, we speculate that contouritic deposits which appear to be more widespread in the northern parts of the slide (Fig. 3.12), should favour an easier sediment disintegration in the area, and hence give rise to more mobile sediment flows. In contrast, the predominance of intact tabular slide blocks (Figs. 3.5 and 3.9) as well as highly irregular and blocky debris flow facies (Figs. 3.4 and 3.8) in the headwall areas of the southern part of the slide suggests that pre-slide sediments in those areas have experienced less disintegration than sediments in the north therefore rendering the resulting southern slide materials stiffer and less mobile.

The two canyon systems that delimit the northern and southern boundaries of the slide complex are seen to merge immediately downslope near the apex of the distal slide to constitute a major single channel system, the Mauritania Channel. As turbidity flows are presumed to generate at the leading edge of debris flows (Middleton and Hampton, 1973; McHugh et al., 2002), we expect the distal debris flows to potentially evolve into a major turbidity flow system which is likely to feed this major channel system for enhanced mass sediment evacuation into the deeper sea.

### *3.7.2 Sedimentary environments and pre-conditioning for slide development.*

Our seismic data (Fig. 3.14) reveal that sediments in the vicinity of the northern parts of the slide that are unaffected by sliding, display contouritic deposition characterised by mounded morphology. In addition, we note that several of the well-layered sediments that separate debris flow deposits within the main depositional area, especially those which infill pre-existing topographic lows, show contouritic characteristics (e.g. Fig. 3.12). These

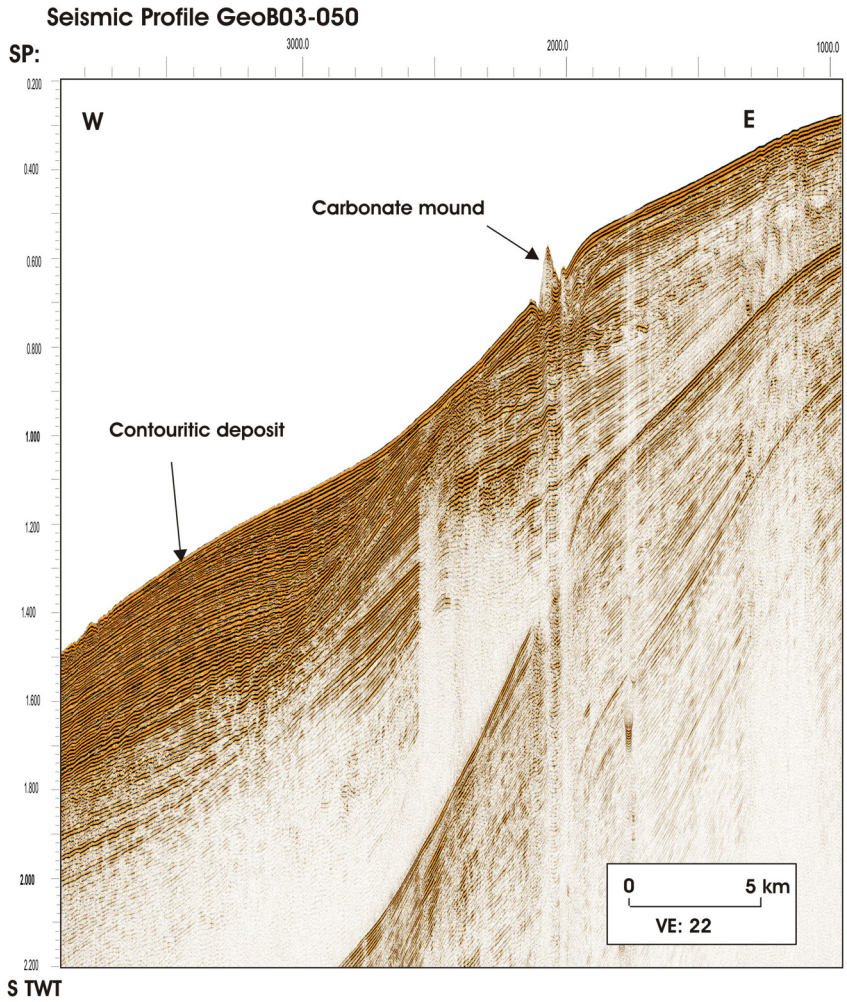


***Figure 3.14:*** *Seismic dip profile GeoB03-050 recorded upslope of Mauritania Slide Complex showing mound-shaped contouritic sediments unaffected by sliding as well as a carbonate mound feature. Location of the profile is shown in Fig. 3.3.*

observations suggest that a great deal of the failed sediments, particularly in the northern parts of the slide, were probably of contouritic origin. The nearby Cape Verde Rise may have aided in focusing bottom current, i.e. the south-flowing NADW, circulation in the area. Consequently, the increased bottom current speed would have actively interacted with sediment depositional processes in the area, arising mainly from upwelling-induced and wind-blown aeolian sediment sources, thereby enhancing contouritic deposition.

Contouritic deposits characterised by sand-rich sediments which are intercalated by fine-grained layers are known to be especially prone to sediment instability (Bryn et al., 2005a). In this case, the fine grained layers often serve as suitable planes of weakness for promoting mass sediment failures. Weak layers facilitate the destabilization of sediments and the formation of slides. Most weak layers are probably much too thin to be resolved by the seismic system but the occurrence of very thin acoustically transparent layers within the

unfailed sediments (Figs. 3.10 and 3.11) in the northern parts suggests that lithologically weak layers probably exist in this area and may have facilitated the slide process within the mostly contouritic deposits. Though contourite deposition becomes less widespread in the southern parts of the slide, the unfailed well-stratified sediments in the area are also intercalated with very thin acoustically transparent layers (Figs. 3.8 and 3.9) which should serve to promote gravity-driven downslope sediment movement, as similarly observed on the Aegean Sea margin (Lykousis et al., 2002) and offshore Norway (Laberg and Vorren, 2000).

Lack of canyons within the arcuate segment of the margin favoured uninterrupted rapid build-up of sediment piles over relatively long time intervals in a sheltered open slope setting. This is in sharp contrast to the adjacent north and south bounding areas of the margin where high concentration of canyons and gullies must have effectively evacuated any sediment supplies through channelised sediment transport, and therefore precluded any significant pile-up of sediments in those areas. The high rates of sediment accumulation, especially in the presence of upwelling-induced organic-rich sedimentation, would have given rise to underconsolidated sediments charged with excess pore pressure, thus making the sediments highly prone to instability, and hence pre-conditioned for slide development.

### *3.7.3 Timing of slide events and failure mechanism*

The seismic data reveal that the main depositional area of the Mauritania Slide Complex is composed of several stacks of debris flow deposits separated by well-stratified sediments. In addition we note in both the seismic and Parasound data, that the uppermost debris flow deposits are made up of several lens-shaped units lying side by side or onlapping each other in places (Figs. 3.7 and 3.10). We also note in both data sets the presence of multiple headwall scars in the source areas (e.g. Figs. 3.4, 3.5, 3.8 and 3.9).

These observations suggest that the stages of development of the slide complex have been characterised by several recurrent mass sediment failure events, which may be grouped into major and relatively minor failure events. We speculate that the termination of each major debris flow depositional event was generally followed by a period of 'normal' sedimentation during which the intervening well-layered sediments were deposited. Also during this period, pre-existing headwall scars as well as seafloor topographic lows, created by sub-surface sediment mobilization or diapiric growths and probably erosional removal, were infilled by 'normal' sediments. That some of the well-layered sediments between 700 – 2500 m water depths (Figs. 3.12 and 3.14) display mounded contouritic characteristics, is

indicative of the prevalent increased bottom current activity, i.e. under the regime of North Atlantic Deep Water, which characterised the sedimentation process.

Many young submarine slides on deep continental margins which exhibit complex and multi-staged behaviour are thought to have usually formed through retrogressive sliding (Canals et al., 2004). The complex internal structure and the step-like headwall morphology displayed by the Mauritania Slide Complex together with the fact that most of the lower headwall scars occur at considerable water depths, i.e. up to ~2000 m deep, suggest that its process of development during a major event was characterised by retrogressive sliding. In this case, the initial sediment failure was started from the lowermost headwalls and was then followed by a series of discrete failures which progressed upslope. In the seismic data (e.g. Figs. 3.8 and 3.9) we observe, especially in the slope areas, the presence of widespread thin acoustically transparent layers intercalated within thick well-layered sediment units. We interpret these thin layers which commonly underlie failed sediments as weak layers which facilitate sediment failure. The process of retrogressive slide development must have exploited the widespread presence of these weak layers as glide planes. As no slides are observed upslope of the linearly aligned cold water carbonate mounds (Fig. 3.3), it is most likely that the mounds played an influential role in halting further upslope slide retrogression particularly in the southern parts of the slide.

C14-age determination of sediment cores from the uppermost debris flow layers recovered from different locations in the slide returned C14-age dating of 10.5 – 10.9 cal. ka B.P. representing the age of the last major slide event (Henrich et al., in review). Slide development during a major event may have been significantly modified by later minor instability events which included remobilization of pre-existing debris flows as well as translational sliding (this is discussed in detail in the last section). However, the time lapse between the phases of multiple instabilities within the last major slide event may have escaped the resolution of the C14-age dating method. The complete age description of the slide complex has, however, not yet been established.

### *3.7.4 Possible trigger mechanisms for slide development*

Following the creation of a slide ‘pre-conditioned’ environment along the Mauritanian margin, i.e. the rapid build up of a thick sediment piles intercalated with widespread weak layers, the stage was then set for a trigger mechanism to initiate the mass sediment failure events which would lead to slide development. We now examine and evaluate the potential trigger mechanisms which are likely to have initiated the development of the Mauritania Slide

Complex based on indications from our data as well as those commonly documented for other passive marginal settings. These are mainly: excess pore-pressure (generated mostly through methane gas, decaying gas hydrates and sea level fluctuations, etc), earthquakes and diapiric movements.

#### *3.7.4.1 Excess pore pressure*

Build-up of excess pore pressure in upper sediment layers is known to be capable of triggering mass sediment failures (Laberg and Vorren, 1995; Vorren et al., 1998). With the high rates of sediment accumulation within the study area, the potential for excess pore-pressure generation would have been quite immense. The rapid pile up of huge quantities of sediments would have entrapped organic matter from upwelling-induced sedimentation as well as fluvial sources which decomposed into methane gas to give rise to increased excess pore-pressures. Our data do not provide any clear indications like enhanced buried reflectors or gas hydrate BSR (bottom simulating reflector) to suggest decaying gas hydrates as being a possible source of the pore-pressure build-up. However, we note the presence of widespread and pervasive acoustically transparent linear vertical zones which are often associated with wavy reflectors in the main slide depositional areas (e.g. Figs. 3.12 and 3.13), and interpret the features as evidence of widespread distribution of excess pore-pressure from over-pressurised gas or fluids within the slide complex.

Sea level fluctuations are also known to generate excess pore pressures within near-bottom seafloor sediments as a result of periodic changes in hydrostatic pressure within the sediments (e.g. Lee et al., 1996). As noted by Henrich et al. (in review), the timing of the last major debris flow depositional event, i.e. 10.5 – 10.9 cal. ka B.P., is suggestive that the youngest major failure event could also have been triggered by the rising sea level during the transition between the last glacial and the present interglacial.

#### *3.7.4.2 Earthquakes as a possible trigger mechanism*

Jacobi (1976) suggested earthquakes associated with the Cape Verde Rise and adjacent fracture zones extensions may have possibly triggered the slide events. Earthquakes have been cited in several studies in Atlantic marginal settings as the commonest trigger mechanism for many large-scale submarine mass sediment failures, e.g. the Storegga Slide (Bryn et al. 2005b), Afen Slide (Wilson et al., 2004) and the Traenadjupet Slide (Laberg and Vorren, 2000) though the margin setting of these slides is different compared to the Mauritania Slide Complex.

Seismic hazard modelling results have shown that nearby thick offshore sediments are able to significantly extend the shaking duration of earthquakes (Lindholm et al., 2005). And for their study of the deep sedimentary More Basin, offshore Norway, Lindholm et al. (2005), concluded that surface sediment layers located ~100 km from the earthquake source experienced more seismic shaking than the source region. As the Mauritania Slide Complex is located within a thickly sedimented rift basin, i.e. up to 10 km deep at its depocenter off Mauritania (Wissmann, 1982), any earthquake activity from nearby Cape Verde Islands is expected to have a more pronounced effect in the slide area. Consequently, earthquake activities from the islands should be considered as a potential trigger mechanism for the formation of the Mauritania Slide Complex.

#### *3.7.4.3 Diapirism as a possible trigger mechanism and its influence on recent slide development*

We note that the Mauritania Slide Complex is located within the area of salt diapirs, which lies between latitudes 16 ° - 19° N (Wissman, 1982), along the Mauritanian margin. Our seismic data interpretation shows that most of the slide area has been subjected to sub-surface sediment mobilization and diapiric growths ( e.g. Figs. 3.9 – 3.11). Salt movements in the margin, believed to have began in Miocene/Pliocene time following sediment overloading from the Senegal River paleo-estuary (Wissman, 1982), appear to have continued up to this time though there might have been several long periods of inactivity. As the depocenter of the paleo-estuary shifted progressively southwards towards its present location near 16° 05'N, high sediment accumulation from upwelling-induced sources and wind-blown sediment must have sustained the salt halokinesis. Consequently, we think destabilization of overlying sediment layers by salt movements has continued over a long time and may constitute an important trigger mechanism for the development of Mauritania Slide Complex. Apart from fracturing and deforming overlying sediments, the upward movement would also have locally created oversteepening of affected slope and rise areas. This observation is consistent with studies elsewhere, e.g. in the Gulf of Mexico (Tripsanas et al., 2004) and off North Carolina (Cashman and Popenoe, 1985) where episodic movements of underlying salt bodies are believed to have triggered slope failures.

Though we do not have data control over the growth history of the diapirs, our data interpretation allows us to envisage the influence of diapiric growths on seafloor stability and recent slide development by a three-stage evolutionary model outlined as follows (Fig. 3.15):

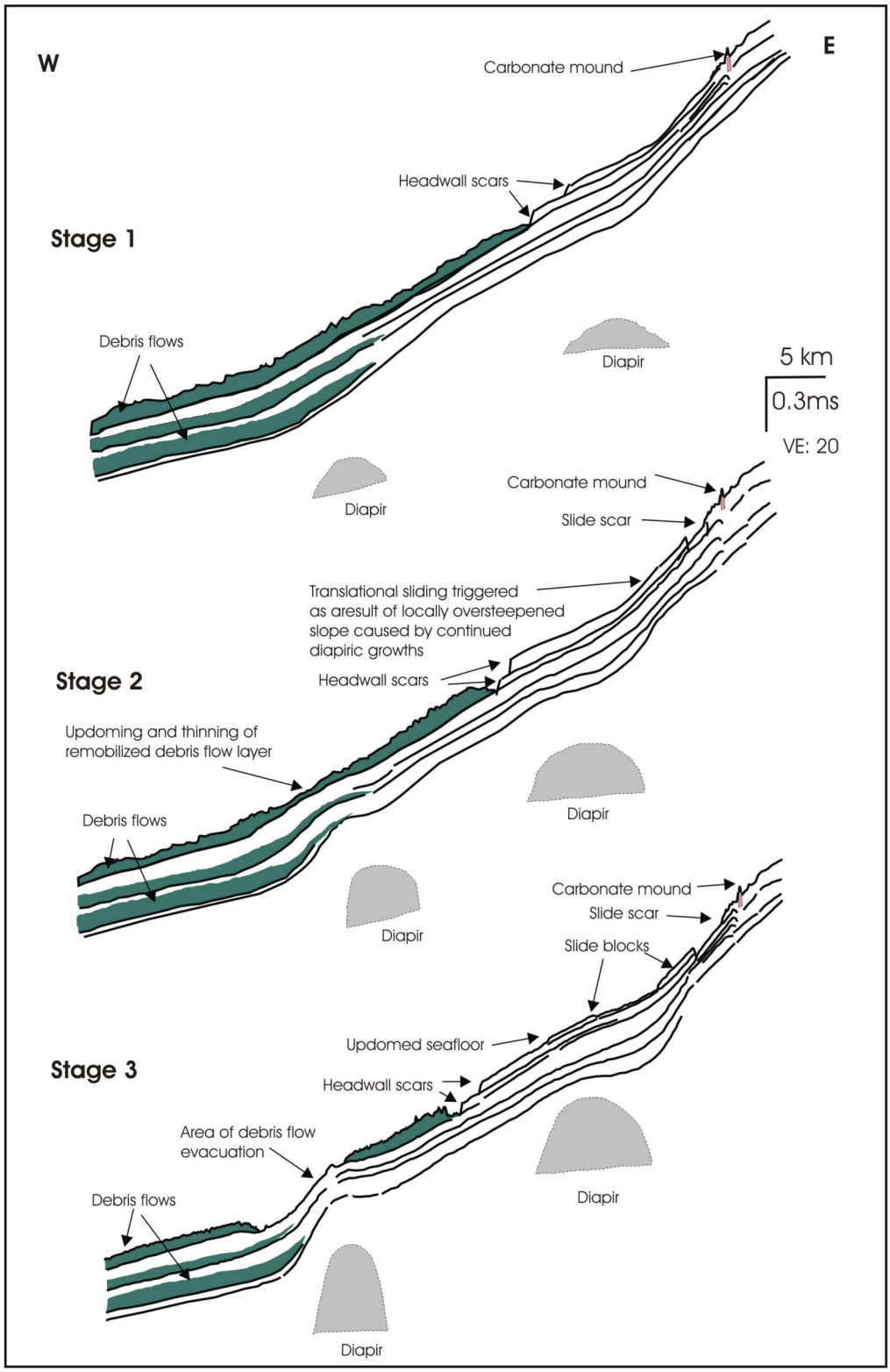


***Figure 3.15:*** *Schematic illustration of the influence of diapiric growths on seafloor stability and recent development of the Mauritania Slide Complex. The model is based on our interpretation of Profile GeoB03-054 (Fig. 9). Stage 1: Deposition of debris flows during last major slide event. Stage 2: Continued diapiric growths cause uplifts of seafloor accompanied by locally increased slope gradients leading to translational sliding and remobilization of pre-existing debris flows. Stage 3: Further diapiric growths lead to more uplifts of overlying sediments and then disintegration of seafloor debris flow deposit. See text for detailed explanation.*

(i) The last major slide event resulted in the formation of widespread debris flow deposits probably through retrogressive slope failure of previously well-layered slope sediments (Fig. 3.15, stage 1). The age of this major event is represented by the 10.5 – 10.9 ka obtained from core dating.

(ii) Following this event continued diapiric growths locally uplifted the upper and lower slope areas, including: (a) the area immediately upslope the upper headwall scar, which previously had undisturbed sediments, and (b) the area downslope the lower scar. In the upper slope area, initial diapiric growths locally increased the seafloor gradient, thereby inducing translational sliding along planar failure surfaces. In this case, the very thin acoustically transparent layers within the well-stratified upslope sediment packages may have facilitated the sliding process by serving as lithological planes of weakness. In the lower slope area, the seafloor debris flow layer responded to diapiric growths by gradually thinning and withdrawing towards the downslope flank of the now uplifting seafloor (Fig. 3.15, stage 2).

(iii) In the upper slope area, progressive upward diapiric growths led to a slight disintegration of the slide blocks accompanied by further downslope movement which may have eventually slowed down or stopped on encountering the detached debris flow deposit. In the lower slope area, the growths led to a complete detachment of the overlying less cohesive and increasingly weakened debris flow layer at the downslope flank of the updomed crest leaving an isolated debris flow remnant in the upslope flank (Fig. 3.15, stage 3).

Our model suggests that diapiric growths have the tendency to later destabilize overlying sediments previously unaffected by retrogressive failures of even major slide events. In the case of pre-existing seafloor debris flow deposits, the growths would thin or considerably weaken the layers and eventually dismember or disintegrate them thereby inducing renewed mobility to the flows.

Translational sliding and debris flow remobilization may still be an active process within the Mauritania Slide Complex as evidenced by recent updoming and seafloor instabilities induced by the apparently, still active diapiric growths. In many cases, seafloor topographic lows created at the flanks of the domed areas have constituted pathways for remobilized debris flows (e.g. Fig. 3.11). Additionally, the rugged seafloor topography created by the isolated and detached remnants of the pre-existing slide materials may locally give rise to increased bottom current velocities, thereby leading to erosional removal of portions of the deposits for further redistribution into the deep sea.

Considering all the scenarios for slide initiation discussed above, it is unlikely that any single trigger mechanism could be solely responsible for initiating all the slide events. In addition, the marked complexity in morphology exhibited by the Mauritania Slide Complex suggests that its stages of development must have been influenced by the interplay between more than one of the triggering mechanisms discussed above. However, because of their more regional character, factors like earthquakes and excess pore pressure may have been more dominant in initiating major slide events which were later modified by diapiric growths and sub-surface sediment remobilization.

## 3.8 Conclusions

- Recentlly acquired Parasound sediment echosounder and high resolution multi-channel seismic reflection data have afforded a more detailed characterisation of the Mauritania Slide Complex than previously reported. Apart from further constraining the seafloor morphology of the slide complex, the new data have allowed a detailed visualization and investigation of the internal structure of the slide including headwall features, basal sliding surfaces as well as the geometry and character of slide deposition.
- The slide has affected an area in the order of 34,000 km² occurring between ~600 m - >3500 m water depths, hence ranking as one of the major slides on the NE Atlantic margin. Headwall scars commonly occur as a series of steps in seafloor morphology ranging between 25 – 100 m high and occurring between 600 - 2000 m water depths.
- The ovate-shaped slide displays a long run-out distance >300 km as a result of higher sediment flow mobility induced in its northern parts by bounding canyon systems and the Cape Verde Rise. In addition, widespread diapiric growths may have enhanced quicker disintegration of overlying weaker contouritic deposits thus contributing to increased sediment flow mobility.
- Slide development was pre-conditioned by uninterrupted deposition of probably upwelling-induced organic-rich sediments in an open slope environment which would have favoured rapid accumulation of poorly consolidated bedded sediments interspersed with thin lithologically weak layers.
- The presence of several vertically stacked debris flow deposits separated by well-layered sediment intervals revealed within the internal structure of the slide is suggestive that the stages of slide development have been characterised by multiple failure events. In addition, the series of step-like headwall scars which extend from

great water depths ~2000 m upslope to~600 m, suggests a retrogressive mode of failure which may have been facilitated by widespread weak layers during a major slide event.

- Slide development during a major slide event may have been significantly modified by later minor instability events which involved remobilization of pre-existing debris flows as well translational sliding mainly as a result of diapiric growths.
- The data interpretation suggests excess pore pressures, resulting from decayed organic matter and/sea level rise, could be the most important trigger mechanism for slide formation. However, seismic shaking could have played a complementary or, at one time or the other, a leading role in triggering the sediment failures. Diapiric growths have also been important in destabilizing overlying sediments including unfailed areas. The combined activities of these factors are the most likely cause of the complex morphology of the Mauritania Slide Complex.

## 3.9 Acknowledgements

The authors deeply acknowledge the invaluable assistance and cooperation enjoyed from fellow cruise participants as well as the Captain and crew members of RV Meteor Cruise M58/1 during data acquisition. This is publication RCOM XXXX of the DFG-Research Center 'Ocean Margins' (University of Bremen).

## References

Antobreh, A. A., and Krastel, S. (in press). Morphology, seismic characteristics and development of Cap Timiris Canyon, offshore Mauritania: a newly discovered canyon preserved off a major arid climatic region. Marine and Petroleum Geology.

Baraza, J., Ercilla, G., and Nelson, C. H. (1999). Potential geologic hazards on the eastern Gulf of Cadiz slope (SW Spain). Marine Geology 155, 191-215.

Bryn, P., Berg, K., Stoker, M. S., Haflidason, H., and Solheim, A. (2005a). Contourites and their relevance for mass wasting along the Mid-Norwegian Margin. Marine and Petroleum Geology 22, 1-12.

Bryn, P., Berg, K., Forsberg, C. F., Solheim, A., and Kvalstad, T. (2005b). Explaining the Storegga Slide. Marine and Petroleum Geology 22, 11-19.

Bugge, T., (1983). Submarine slides on the Norwegian continental margin, with special emphasis on the Storegga area. Publ. Cont. Shelf Inst. 110, 152.

Canals, M., Lastras, G., Urgeles, R., Casamor, J. L., Mienert, J., Cattaneo, A., De Batist, M., Haflidason, H., Imbo, Y., Laberg, J. S., Locat, J., Long, D., Longva, O., Masson, D. G., Sultan, N., Trincardi, F., and Bryn, P. (2004). Slope failure dynamics and impacts from seafloor and shallow sub-seafloor geophysical data: case studies from COSTA project. Marine Geology 213, 9-72.

Casas, D., Ercilla, G., Baraza, J., Alonso, B., and Maldonado, A. (2003). Recent mass-movement processes on the Ebro continental slope (NW Mediterranean). Marine Geology 20, 445-457.

Cashman, K. V., and Popenoe, P. (1985). Slumping and shallow faulting related to the presence of salt on the continental slope and rise off North Carolina. Marine and Petroleum Geology 2, 260-271.

Colman, J. G., Gordon, D. M., Lane, A. P., Forde, M. J., and Fitzpatrick, J. J. (2004). Carbonate mounds off Mauritania, Northwest Africa: status of deep-water corals and implications for management of fishing and oil exploration activities. In: A. Freiwald, and J. M. Roberts, (Eds.), Cold-water Corals and Ecosystems. Springer-Verlag, Berlin Heidelberg. pp. 379-403.

Dawson, A. G. (1999). Linking tsunami deposits, submarine slides and offshore earthquakes. Quaternary International 60, 119-126.

Fine, I. V., Rabinovich, A. B., Bornhold, B. D., Thomson, R. E., and Kulikov, E. A. (2005). The Grand banks landslide-generated tsunami of November 18, 1929: preliminary analysis and numerical modeling. Marine Geology 215, 45-57.

Fryer, G. J., Watts, P., and Pratson, L. F. (2003). Source of the great tsunami of 1 April 1946: a landslide in the upper Aleutian forearc. Marine Geology 203, 201-218.

Gee, M. J. R., Masson, D. G., and Watts, A. B. (2001). Passage of debris flows and turbidity currents through a topographic constriction: seafloor erosion and deflection of flow pathways. Sedimentology 48, 1389-1409.

Grant, J. A., and Schreiber, R. (1990). Modern swathe sounding and sub-bottom profiling technology for research applications: The Atlas Hydrosweep and Parasound Systems. Marine Geophysical Researches 12, 9-19.

Haflidason, H., Sejrup, H. P., Nygard, A., Mienert, J., Bryn, P., Lien, R., Forsberg, C. F., Berg, K., and Masson, D. G. (2004). The Storegga Slide: architecture, geometry and slide development. Marine Geology 213, 201-234.

Hampton, M. A., Lee, H. J., and Locat, J. (1996). Submarine lanslides. Rev. Geophys. 34, 33-59.

Imbo, Y., De Batist, M., Canals, M., Prieto, M. J., and Baraza, J. (2003). The Gebra Slide: a submarine slide on the Trinity Peninsula Margin, Antarctica. Marine Geology 193, 235-252.

Jacobi, R. D. (1976). Sediment slides on the northwestern continental margin of Africa. Marine Geology 22, 157-173.

Jacobi, R. D., and Hayes, D. E. (1982). Bathymetry, Microphysiography and Reflectivity Characteristics of the West African Margin Between Sierra Leone and Mauritania. In: U. von Rad, K. Hinz, M. Sarnthein, and E. Seibold (Eds.), Geology of the Northwest African Continental Margin. Springer-Verlag, Berlin pp. 182-212.

Jansa, L. F., and Wiedmann, J. (1982). Mesozoic-Cenozoic development of the Eastern North American and Northwest African Continental Margins: a comparison. In: U. von Rad, K. Hinz, M. Sarnthein, and E. Seibold (Eds.), Geology of the Northwest African Cantinental Margin. Springer-Verlag, Berlin, pp. 215-269.

Klaus, A., and Ledbetter, M. T. (1988). Deep-sea sedimentary processes in the Argentine Basin revealed by high resolution-seismic records (3.5 kHz echograms). Deep-Sea Research 35, 899-917.

Koopmann, B. (1981). Sedimentation von Saharastaub im subtropischen Nordatlantik während der letzten 25.000 Jahre. Meteor Forschungsergebnisse 35, 23-59.

Krastel, S., Hanebuth, T. J. J., Wynn, R. B., Antobreh, A. A., Henrich, R., Holz, C., Kölling, M., Schulz, H. D., and Wien, K. (2004). Cap Timiris Canyon: A newly discovered channel-system off Mauritania. EOS, Transactions 85, 417-423.

Krastel, S., Scminke, H. U., Jacobs, C. L., Rihm, R., Le Bas, T. P. and Alibes, B. (2001). Submarine landslides around the Canary Islands. Journal of Geophysical Research 106, 3977-3997.

Laberg, J. S., and Vorren, T. O. (1995). Late Weichselian submarine debris flow deposits on the Bear Island Trough Mouth Fan. Marine Geology 127, 45-72.

Laberg, J. S., and Vorren, T. O. (1996). The Middle and Late Pleistocene evolution of the Bear Island Trough Mouth Fan. Global and Planetary Change 12, 309-330.

Laberg, J. S., and Vorren, T. O. (2000). The Traenadjupet Slide, offshore Norway- morphology, evacuation and triggering mechanisms. Marine Geology 171, 95-114.

Lee, H. J., Chough, S. K., and Yoon, S. Y. (1996). Slope stability change from late Pleistocene to Holocene in the Ulleung Basin, East Sea (Japan Sea). Sedimentary Geology 104, 39-51.

Lindholm, C., Roth, M., Bungum, H., and Faleide, J. I. (2005). Probabilistic an deterministic seismic hazard results and influence of the sedimentary More Basin, NE Atlantic. Marine and Petroleum Geology 22, 149-160.

Lonsdale, P. (1982). Sediment drifts of the Northeast Atlantic and their relationship to the observed abyssal currents. Bull. Inst. Geol. Bassin d'Aquitaine 31, 141-149.

Lykousis, V., Roussakis, G., Alexandri, M., and Pavlakis, P. (2002). Sliding and regional slope stability in active margins: North Aegean Trough (Mediterranean). Marine Geology 186, 281-298.

Masson, D. G., Canals, M., Alonso, B., Urgeles, R., and Hühnerbach, C. (1998). The Canary Debris Flow: source area morphology and failure mechanisms. Sedimentology 45, 411-432.

McAdoo, B. G., Pratson, L. F., and Orange, D. L. (2000). Submarine Landslide geomorphology, US continental slope. Marine Geology 169, 103-136.

McHugh, M. G. C., Damuth, J. E., and Mountain, S. G. (2002). Cenozoic mass-transport facies and their correlation with sea level change, New Jersey continental margin. Marine Geology 184, 295-334.

Middleton, G. V., and Hampton, M. A. (1973). Sediment gravity flows: mechanics of flow and deposition. Pacific Section, Short Course Lecture Notes on "Turbidites and Deep Water Sedimentation". SEPM, 1-38.

Piper, D. J. W., and Ingram, S. (2003). Major Quaternary sediment failures on the east Scotian Rise, eastern Canada. Geological Suvey of Canada, Current Research 2003-D1, 7.

Sarnthein, M., Thiede, J., Pflaumann, U., Erlenkeuser, K., Fütterer, D., Koopmann, B., Lange, H., and Seibold, E. (1982). Atmospheric and Oceanic Circulation Patterns off Northwest Africa During the Past 25 Million Years. In: U. von Rad, K. Hinz, M. Sarnthein, and E. Seibold (Eds.), Geology of the Northwest African Continental Margin. Springer-Verlag, Berlin. pp. 545-604.

Schulz, H. D., and Cruise participants., (2003). Report and preliminary results of METEOR Cruise M 58/1, Dakar-Las Palmas, 15.04.2003-12.05.2003, Berichte, Fachbereich Geowissenschaften, Universität Bremen, Bremen. pp. 186.

Seibold, E., and Hinz, K. (1974). Continental slope construction and destruction, West Africa. In: C. A. Burk, and C. L. Drake (Eds.), The geology of continental margins. Springer, New York. pp. 179-196.

Spieß, V. (1993). Digitale Sedimentechograpraphie - Neue Wege zu einer hochauflösenden Akustostratigraphie. Berichte Fachbereich, Geowissenschaften. Universität Bremen, Bremen. pp. 1-199

Trifunac, M. D., Hayir, A., and Todorovska, M. I. (2003). A note on tsunami caused by submarine slides and slumps spreading in one dimension with nonuniform displacement amplitudes. Soil dynamics and Earthquake Engineering 23, 41-52.

Tripsanas, E. K., Bryant, W. R., and Phaneuf, B. A. (2004). Slope instability processes caused by salt movements in a complex deep-water environment, Bryant Canyon area, northwest Gulf of Mexico. AAPG Bulletin 88, 801-823.

Vörösmarty, C. J., Fekete, B. M., Meybeck, M., and Lammers, R. B. (2002). Global system of rivers: Its role in organizing continental land mass and defining land-to-ocean linkages. Global Biogeochemical Cycles 14, 599-621.

Vorren, T. O., Laberg, J. S., Blaume, F., Dowdeswell, J. A., Kenyon, N. H., Mienert, J., Rumohr, J., and Werner, F. (1998). The Norwegian-Greenland Sea continental margins: morphology and Late Quaternary sedimentary processes and environment. Quaternary Science Review 17, 273-302.

Wilson, C. K., Long, D., and Bulat, J. (2004). The morphology, setting and processes of the Afen Slide. Marine Geology 213, 149-167.

Wissmann, G. (1982). Stratigraphy and Structural Features of the Continental Margin Basin of Senegal and Mauritania. In: U. von Rad, K. Hinz, M. Sarnthein, and E. Seibold (Eds.), Geology of the Northwest African Cantinental Margin. Springer-Verlag, Berlin. pp. 160-181.

Wynn, R. B., Masson, D. G., Stow, D. A. V., and Weaver, P. P. E. (2000). The Northwest African slope apron: a modern analogue for deep water systems with complex seafloor topography. Marine and Petroleum Geology 17, 253-265.

# 4 Sedimentation processes along the slope and rise offshore Uruguay inferred from reconnaissance high resolution seismic reflection survey

Andrew A. Antobreh, Sebastian Krastel and Volkhard Spieß

*To be submitted to Marine Geology*

## 4.1 Abstract

Our interpretation of recently acquired high resolution multichannel seismic reflection data from the continental margin off Uruguay suggests that sedimentation processes in the slope and rise areas, whilst dominated by gravity-driven processes, have been significantly influenced by bottom current activity and recent structural deformation in the margin. The highly unstable slope area is dominated by extensive mass sediment movements. In particular, several discrete slide and slump blocks, measuring >5 km in width and >70 ms TWT in thickness in dip direction, occur at the upper and middle slope. Downslope mass sediment movements have been facilitated by widespread lithological weak layers which serve as glide planes. The continental rise is dominated by widespread debris flow deposits occurring as stacks of lenses, extensive sheet-like forms and massive bodies separated by thin veneers of well-layered hemi-pelagic deposits. Three regionally traceable seismic reflectors associated with hemi-pelagic deposition, group the debris flow units into distinct stratigraphic horizons.

Build-up of excess pore pressure, mainly from entrapped water during the rapid sediment accumulation and decayed organic matter from terrigenous inputs as well as high productivity, appears to constitute the most important trigger mechanism for large sediment failures in the margin. Though slope oversteepening may also be very important for triggering the large scale slope failures, its influence is mostly observed for the relatively smaller-scale failure events. Recent structural deformation in the margin has resulted in an intensely faulted and deformed bathymetric swell at the toe of the slope which now acts as a local topographic barrier to downslope sediment movement. The resulting rugged seafloor topography serves as a site for enhanced bottom current activity. Our study suggests that the slope has been unstable for quite a long time. The mass sediment movement events may have been dominant during lowered sea level stages, and curtailed during the subsequent rise in sea level when sedimentation was dominated by hemi-pelagic deposition.

Keywords: slide blocks, weak layers, glide planes, debris flows, bottom current, slope oversteepening, excess pore pressure.

## 4.2 Introduction

Huge quantities of terrigenous sediments discharged into the South Atlantic by the Rio de la Plata are swept northwards from the estuary by longshore currents, and deposited at the Uruguayan continental shelf and slope (Lonardi and Ewing, 1971, Spiess et. al., 2002). The high rate of sediment accumulation is accompanied by high water retention and low sediment rigidity. Consequently, the deposits become potentially unstable on the steep slope and often result in extensive mass wasting activities (Klaus and Ledbetter, 1988; Spiess et. al., 2002). In addition, the Uruguayan continental margin is uniquely located within a region of intense oceanic mixing (Fig. 4.1) involving south-flowing tropical and north-flowing Antarctic water masses (Peterson and Stramma, 1991).

Current knowledge about the sedimentation processes along the Uruguayan margin has largely been derived from more regionally based studies of the Argentine margin and related provinces (e.g., Lonardi and Ewing, 1971, Ewing and Lonardi, 1971, Klaus and Ledbetter, 1988, Milliman, 1988). However, the complexity of sedimentary structures along the slope and rise (Lonardi and Ewing 1971) and the strong influence of bottom current activity in the region (Peterson and Stramma, 1991) call for a more focused study in order to afford reliable interpretations of the factors and processes that have governed the sedimentary dynamics of the margin. This is especially important for a better understanding of the sedimentation process history of the region which is crucial for resolving the palaeoceanographic circulation patterns as well as climatic events in the South Atlantic since the late Neogene.

From their regional study of deep-sea sedimentary processes in the Argentine Basin using 3.5 kHz echograms, Klaus and Ledbetter (1988) identified large mass flow deposits east of the Rio de la Plata and the adjacent abyssal plain. Interpretations of Parasound sediment echosounder data by Bleil et al. (1994) and Hensen et al. (2003) also suggest frequent and widespread downslope mass movements of the near-surface sediments in the margin. Widespread episodic downslope mass sediment movement events have been recognised in many passive continental margins, e.g., the eastern Scotian margin (Piper and Ingram, 2003), the New Jersey continental margin (McHugh et al., 2002), the Norwegian-Greenland Sea continental margins (Vorren et al., 1998), the northwest African (Wynn et al., 2000) and the northeast Atlantic continental margins (Weaver et al., 2000), and are perceived as being important components of the modern stratigraphic record. Consequently, the events have been associated with global climatic cycles, particularly sea level changes (McHugh et al., 2002). In recent years, the growing interest in the study of mass sediment transport processes has

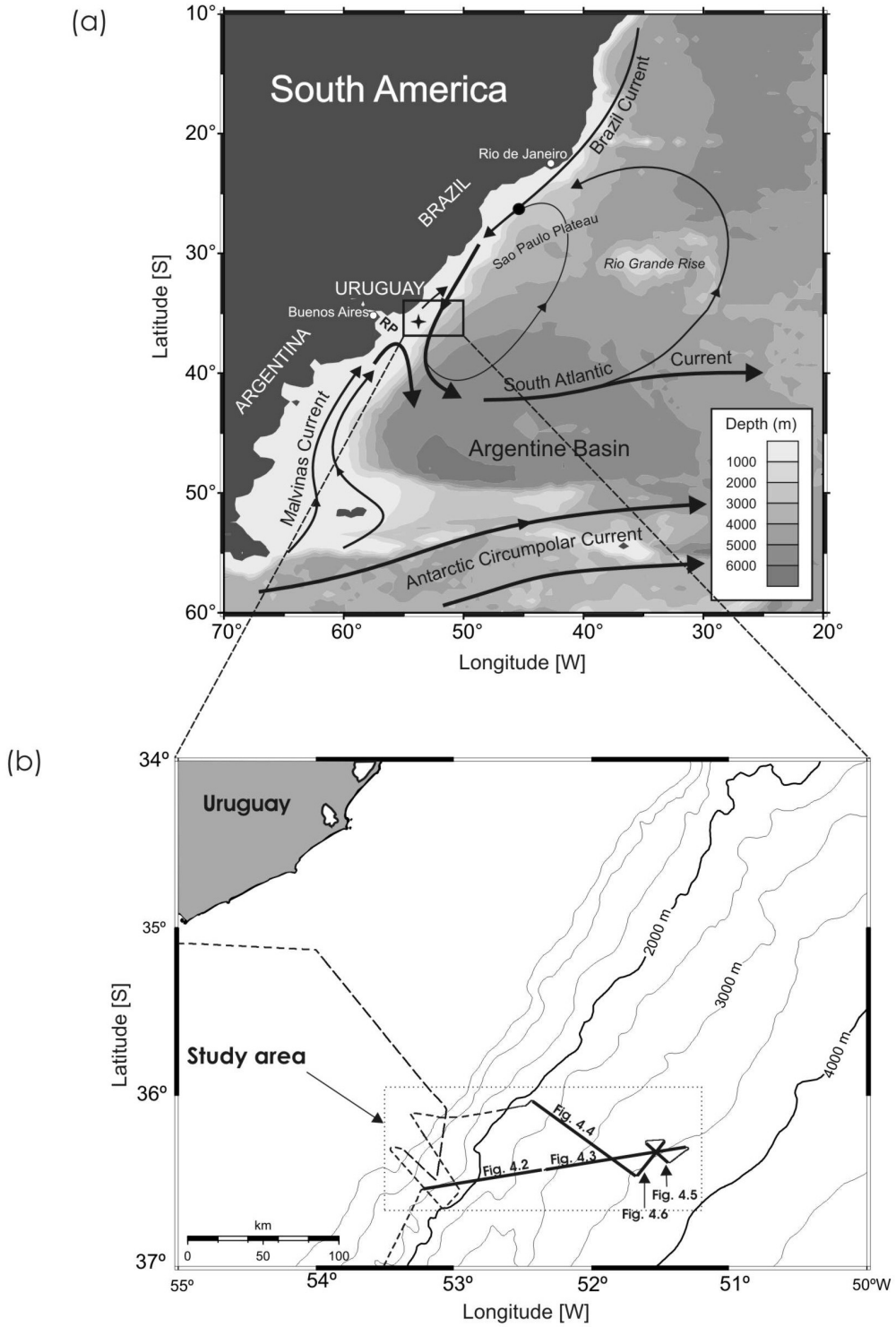


***Figure 4.1:*** *(a) General bathymetry of SW Atlantic continental margin showing the location of study area (in box) in relation to large-scale upper-level current circulation patterns in the South Atlantic Ocean (modified after Peterson and Stramma, 1991 and Wefer et al., 1999). RP = Rio de la Plata estuary; Black star = location of recent recorded seismicity in the margin (U.S.G.S., 2004). (b) Bathymetric map of a close-up of the study area (Gebco, 2003), enclosed in dotted-line box, showing Meteor Cruise M49/2 ship track lines. Locations of selected high resolution MCS profiles presented in this study are shown in thick black lines.*

further been boosted by their crucial importance in geo-hazard assessment studies for engineering and environmental projects connected with offshore economic resource exploitation and development (Baraza et al., 1999, Piper and Ingram, 2003). Furthermore, several analyses aim at studying the tsunami generation potential of the failed sediments (e.g., Dawson, 1999; Fryer et al., 2003; Trifunac et al., 2003; Fine et al., 2004).

In this present study, we interpret reconnaissance high resolution multi-channel seismic reflection (MCS) data, to investigate slope processes and sedimentation patterns along the Uruguayan continental margin. In particular, we analyse the mechanisms of mass sediment transport and re-deposition along the slope and rise, and attempt to derive their relationships with sea level fluctuations, bottom current circulation and structural deformations.

## 4.3 Physiography and oceanographic setting

The study area is located within 36° - 37° S and 51° - 53° 30’ W along the Uruguayan continental margin (Fig. 4.1). The area is slightly to the northeast of the Rio de la Plata estuary. Structurally, the Uruguayan margin is located in the northwestern part of the continental rim of the extensive Argentine Basin. Descriptions of the main physiographic features and sedimentary structure of the Argentine margin and related provinces are provided by Lonardi and Ewing (1971) and Ewing and Lonardi (1971). In the study area, the shelf break occurs between 130 and 150 m, and is thought to coincide with a relict erosional surface. From a relatively wide width of up to ~300 km south of 38° S, the shelf becomes narrower north of this point to widths <150 km offshore Uruguay. At the same time, the slope becomes broader northwards from the Uruguayan margin. In the interval between 36° 30’ and 37° 10’, the slope is quite steep, attaining 3 – 3.5° around 2500 m water depth. Several submarine canyons incise the slope and rise off the Rio de la Plata. The continental rise is characterised by a gentle gradient and occurs from depths around 2900 m seaward. The presence of the N-S striking Polonio Fault (Ewing and Lonardi, 1971), which cuts across the slope and rise north of the Rio de la Plata, and other minor faults observed on the slope off the Rio de la Plata, might provide indications of a recent tectonic event along the margin.

The Uruguayan margin, together with the adjacent lying southern Brazilian and Argentine margins, is situated within the confluence region of intense mixing of oceanic currents (Fig. 4.1) where the northward flowing cold Antarctic water masses of the Falkland (Malvinas) Current meet the southward flowing warm and saline tropical waters of the Brazil Current (Peterson and Stramma, 1991). These mixing water masses control the dynamics of

the upper-level current regimes, and the front separating them currently migrates between 32° and 40° S in response to the relative strengths of the currents (Olson et al., 1988). Apart from giving rise to a high regional productivity, the intense mixing leads to increases in current velocities extending to the seafloor (Antoine et al., 1996; Peterson et al., 1996). Along the shelf and upper slope offshore Uruguay, the increased current velocities are thought to be mainly responsible for winnowing and re-distribution of the huge terrigenous sediment inputs received from the Rio de la Plata (Peterson et al., 1996). The confluence region is also set within the crossroads of several major deep-water masses including the northward flowing Antarctic Intermediate Water (AAIW) and the southward flowing North Atlantic Deep Water (NADW) operating between 500 – 4000 m water depths. In addition, from water depths below 3800 – 4000 m, current circulation is dominated by the Antarctic Bottom Water (AABW) which forms a strong deep-water circulation gyre centred around the Argentine Basin (Reid, 1989; Flood and Shor, 1988; von Lom-Keil et al., 2002).

**4.4 Seismic data**

Our study is based on MCS data acquired offshore Uruguay during R/V Meteor Cruise M49/2 undertaken by the University of Bremen in February 2001. The data were primarily collected as part of a larger geophysical survey of the South Atlantic continental margins in connection with a pre-site survey for the ODP (Ocean Drilling Program) drilling proposal 'Brazil-Falkland (Malvinas) Confluence: Paleoceanography of a Mixing Region' prepared by Wefer et al. (1999). Seismic data recorded within the study area comprised ~325 km total length of profiles, and coverage included areas in the upper slope, at ~1200m water depth, down to the continental rise, at ~3600 m water depth.

The data were acquired using a 1.7 l GI-Gun as seismic source. The gun was shot at ~25 m intervals, being operated by a high pressure air of 150 bar. A 600 m-long Syntron streamer, equipped with separately programmable hydrophone subgroups, was used to receive the data. Recording was done by 48 groups at a group distance of 12.5 m. The data were digitally recorded at a sampling frequency of 4 kHz over 3 s time. Positioning was based on GPS (Global Positioning System). The MCS data were processed using a combination of 'in-house' and the 'Vista' (Seismic Image Software Ltd) softwares. Processing procedures involved trace editing, setting up geometry, static and delay corrections, velocity analysis, normal moveout corrections, bandpass frequency filtering, stack and time migration. A CMP spacing of 10 m was used throughout.

## 4.5 Results and data interpretation

We present four dip-oriented seismic profiles, GeoB01-147a, GeoB01-147b, GeoB01-149 and GeoB01-152 (Figs. 4.2 – 4.5), and one strike-oriented profile, GeoB01-151 (Fig. 4.6), to describe the dominant features and that characterize the shallow sedimentary structure of the continental slope and rise areas of the Uruguayan margin. The seismic data have generally afforded a high resolution image of the sedimentary features within the upper ~600m (i.e., 800 ms TWT) of the seafloor cover.

### *4.5.1 Continental slope*

Profile GeoB01-147a (Fig. 4.2) extends from the upper slope area at a water depth of ~1150 m down to the upper rise at a water depth of ~2900 m. The roughly ENE-WSW oriented profile is slightly oblique to the margin. The profile shows that the sedimentary cover of the slope, i.e., from Shot Points 0 - 4000, is made up of a thick sediment package (>400 ms TWT) characterised seismically by parallel to sub-parallel well-layered medium to high amplitude reflectors which are intercalated by thin units (<70 ms TWT) of very low amplitude to transparent reflection events. The continuity of these slope reflection events, especially in the steepest part of the slope between Shot Points 2200 and 4000, is interrupted by several glide planes and listric faults. The well-layered reflectors are sharply truncated in the upper slope, e.g., between Shot Point 1800 and 2500, by what appears to be buried slide or slump scars, and in the uppermost slope, the sediment package is down-faulted into a depression measuring ~6 km wide and >50 m deep. The entire seafloor of the slope, especially between Shot Points 800 to 3700, is disrupted by a number of scars. In addition, the seafloor morphology displays several isolated blocks, some with disturbed internal structure, which measure up to 5 km wide and 70 ms TWT. We interpreted these as either slump or slide blocks.

At the lower part of the slope, a broad updomed zone, ~30 km wide, is seen to occur between Shot Points 4000 and 7000. This zone which is associated with a number of fault-bounded blocks, shows intense deformation as well. To the immediate west of Shot Point 4000, a wedge shaped down-faulted block, ~ 4 km wide and bounded in the west by shallow faults, shows slightly folded internal reflectors. Lying immediately east of this block, is a much larger block, ~9 km wide, characterised by intensely folded and deformed, very low amplitude internal reflectors. This second block is bounded by very steeply dipping to near-vertical faults. The intensity of folding within the block appears to progressively increase upwards. The two blocks appear to be downthrown in a step-wise fashion forming a ~16 km

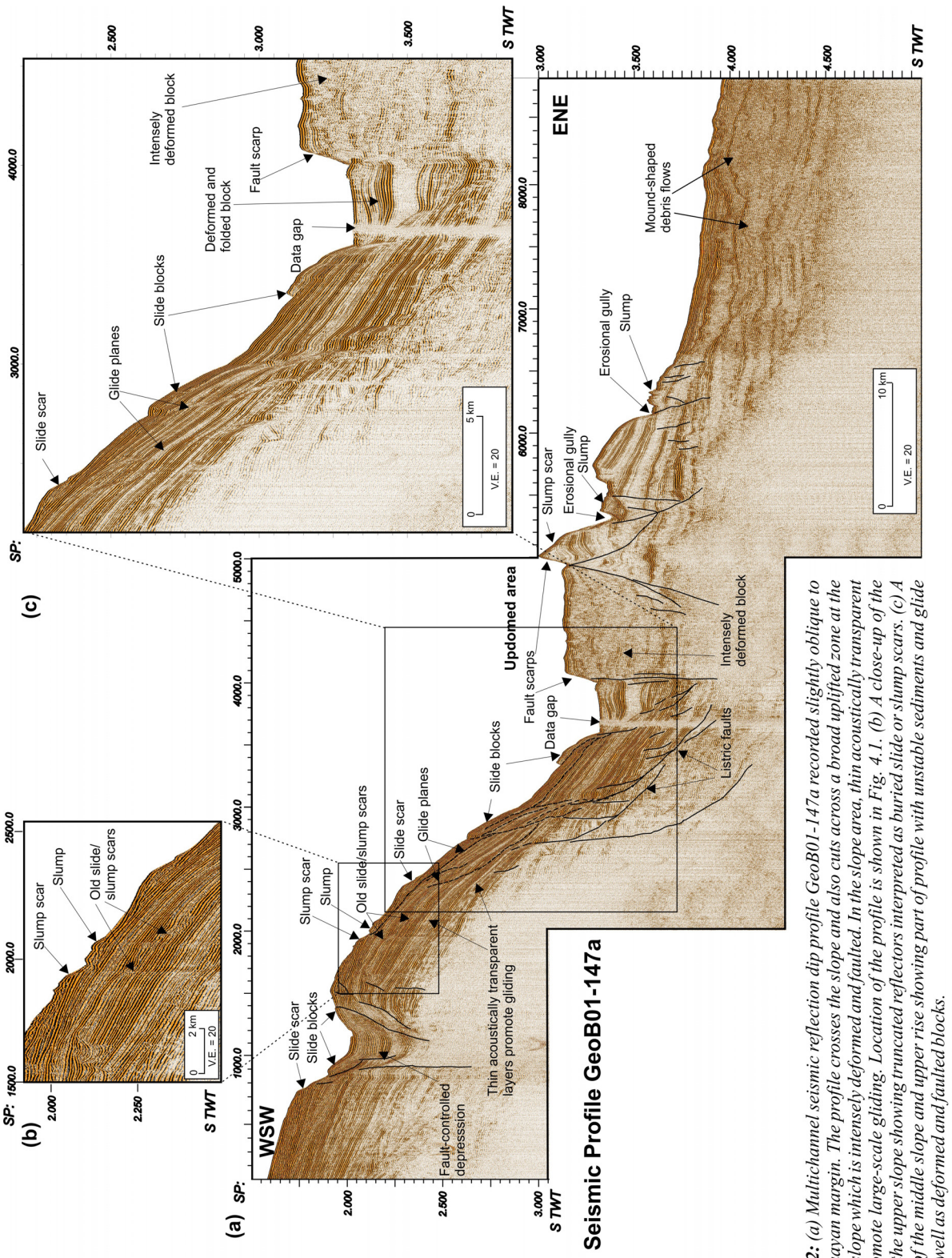


***Figure 4.2:*** *(a) Multichannel seismic reflection dip profile GeoB01-147a recorded slightly oblique to the Uruguayan margin. The profile crosses the slope and also cuts across a broad uplifted zone at the toe of the slope which is intensely deformed and faulted. In the slope area, thin acoustically transparent layers promote large-scale gliding. Location of the profile is shown in Fig. 4.1. (b) A close-up of the profile in the upper slope showing truncated reflectors interpreted as buried slide or slump scars. (c) A close-up of the middle slope and upper rise showing part of profile with unstable sediments and glide planes as well as deformed and faulted blocks.*

wide depressed zone. Another fault-bounded block is seen close to Shot Point 5000. This block which is wedge-shaped, tapers from a >7 km base to less than 2.5 km in its upper part, and internally displays folded and deformed low to medium amplitude reflections. The upper surface of this wedge-shaped block shows a scar. A sediment slump which displays chaotic internal and blocky surface reflections is observed to the immediately east of the seafloor scar. This slump material is associated with a gully which coincides with the upward trace of a fault. To the east of the wedge-shaped block is a much broader block, ~ 9 km wide. This block is, however, less deformed and displays thin (<100 ms TWT) units of well-layered medium amplitude reflectors separated by thicker (up to 200 ms TWT thick) very low amplitude to transparent reflection zones. The eastern surface of this block also shows a scar and a gully associated with faulting. Again, a sediment slump with a blocky seismic structure at its upper surface is observed immediately to the east of the scar. East of Shot Point 6700, and within what appears to be the transition to the continental rise, the area is dominated by widespread debris flow deposits acoustically imaged as several stacked units of chaotic to transparent internal reflections often with mound-shaped external geometry. The deposits are draped on the seafloor by a thin, well-layered medium to strong amplitude reflector packet which in-fills a locally depressed zone between Shot Point 6500 and 8300.

### *4.5.2 Continental rise*

All the profiles located in the continental rise (Figs. 4.3 – 4.6), show the presence of widespread debris flow deposition. The debris flow deposits are imaged predominantly as stacks of acoustically chaotic to transparent lenses, as well as massive units of very weak or chaotic reflections, separated by thin veneers of well-layered medium to strong amplitude reflectors. The dip-oriented profiles GeoB01-147b (Fig. 4.3) and GeoB01-152 (Fig. 4.4) show that the debris flow units assume more sheet-like geometry seaward from the mainly mound-like shapes which characterise the upslope deposits, e.g., as described earlier in the easternmost part of Profile GeoB01-147a (Fig. 4.2).

The debris flow units appear to group within a number of distinct stratigraphic horizons whereby the base of each group of debris flows is defined by a key reflector which separates it from an underlying thin sediment veneer. We recognise at least three key reflectors which are traceable in the dip-oriented profiles in the rise (Figs. 4.3 – 4.5) as well as the strike-oriented profile (Fig. 4.6) over a wide area in the continental rise. We denote these reflectors, from the deepest to the shallowest, as DR, MR and SR respectively.

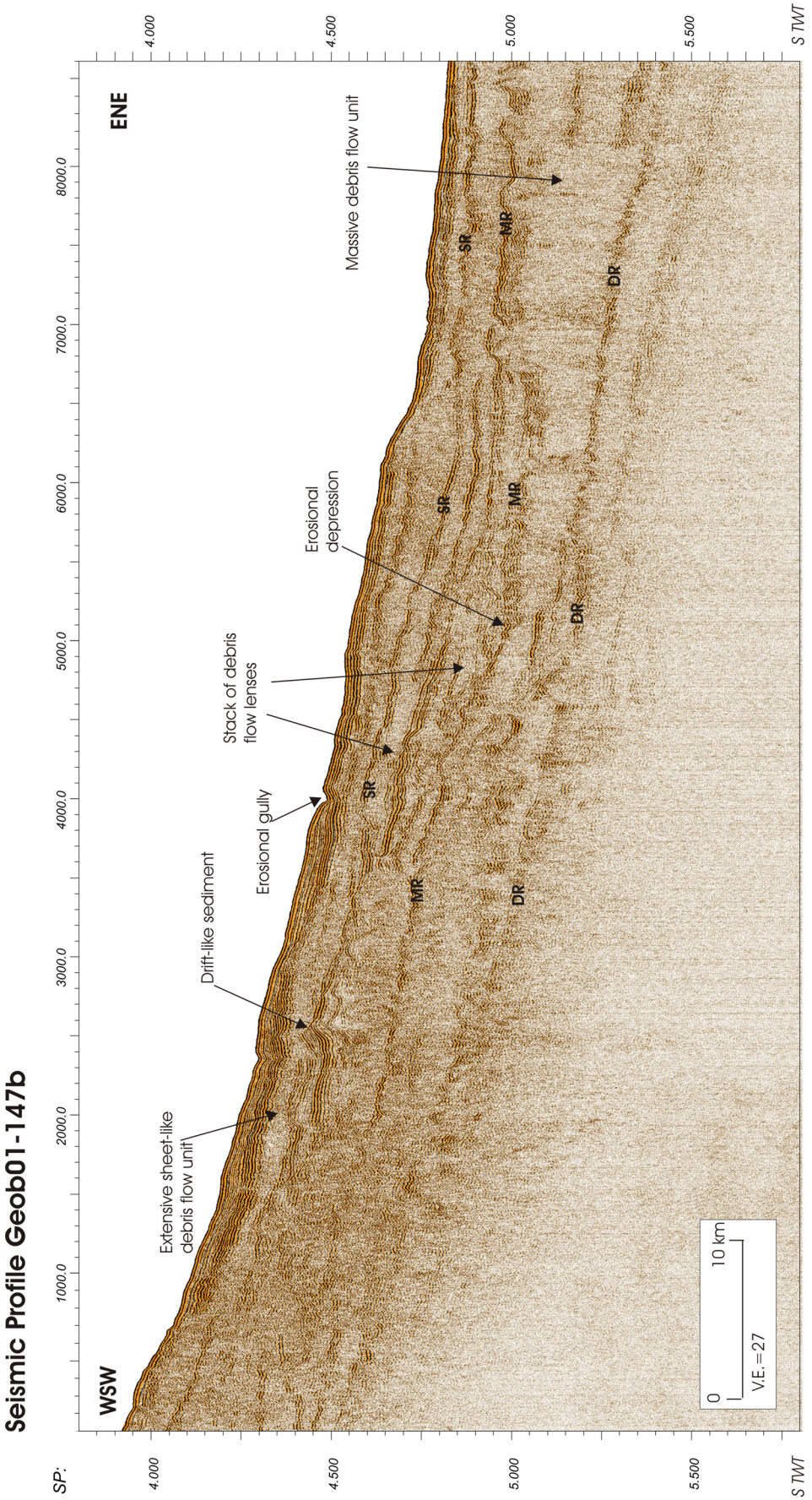


***Figure 4.3:*** *Multi-channel seismic reflection dip profile GeoB01-147b, which is an extension of GeoB01-147a into the continental rise. The profile is dominated by different forms of debris flow deposits, here imaged as massive as well as stacks of lens-shaped and sheet-like bodies with acoustically chaotic to transparent internal reflections. The deposits are separated by thin veneers of well-layered reflections, with the most prominent of them giving rise to three widely traceable key reflectors, DR, MR and SR. Location of the profile is shown in Fig. 4.1.*

Reflector DR is generally characterised by a blocky and hyperbolic seismic reflection signature upslope (Figs. 4.3 and 4.4), but which becomes slightly undulating seaward, e.g. as observed on Profile GeoB01-149 (Fig. 4.5). In dip profiles (Figs. 4.3 – 4.5), DR has quite a low relief, which is sub-parallel to the seafloor. It is moderately continuous within the rise, and can be traced with a fair degree of confidence from depths >5400 ms TWT upslope to depths of ~4500 ms TWT (Fig. 4.3) beyond where the reflection becomes generally weaker, and is eventually lost. DR is in places associated with broad depressed zones, up to 30 km wide and >50 m deep, e.g. between Shot Points 2000 – 5000 in Profile GeoB01-152 (Fig. 4.4). DR is overlain by a generally thick, relatively massive sheet of debris flow unit which may attain up to 300 ms TWT thick, although it shows what appears to be several sections of intense erosion (Figs. 4.3 – 4.6). Strike profiles (Figs. 4.3 and 4.4) show that this unit can be followed more than 80 km downslope from the upper rise. However, we do not know how far the unit continues downslope due to missing data coverage in water depth >3600 m.

Reflector MR is also characterised by blocky and irregular reflection signature upslope (Figs. 4.3 and 4.4) but develops broader waveforms seaward, with wavelengths reaching up to 2.5 km, e.g., Profile GeoB01-149 (Fig. 4.5). The waveforms commonly form the upper surface of drift-like bodies which internally display well-stratified wavy medium amplitude layers (Figs. 4.3 – 4.5) with upslope migration (Fig. 4.5). The reflector is also generally sub-parallel to the low seafloor relief, and may be followed within the rise from ~5000 ms TWT depth (Figs. 4.3 and 4.4) upslope with a good degree of confidence to the slope/rise transitional area (Fig. 4.3), where it is lost among the several other strong reflections that bound the mound-shaped debris flow lenses. MR is also locally associated with depressed zones (Figs. 4.3, 4.4 and 4.6). The immediately overlying debris flow package is especially characterised by several relatively large discrete flat lenses, >32 km long and <70 ms TWT thick, some of which locally infill the underlying depressed zones.

The shallowest reflector, SR, has a relatively linear seismic signature upslope which gradually develops into smaller waveforms in deeper waters (Figs. 4.3 – 4.5). Locally, SR is associated with drift-like bodies which measure up to 17 km wide (Fig. 4.3). SR has good continuity and may be traced from within ~4900 ms TWT in the rise, close and sub-parallel to the seafloor, with a good degree of confidence up to the lower slope where its continuity is lost under the deformed zone (Fig. 4.2). The overlying debris flow unit is particularly extensive and sheet-like, and is ~ 100 ms TWT thick and exceeds 80 km long in strike profiles (Figs. 4.3 and 4.4). The top of this debris flow sheet is dominated by irregular, often relatively smaller blocky and hyperbolic reflection events. The unit is draped on the seafloor

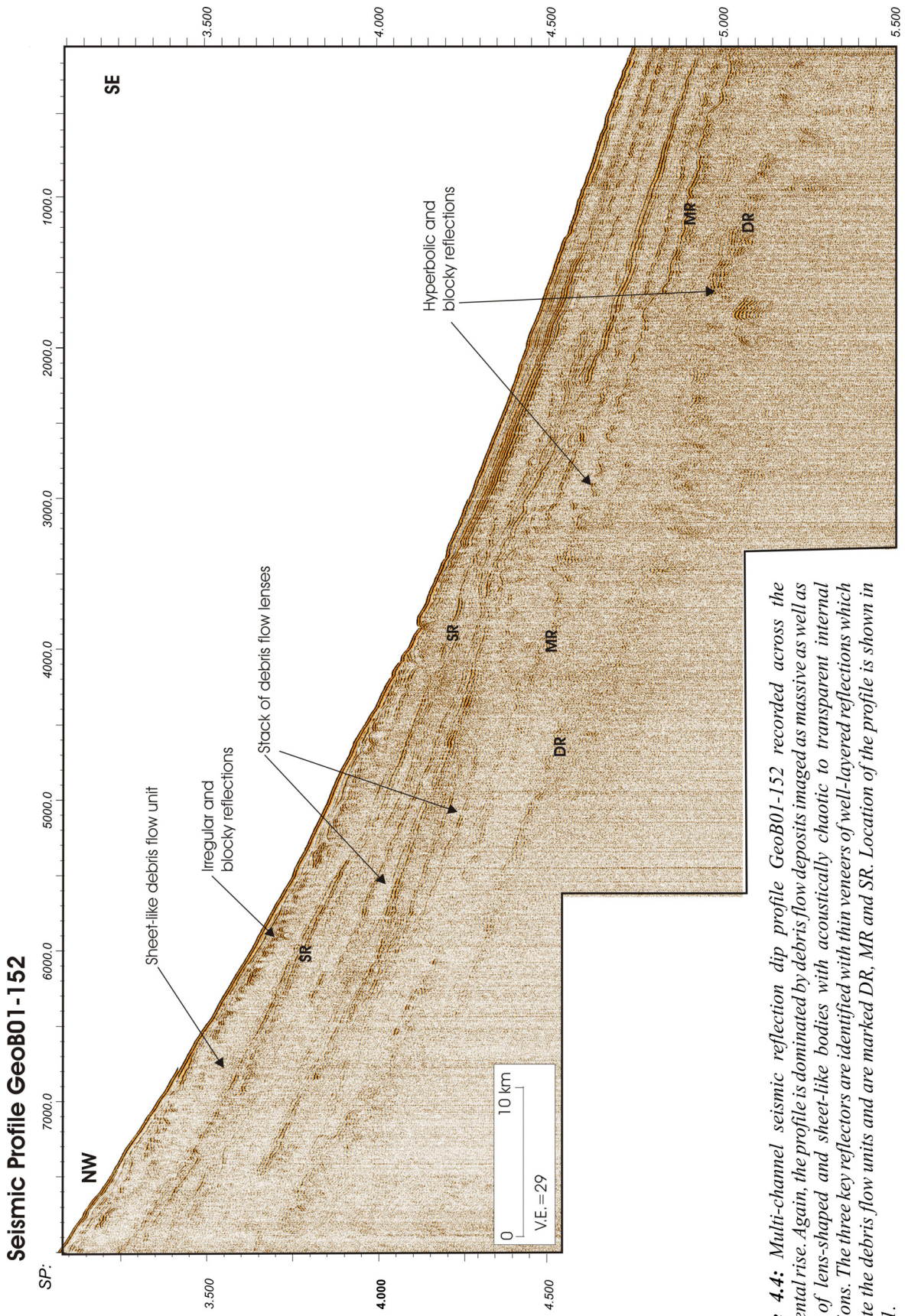


***Figure 4.4:*** *Multi-channel seismic reflection dip profile GeoB01-152 recorded across the continental rise. Again, the profile is dominated by debris flow deposits imaged as massive as well as stacks of lens-shaped and sheet-like bodies with acoustically chaotic to transparent internal reflections. The three key reflectors are identified with thin veneers of well-layered reflections which separate the debris flow units and are marked DR, MR and SR. Location of the profile is shown in Fig. 4.1.*

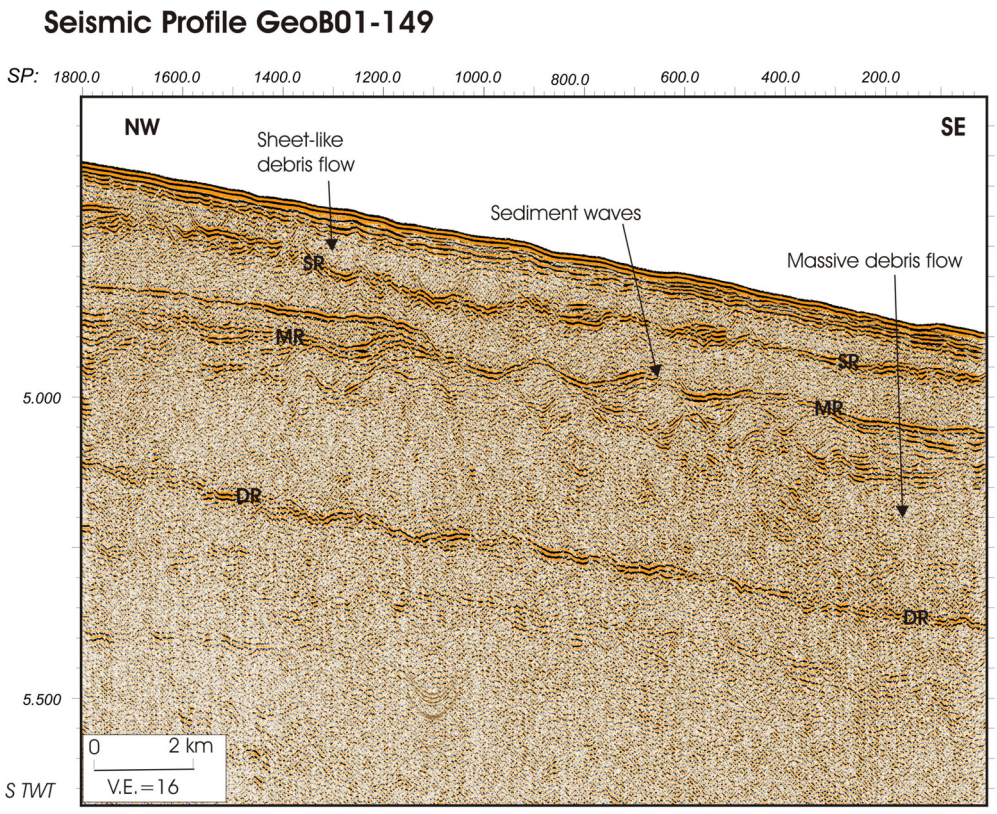


***Figure 4.5:*** *Multi-channel seismic reflection dip profile GeoB01-149 located slightly deeper in the rise. Here, the three key reflectors, DR, MR and SR, are very prominent and show various waveforms. The interval between DR and MR is dominated by a massive debris flow unit. Location of the profile is shown in Fig. 4.1.*

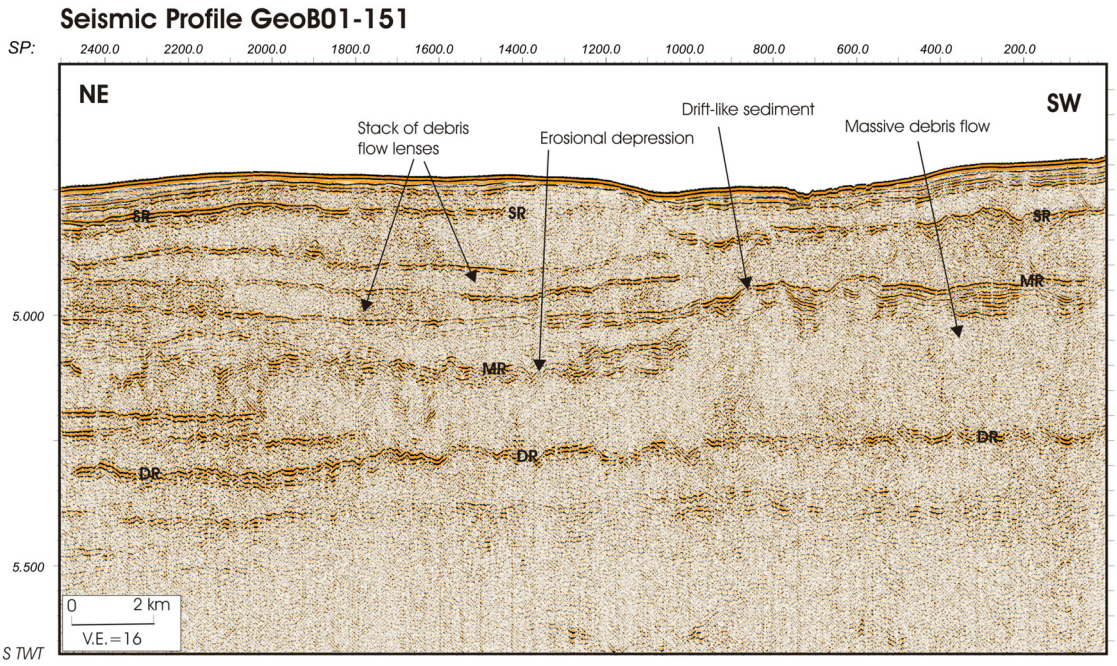


***Figure 4.6:*** *Multi-channel seismic reflection strike profile GeoB01-151 also recorded in the continental rise. Again, the three key reflectors, DR, MR and SR, are associated with thin veneers of well-layered reflections which separate the debris flow units. We also notice the massive debris flow unit between DR and MR. Location of the profile is shown in Fig. 4.1.*

by an acoustically well-stratified thin sheet (<70 ms TWT) of medium to high amplitude reflection events which may thicken to infill locally depressed zones. The seafloor sediment layers are locally associated with gully-like features (Fig. 4.4).

## 4.6 Discussion

### *4.6.1 Patterns of debris flow deposition*

Our data (Figs. 4.2 – 4.6) show the increasing dominance of debris flow deposition from the lower slope towards deeper waters. The continental rise, especially, is dominated by widespread debris flow deposits which occur in various forms including stacks of lenses, extensive sheet-like forms and massive bodies separated by thin veneers of well-layered hemi-pelagic deposits. The mound-shaped geometry displayed by the deposits in the upper rise might have been locally induced by slow creeping of sediments on the eastern flank of the bathymetric swell.

The three key reflectors, DR, MR and SR, identified with the debris flow units in the rise, group the units under at least four major depositional periods. The morphology, scale and surface boundary characteristics displayed by the upper surface of the different groups of debris flow units in seismic profiles, suggest that they formed through the deposition of sediments sourced from different scales of mass sediment failures in the slope.

The extensive blocky and hyperbolic seismic signature displayed by the deepest reflector, DR, suggests that the reflector constitutes the upper surface of an underlying extensive group of debris flow units that is probably dominated by massive bodies, but whose geometry is unresolved by the limit of seismic penetration. We note also that the upper surface of the debris flow units that overlie reflector DR is similarly associated with extensive blocky and hyperbolic reflection events. This group has been shown to be dominated by massive debris flow units with only a few lenses in places (Figs. 4.3, 4.4 and 4.6). We speculate that the deposition of these two earliest dominantly massive debris flow deposits, involved huge volumes of mass sediment movement and included several large sediment block fragments. The mass sediment flows must have been sourced mainly from large-scale or catastrophic sediment failure events in the slope and probably shelf areas, punctuated only by intermittent small scale failure events which we associate with the few debris flow lenses.

In contrast to the earliest massive debris flow units, the deposits which lie between reflectors MR and SR have been shown to be dominated by several stacked lenticular shapes suggesting that their deposition involved sediments derived mainly from repeated and relatively smaller-scale slope failures. Consequently, the deposition of these debris flow

lenses probably resulted predominantly from the persistent release of discrete slide or slump blocks in the slope. The data show that the youngest debris flow deposit, i.e. which overlies reflector SR, is sheet-like and quite extensive. The irregular, often blocky and hyperbolic seismic signature of its upper surface imply that this unit also contains several block fragments. However, quite unlike the two earliest debris flow deposits, this unit probably contains a greater percentage of smaller block fragments, as depicted by the seismic signature. Large sediment volumes are known to give rise to increased sediment flow mobility (Laberg and Vorren, 1995). That both the earliest and most recent debris flow units can be followed downslope over 80 km from the upper rise, implies that their depositional events involved the movement of large volumes of sediment, thereby favouring long run-out distances of the mass sediment flows.

### *4.6.2 Source of the debris flows and pre-conditioning for mass sediment failure*

The mostly well-layered nature of the slope sediments in Profile GeoB01-147b (Fig. 4.2) suggests relatively long periods of uninterrupted sediment accumulation in this area. In addition, we see no indications like remnants of major headwall scars in this part of the slope to suggest previous removal of huge volumes of sediments. Hence, whereas the profile shows indications of recent instability and downslope mass sediment movement in the slope area, it is unlikely that this portion of the Uruguayan slope has been the main sediment source for the extensive debris flow units seen in the rise. However, because of the paucity of data in the adjacent slope areas, we can only speculate that the bulk of the debris flow sediments has been sourced from the slope and shelf areas to the immediate north of Profile GeoB01-147b (Fig. 4.2). Presumably, this area is the most likely source area for the debris flow sediments as sediments remobilized immediate north of Profile GeoB01-147b and following the maximum slope gradient would be re-deposited in the debris flow area surveyed by us. We also note that unlike the slope areas off the Rio de la Plata and the adjacent south where downslope sediment transport is facilitated by several deeply incised canyons, the absence of any major canyon systems in the study area must have created a depositional environment that allowed rapid and widespread sediment accumulation in an open slope setting. It is from this setting that the failed sediments moved downslope towards the southeast direction to the present depositional area in the rise.

Our slope profile (Fig. 4.2) clearly shows that the entire slope is currently undergoing extensive gravity-controlled mass sediment movement occurring both as large-scale and relatively smaller-scale sediment failures in the form of slides and slumps. Our interpretation

suggests that the thin acoustically transparent layers, which alternate with the thick well-layered high amplitude reflection packages, are associated with widespread sediment glide planes in the slope area. We accordingly interpret these thin layers as lithological planes of weakness which promote widespread slope instabilities in the area. Similar examples where thin mud-rich sediment layers have facilitated large slope failures of thick well-stratified sand rich turbidites have been reported elsewhere, e.g., in the Barents Sea (Laberg and Vorren,1996) and the Aegean Sea (Perissoratis and Papadopoulos, 1999; Lykousis et al., 2002). The rapid deposition of huge quantities of fluvial sediments along the Uruguayan margin from the Rio de la Plata would have favoured the formation of thin clay-rich sediment layers within thick well-layered, probably, sand-rich sediment packages. The depositional setting along the Uruguayan margin would therefore have already pre-conditioned the slope area for massive sediment instability, and thus needed only a trigger mechanism to set off the massive sediment failures.

### *4.6.3 Possible trigger mechanisms for the mass sediment movement*

We list potential trigger mechanisms for the failure events along the margin including slope oversteepening, build-up of excess pore pressure and earthquakes. The several isolated blocks which characterise the present upper slope seafloor morphology have been identified as either slide or slump blocks. The presence of slide/slump scars immediately upslope of these blocks and the fact that most of the blocks have their layered internal structure preserved, suggest that they may have been recently released, having moved only short distances away from their points of release. Again, the presence of buried slump/slide scars in older well-stratified sediments of the steeper parts of the upper slope indicates that the slope had in previous times persistently released several of similar sediment slides and slumps. It is also likely that a number of the subsequent failures had been induced by locally increased slope gradients created from earlier scars. That the scars are particularly widespread in the steep upper slope areas, suggests that slope oversteepening from the rapid sediment accumulation constituted a very important triggering mechanism for sediment failures in the slope area. Our data also show that the downslope movement of sediment blocks in the slope area are also associated with widespread faulting most of which we interpret as listric growth faults. These faults may have contributed in oversteepening the slope so as to trigger off sediment failure.

Build-up of excess pore-pressures is known to be capable of triggering sediment failures (Laberg and Vorren, 1995; Vorren et al., 1998). The large fluvial terrigenous

sediments supplied to the margin by the Rio de la Plata would have included significant amounts of organic-rich material (Lonardi and Ewing, 1971, Spiess et. al., 2002; Hensen et al., 2003). In addition, we note that the Uruguayan margin is located within a region of high primary productivity as arising from intensely mixing surface waters (Behrenfeld and Falkowski) which would also give rise to additional large export of organic matter to the seafloor (e.g. Hensen et al., 2003). Consequently, increased pore pressure would have been generated from bogenic gas formed through the decomposition of organic matter (Hensen et al., 2003) as well as the high amounts of water entrapped during the rapid sediment build-up. In addition, rapid falls in sea level have been shown (e.g. Lee et al., 1996) to directly lead to a lowering of hydrostatic pressure on near-bottom seafloor sediments, thus generating excess pore pressures within the sediments. The influence of sea level fluctuations on sedimentation in the margin (discussed in the next section) is also likely to be another potential source for episodic build-up of high pore pressures in the upper sediment layers. Though our data do not show any clear evidence of gas charged sediments, the several potential sources of excess pore-pressure generation in the margin suggest that build-up of excess pore pressure may be the most important trigger mechanism for mass sediment failure along the margin.

Evidence of recent seismicity in the vicinity recorded during the last 30 years (U.S.G.S., 2004) suggests earthquakes as a possible triggering mechanism for some of the slope sediment failures in the area. Since sedimentation in the margin had already pre-conditioned the slope for sediment instability, especially with the introduction of widespread lithological weak layers, a number of even small single earthquakes, occurring in succession, could potentially trigger large-scale failures (e.g. O'Leary 1991; Laberg and Vorren, 2000). The sustained seismic shaking would have caused continued deterioration of the shear strength along failure planes (Laberg and Vorren, 2000). Consequently, large slabs of sediment are released in the slope, and these undergo progressive fragmentation as they move downslope subsequently evolving into debris flows. In the absence of sufficient data about the earthquake history in the margin, however, we can only speculate about earthquakes as a potential trigger mechanism for failures in the margin.

### *4.6.4 Sea level fluctuations and bottom current influence on sedimentation*

The presence of alternating thin acoustically transparent layers within thick well-layered high amplitude reflection packages that dominate the thick slope sediments (Fig. 4.2) suggests that the margin has experienced marked cyclicity in sedimentation patterns probably in response to glacial eustatic controls on the sedimentary environment, as similarly reported,

e.g., in the Aegean Sea (Lykousis et al., 2002). We interpret the deposition of the thick well-layered high amplitude reflection packages as representing periods of increased sediment influx of mainly coarse-grained or sand-rich terrigenous sediment into the margin. These periods correspond to stages of glacial sea level lowstands when the exposed proximal margin was likely to have received huge quantities of terrigenous sediment supplies. The thin transparent layers represent deposits of fine-grained or mud-rich material associated with the intervening periods of reduced sediment input under an inter-glacial sea level highstand regime.

Our seismic data show that most of the present seafloor, especially in the continental rise, is draped with a thin veneer of well-layered reflectors which may presumably represent hemi-pelagic sediment deposited under the recent interglacial highstand regime. Accordingly, we infer that the three key seismic reflectors, DR, MR and SR, identified in the rise, constitute the top of thin well-layered sediment veneers, and mark the end of relatively short intervals of hemi-pelagic sediment deposition of intervening highstand periods. Due to lack of borehole data in the vicinity, we are unable to determine the age calibration for the reflectors. However, we accordingly speculate that most of the debris flow depositional events occurred under glacial stages of falling sea level which generally followed the transient intervals of hemi-pelagic deposition.

We note that the Uruguayan margin is located within a region of intense oceanic mixing of major geostrophic currents (Fig. 4.1). Mixing of water masses of different origin are thought to generate drift-like morphologies in hemi-pelagic sediments (Knutz et al., 2002). Along the Uruguayan margin, the intervals of hemi-pelagic deposition coincided with periods of increased bottom water influence on sedimentation as depicted by the presence of erosional features, drift-like bodies and sediment waves, particularly, from water depths >3000 m (Figs. 4.3 – 4.6), possibly, in a current domain controlled by the NADW. However, interpretation of erosional features in Parasound profiles located in the adjacent slope south of the study area shows contour current activity extended upslope to about 850 m water depth (Bleil et al., 1994), and was probably influenced by the AAIW. Because reflectors MR and SR are associated with pronounced erosional depressions and better developed contourite drifts and sediment waves, their time were probably marked by the most intense bottom current activity. Apparently, with its better contourite development in the upper rise, SR time may have witnessed much stronger bottom current circulation in less deeper waters, i.e. around 3000 m water depth (Figs. 4.3 and 4.4). However, with its more pronounced erosional depressions and sediment drifts in the lower rise, MR time apparently produced the stronger bottom water

circulation in deeper waters, i.e. >3500 m water depth. These bottom water circulation regimes must have been governed by the NADW.

### *4.6.5 Influence of recent structural deformation on sedimentation*

Recent structural deformation of the proximal margin may have significantly influenced present sedimentation processes as well as bottom current activity in the region. Being located on the passive SW Atlantic margin, the Uruguayan margin is expected to generally remain tectonically stable during the post-rift period (Rabinowitz and LaBrecque, 1979 ). Consequently, the updomed area and associated faulting observed at the toe of the slope may be ascribed to gravitational gliding or spreading of the upper sediment layers over a weak regional detachment surface as similarly observed for passive deltaic margins e.g. the Gulf of Mexico (Cobbold and Szatmari, 1991) and the Niger Delta (Cohen and McClay, 1996). However, further evidence like the presence of a detachment plane, tilting of faulted blocks against listric faults as well as regionally remobilized salt or shale to facilitate such large-scale gravitational failure (Cohen and McClay, 1996; Mauduit et al., 1997) from more extensive, and probably deeper seismic survey method, would be required to substantiate a gravitational origin for this feature. Ewing and Lonardi (1971) provide some evidence for the N-S striking Polonio Fault, which they ascribe to possible tectonic origin. Therefore tectonics might have played a role during the evolution of the margin and the updomed area and associated faulting. However, for the scenario described above, additional deep seismic data would be necessary to support it.

Though the paucity of our data neither allows us to determine the areal extent of the updomed area on the lower slope nor the causes for this feature, our interpretation of Profile GeoB01-147a (Fig. 4.2) allows us to outline a schematic model (Fig. 4.7) to illustrate the influence of recent structural deformation observed in the area on sedimentation processes and bottom current activity along the margin. We are also aware that Profile GeoB01-147a is slightly oblique to the margin and therefore we would like to stress the fact that we only present a schematic model not taking into account the three-dimensionality of this problem.

The initial updoming process gave rise to a broad bathymetric swell, about 30 km wide, in the lower slope accompanied by widespread extensional faulting within the upper sediment layers (Fig. 4.7a). Downward movements of large faulted blocks along high angle faults (Fig. 4.7b) gave rise to the development of a graben and horst-like feature in the updomed area. The graben created at the toe of the slope must have induced massive downslope sediment movement in the slope area as a result of a local increase in seafloor

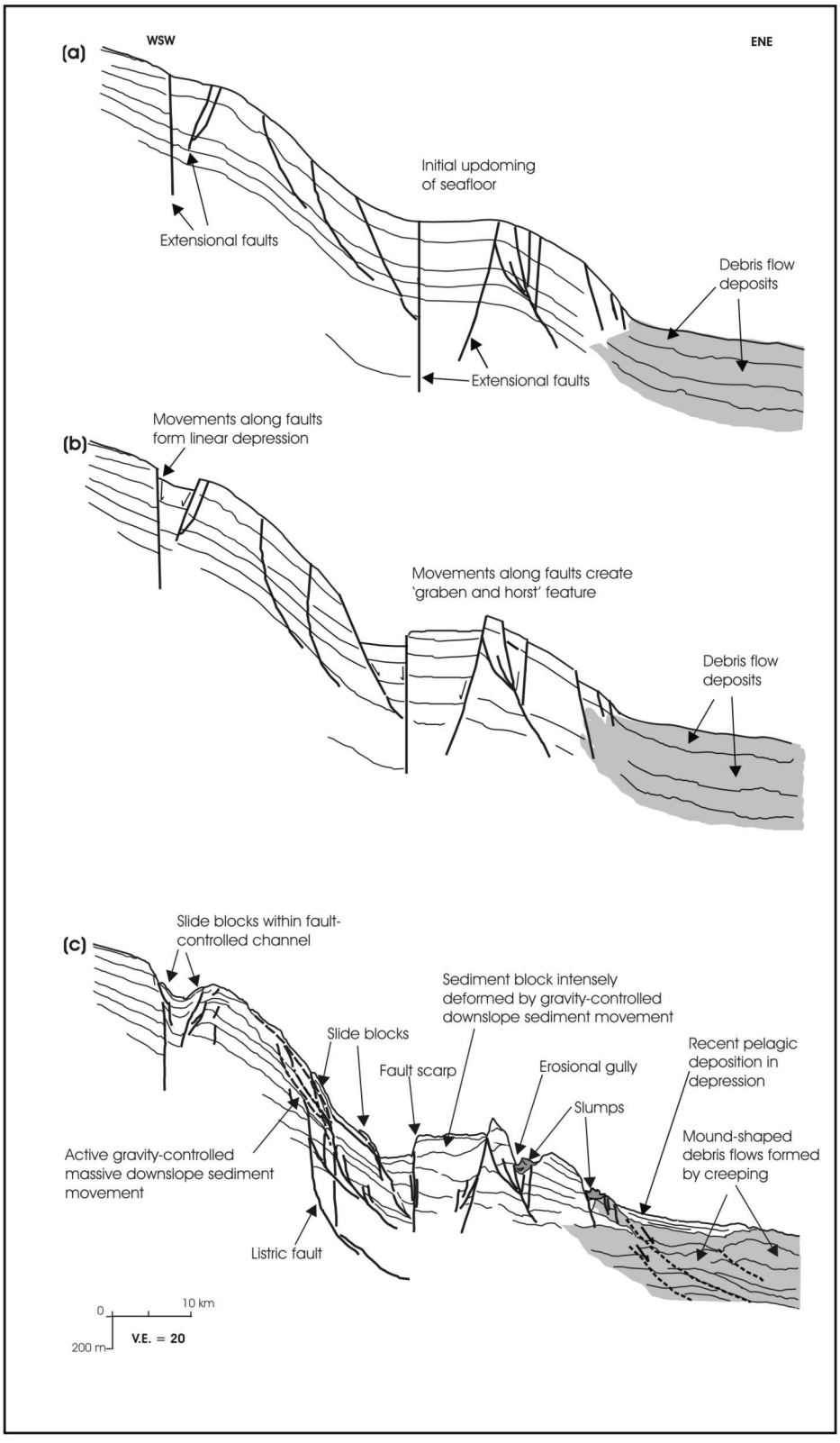


***Figure 4.7:*** *Schematic representation of recent structural deformation on sedimentation processes offshore Uruguay. The cause of the deformation is unknown. The model is based on our interpretation of Profile GeoB01-147a (Fig. 4.2). (a) Onset of updoming process leading to bathymetric swell (in lower slope) and extensional faulting (in the uppermost and lower slope). (b) Formation of fault scarps as well as 'graben and horst' feature following downward movement along faults. (c) Present shape of margin. See text for detailed explanation.*

gradient. However, as the gravity-flow process of the slope sediments is obstructed by the action of the updomed zone, intense compressive stresses are applied by the sliding sediments on the intervening sediment blocks, i.e. at the toe of the slope and on the western flank of the updomed area, leading to systematic folding and deformation of the blocks (Fig. 4.7c). The especially intense folding and deformation of the sediment blocks against the fault planes on the western flank of the uplifted zone, clearly demonstrate that the bathymetric swell is currently acting as a topographic barrier to active downslope mass sediment movement. Whilst our data coverage is not dense enough to allow a good determination of the strike extent of the swell, the presence of widespread recent terrigenous deposits in the rise (Bleil et al., 1994; Hensen et al., 2003) suggests that a great deal of the slope-derived mass sediment flows from the adjacent slope areas are able to by-pass this barrier. Hence, the bathymetric swell may be viewed as a local, albeit prominent, topographic barrier to recent downslope mass sediment movement.

Complex topographic irregularities on the sea floor are known to significantly intensify bottom current flow (Stoker, 1998). The ‘graben and horst’-like features associated with the bathymetric swell have created a local rugged seafloor topography hence giving rise to an intensification of bottom current activity, possibly dominated by the NADW. In addition, the associated fault scarps on the seafloor serve as sites of enhanced erosion by the increased current strength, resulting in the development of several contour-parallel erosional gullies. Furthermore, the highly unstable nature of the fault scarps, commonly results in slumping into the adjacent gullies and a further widening of the upper gully walls, thereby facilitating stronger bottom current circulation. The partly eroded slump deposits within the gullies attest to the efficiency of the powerful currents in evacuating slump sediments for onward re-deposition into the deep sea. The especially intense deformation of sediments on the western flank of the swell may have rendered the soft sediments more susceptible to erosion by strong bottom currents. Consequently, the swell constitutes a potential area for future sediment re-working for further re-distribution.

The influence of recent structural deformation on sedimentation and the structural model presented above only discusses possible scenarios which we consider as plausible based on the available data. A complete appreciation of the nature and scale of the influence of this bathymetric swell on sedimentation in the margin would require a detailed seismic investigation of the adjacent areas.

## 4.7 Conclusions

1. The slope of the Uruguayan margin is highly unstable, and is characterised by extensive gravity-flow processes. The slope seafloor morphology is dominated by slide/slump scars and several isolated slide and slump blocks. Downslope mass sediment transport has been facilitated by widespread lithological weak layers which serve as glide planes for sediment failures.
2. Slope oversteepening as well as build-up of excess pore pressure generated mainly from decayed organic matter and entrapped water during the rapid sediment build-up may be the most important trigger mechanism for the slope failures. Fluctuations in sea level could also be important in generating high pore pressures to trigger failures. However, the relatively smaller-scale failures associated with slide blocks and slumps may have been largely caused by slope oversteepening. Earthquakes may also constitute a potential trigger mechanism but in the absence of adequate data about earthquake activity in the margin, their influence could only be speculative.
3. The continental rise is dominated by widespread debris flow deposits occurring as stacks of lenses, extensive sheet-like forms and massive bodies separated by thin veneers of well-layered hemi-pelagic deposits. Three regionally traceable seismic reflectors associated with the hemi-pelagic sediments, group the debris flow units into distinct stratigraphic horizons. In deeper waters, the key reflectors are commonly associated with sediment waves and drift-like bodies as well as large erosional depressions, pointing to strong bottom current influence on hemi-pelagic depositional events.
4. The debris flow deposits were sourced from mass sediment movements originating from the adjacent shelf and slope areas through large-scale, or catastrophic, as well as small-scale failure events. The mass movement events must have been largely episodic, with each major depositional event of the debris flow units having occurred within a lowered sea level stage and terminated by the deposition of thin hemi-pelagic sediments under the influence of increased bottom current circulation during the subsequent rise in sea level.
5. Recent structural deformation in the margin has given rise to an intensely faulted and deformed bathymetric swell at the toe of the slope which now acts as a local topographic barrier to downslope sediment movement. The resulting rugged seafloor topography, which is dominated by fault scarps and a ‘graben and horst’ feature, serves as a site for enhanced bottom current activity.

6. Whilst the study provides new insights for understanding controls on slope processes, sediment transport mechanisms and re-deposition along the Uruguayan margin, a complete understanding of the sedimentation process history of the margin would require a more detailed and broader seismic investigation, also including age calibrations of key reflectors.

## 4.8 Acknowledgements

The immense contribution of the captain and crew members as well as all cruise participants of RV Meteor Cruise M49/2 for successful data acquisition, is most gratefully acknowledged. This is publication RCOMXXXX of the DFG-Research Center 'Ocean Margins' (University of Bremen).

## References

Antoine, D., Andre, J.M. and Morel, A., 1996. Oceanic primary production. 2. Estimation at global scale from satellite (coastal zone color scanner) chlorophyll. Global Biogeochem. Cycle, 10: 43-55.

Baraza, J., Ercilla, G. and Nelson, C.H., 1999. Potential geologic hazards on the eastern Gulf of Cadiz slope (SW Spain). Marine Geology, 155: 191-215.

Bleil, U. and Cruise participants., 1994. Report and preliminary results of Meteor Cruise M 29/2, Montevideo - Rio de Janeiro, 15.07. - 08.08.1994. Berichte, Fachbereich Geowissenschaftlichen, Universität Bremen. 59,

Cobbold, P.R. and Szatmari, P., 1991. Radial gravitational gliding on passive margins. Tectonophysics, 188: 249-289

Cohen, H.A. and McClay, K., 1996. Sedimentation and shale tectonics of the northwestern Niger Delta front. Marine and Petroleum Geology, 13: 313-328.

Dawson, A.G., 1999. Linking tsunami deposits, submarine slides and offshore earthquakes. Quaternary International, 60(1): 119-126.

Ewing, M. and Lonardi, A.G. (Editors), 1971. Sediment transport and distribution in the Argentine Basin. 5. Sedimentary structure of the Argentine Margin, Basin and related provinces. In: L.H. Ahrens et al., (Eds.), Physics and Chemistry of the Earth, 8. Pergamon Press, Oxford., 8, 123-251 pp.

Fine, I.V., Rabinovich, A.B., Bornhold, B.D., Thomson, R.E. and Kulikov, E.A., 2005. The Grand banks landslide-generated tsunami of November 18, 1929: preliminary analysis and numerical modeling. Marine Geology, 215: 45-57.

Flood, R.D. and Shor, A.N., 1988. Mud waves in the Argentine Basin and their relationship to regional bottom circulation patterns. Deep-Sea Research, 35: 943-971.

Fryer, G.J., Watts, P. and Pratson, L.F., 2003. Source of the great tsunami of 1 April 1946: a landslide in the upper Aleutian forearc. Marine Geology, 203(3-4): 201-218.

Hampton, M.A., Lee, H.J. and Locat, J., 1996. Submarine lanslides. Rev. Geophys., 34: 33-59.

Hensen, C. et al., 2003. Control of sulphate pore-water profiles by sedimentary events and the significance of anaerobic oxidation of methane for burial of sulfur in marine sediments. Geochimica et Cosmochimica Acta, 67(14): 2631-2647.

Klaus, A. and Ledbetter, M.T., 1988. Deep-sea sedimentary processes in the Argentine Basin revealed by high resolution-seismic records (3.5 kHz echograms). Deep-Sea Research, 35: 899-917.

Knutz, P.C., Jones, E.J.W., Austin, W.E.N. and van Weering, T.C.E., 2002. Glacimarine slope sedimentation, contourite drifts and bottom current pathways on the Barra Fan, UK North Atlantic margin. Marine Geology, 188: 129-146.

Laberg, J.S. and Vorren, T.O., 1995. Late Weichselian submarine debris flow deposits on the Bear Island Trough Mouth Fan. Marine Geology, 127: 45-72.

Laberg, J.S. and Vorren, T.O., 1996. The Middle and Late Pleistocene evolution of the Bear Island Trough Mouth Fan. Global and Planetary Change, 12: 309-330.

Laberg, J.S. and Vorren, T.O., 2000. The Traenadjupet Slide, offshore Norway- morphology, evacuation and triggering mechanisms. Marine Geology, 171: 95-114.

Lee, H.J., Chough, S.K. and Yoon, S.Y., 1996. Slope stability change from late Pleistocene to Holocene in the Ulleung Basin, East Sea (Japan Sea). Sedimentary Geology, 104: 39-51.

Lonardi, A.G. and Ewing, M. (Editors), 1971. Sediment transport and distribution in the Argentine Basin. 4. Bathymetry of the continental margin, Argentine Basin and related provinces. Canyons and sources of sediments. In: L.H. Ahrens et al., (Eds.), Physics and Chemistry of the Earth. Pergamon Press, Oxford., 8, 123-251 pp.

Lykousis, V., Roussakis, G., Alexandri, M. and Pavlakis, P., 2002. Sliding and regional slope stability in active margins: North Aegean Trough (Mediterranean). Marine Geology, 186: 281-298.

Mauduit, T., Gaullier, V. and Brun, J.P., 1997. On the asymmetry of turtle-back growth anticlines. Marine and Petroleum Geology, 14: 763-771.

McHugh, M.G.C., Damuth, J.E. and Mountain, S.G., 2002. Cenozoic mass-transport facies and their correlation with sea level change, New Jersey continental margin. Marine Geology, 184: 295-334.

Milliman, J.D., 1988. Correlation of 3.5 kHz acoustic penetration and deposition/erosion in the Argentine Basin: a note. Deep-Sea Research, 35: 919-927.

O'Leary, D.W., 1991. Structure and morphology of submarine slab slides: clues to origin and behaviour. Mar. Geotechnol., 10: 53-69.

Olson, D.B., Podesta, G.P., Evans, R.H. and Brown, O.B., 1988. Temporal variations in the separation of Brazil and Malvinas Currents. Deep-Sea Research, 35: 1971-1990.

Perissoratis, C. and Papadopoulos, G., 1999. Sediment instability and slumping in the southern Aegean Sea and the case history of the 1956 tsunami. Marine Geology, 161: 287-305.

Peterson, R.G., Johnson, C.S., Krauss, W. and Davis, R.E. (Editors), 1996. Langrangian measurements in the Malvinas Current. The South Atlantic: present and past circulation. Springer, 239-247 pp.

Peterson, R.G. and Stramma, L., 1991. Upper-level circulation in the South Atlantic Ocean. Prog. Oceanogr., 26: 1-73.

Piper, D.J.W. and Ingram, S., 2003. Major Quaternary sediment failures on the east Scotian Rise, eastern Canada. Geological Suvey of Canada, Current Research, 2003-D1: 7.

Rabinowitz, P.D. and LaBrecque, J., 1979. The Mesozoic South Atlantic Ocean and evolution of its continental margins. J. Geoph. Res., 84: 5973-6002.

Reid, J.L., 1989. On the total geostrophic circulation of the South Atlantic Ocean: flow patterns, tracers and transports. Prog. Oceanogr., 23: 149-244.

Spiess, V. and participants, c., 2002. Report and preliminary results of Meteor Cruise M 49/2, Montevideo (Uruguay) - Montevideo, 13.02. - 07.03.2001. 203, University of Bremen.

Stoker, M.S. (Editor), 1998. Sediment drift development on the Rockall continental margin off NW Britain. Geological processes on continental margins: Sedimentation mass wasting and stability, 129. Geological Society, London, 229-254 pp.

Trifunac, M.D., Hayir, A. and Todorovska, M.I., 2003. A note on tsunami caused by submarine slides and slumps spreading in one dimension with nonuniform displacement amplitudes. Soil dynamics and Earthquake Engineering, 23(3): 41-52.

U.S.G.S., 2004. Earthquakes program: Seismicity of the South Atlantic Ocean. http://neic.usgs.gov/neis/general/seismicity/s_atlantic.html

von Lom-Keil, H., Spiess, V. and Hopfauf, V., 2002. Fine-grained sediment waves on the western flank of the Zapiola Drift, Argentine Basin: evidence for variations in Late Quaternary bottom flow activity. Marine Geology, 192: 239-258.

Vorren, T.O. et al., 1998. The Norwegian-Greenland Sea continental margins: morphology and Late Quaternary sedimentary processes and environment. Quaternary Science Review, 17: 273-302.

Weaver, P.P.E., Wynn, R.B., Kenyon, N.H. and Evans, J., 2000. Continental margin sedimentation, with special reference to north-east Atlantic margin. Sedimentology, 47 (Suppl. 1): 239-256.

Wefer, G. et al., 1999. Preliminary Proposal for the Ocean Drilling Program: Brazil-Falkland (Malvinas) Confluence: Paleoceanography of a Mixing Region.

Wynn, R.B., Masson, D.G., Stow, D.A.V. and Weaver, P.P.E., 2000. The Northwest African slope apron: a modern analogue for deep water systems with complex seafloor topography. Marine and Petroleum Geology, 17: 253-265.

# Chapter 5: Summary and perspectives

Processes of mass sediment transport in two geologically diverse Atlantic margins which are associated with high marine productivity, i.e. the Mauritanian margin and the Uruguayan margin, were investigated using hydroacoustic (Hydrosweep swath bathymetry and Parasound echosounder) and high resolution multi-channel seismic reflection (MCS) methods. The Mauritanian margin is dominated by hyper-arid conditions and receives large amounts of offshore wind-blown eolian sediments. The margin is also the site of high rates of sediment accumulation related to upwelling-induced high productivity. The Uruguayan margin, on the other hand, is a fluvial-dominated margin which receives large volumes of organic-rich terrigenous sediments from the Rio de la Plata, but is also additionally influenced by high primary productivity arising from intensely mixing surface waters. Though both margins offer good opportunities for studying mass sediment transport processes, especially geologically recent events in two geologically unique settings, the margins are poorly surveyed. The main investigations in this thesis are centred around two major features associated with processes of mass sediment transport off the Mauritanian margin, i.e. the Cap Timiris Canyon and the Mauritania Slide Complex, both of which were surveyed in detail with hydrocoustic methods and high resolution MCS profiling during RV Meteor Cruise M58/1 in April/May 2003. An additional area offshore Uruguay, which is dominated by extensive slope instabilities and mass sediment transport, was also investigated based on high resolution MCS data acquired from the area during RV Meteor Cruise M49/2 in February 2001.

Results of the thesis document for the first time the detailed morphology and seismic structure of Cap Timiris Canyon, which was discovered during RV Meteor Cruise M58/1. The combined interpretation of Hydrosweep swath bathymetry and high resolution MCS data acquired over the canyon has afforded deep insights into processes leading to canyon development as well as the role it has played in the sedimentary dynamics of the margin. Cap Timiris Canyon is dominantly V-shaped and displays many fluvial features. The head region is composed of a series of dendritic canyons and gullies that funnel sediments from a large area, >5000 km², along the Mauritanian margin into the main canyon. Canyon incision and meander evolution have given rise to a number of terraces of different genetic origin. Seismic characterization of the terraces reveal a variety of internal structures which suggest that they originated through a number of different processes including sliding/slumping, uplift-induced incision and lateral accretion. Canyon development is strongly influenced by variations in underlying geology, seafloor gradient, sediment supply and tectonic controls. The nature of

the influence is directly reflected in the style and patterns of meandering as well as processes of terrace formation.

The origin of Cap Timiris Canyon is ascribed to an ancient river system that flowed in the adjacent presently arid Sahara Desert and breached the shelf during a Plio/Pleistocene sea level lowstand in order to deliver sediment directly into the slope area. The data interpretation suggests that the initial invading unchannelised sheet of sand-rich turbidity flows initiated canyon formation by gradually mobilizing along linear seafloor depressions and fault-controlled zones of weakness. The study proposes that the development of canyon morphology and structure was influenced by the stages of active flow of the coupling river system, and hence could act as a proxy for understanding the paleo-climatic evolution of a 'green' Sahara since Neogene time. Though the canyon is currently decoupled from any potential river point source under the present highstand regime, it has been kept preserved mainly through sediment supplies from a number of sources including upwelling-induced sedimentation, offshore wind-blown sediments from the Sahara Desert and remobilized sediment from the shelf areas and canyon vicinities.

The extensive coverage of the Mauritania Slide Complex by Parasound and high resolution MCS profiling during RV Meteor Cruise M58/1 afforded a more detailed characterisation of the slide complex than previously reported. The seafloor morphology reveals that the Mauritania Slide Complex is a major feature that has destabilized an area in the order of 34,000 km² which lies between ~600 - >3500 m water depths. The headwall scars is characterised by a series of steps in seafloor morphology ranging between 25 – 100 m high and occurring between 600 - 2000 m water depths. The slide, which is ovate-shaped, displays a long run-out distance >320 km as a result of higher sediment flow mobility induced in its northern parts by bounding canyon systems and the Cape Verde Rise. In addition, the increased mobility in the northern parts may have been aided by diapiric growths which promoted the disintegration of overlying widespread contouritic deposits. The area became slide-prone as a result of a number of pre-conditioning factors which include undisturbed rapid sediment accumulation from upwelling-induced organic-rich sediments and wind-blown eolian sediments in a sheltered open slope setting as well as the formation of widespread thin lithologically weak layers interbedded within thick well-stratified, often contouritic, sediment piles.

The data interpretation suggests that the development of the Mauritania Slide Complex was characterised by multi-staged processes of slide formation which took place under major and minor failure events. Slide formation during major failure events was dominated by

retrogressive sliding which was promoted by lithological weak layers. However, later minor instability events mainly remobilized pre-existing slide deposits and also, locally, gave rise to translational sliding. Excess pore pressures, resulting from decayed organic matter and/or sea level rise, appear to be the most important trigger mechanism for slide formation. However, seismic shaking may have played a complementary or, at one time or the other, a leading role in triggering the sediment failures. The effects of diapiric growths are mostly observable as minor instability events. The combined activities of these factors are the most likely cause of the complex morphology of the Mauritania Slide Complex.

The studied area in the Uruguayan margin is dominated by extensive mass sediment movements. Slope instabilities have given rise to the downslope movement of large sediment packages as well as several discrete slide and slump blocks which are observed in the upper and middle slope areas. As similarly observed in the Mauritanian margin, the mass sediment movements here have been facilitated by lithological weak layers which served as glide planes. Extensive debris flow depositions dominate the continental rise. The debris flow deposits occur variously as stacks of lenses, extensive sheet-like forms as well as massive bodies separated by thin veneers of well-layered pelagic sediments. Regionally traceable reflectors associated with the thin hemi-pelagic intervals group the debris flow deposits into distinct stratigraphic horizons.

Slide development was also pre-conditioned by the formation of widespread weak layers during rapid sediment build-up. Mass sediment failures may have been triggered mostly by build-up of excess pore pressure arising from entrapped water during the rapid sediment accumulation process as well as decayed organic matter from fluvial sources and high primary productivity. Slope oversteepening may also be important in triggering large scale slope failures, but its influence is mostly observed for the relatively smaller-scale failure events. Earthquakes appear to constitute a potential trigger mechanism but in the absence of adequate data about the earthquake history of the margin, their influence could only be speculative. Evidence of block faulting associated with a locally updomed seafloor suggests part of the Uruguayan margin has experienced recent structural deformation. The updomed feature acts as a local topographic barrier for recent mass sediment movement and also enhances bottom current circulation. The study suggests that the sedimentation process history of the margin has been characterised by episodic major mass sediment movement events which predominated during lowered sea level stages, and was curtailed during the subsequent rise in sea level when sedimentation was dominated by hemi-pelagic deposition.

In general, the main results of the thesis indicate that margin physiography may have played a key role in determining the style of mass sediment transport. Along both the Mauritanian and Uruguayan margins the style of mass sediment transport displays a sharp transition from channelised flow processes to large scale mass sediment movements in open slope environments. Entry points of major fluvial systems along the coast were likely to have given rise to canyon processes as noted for both margins. Subsequent canyon evolution may have been influenced by the stages of flow of the connecting river system. Where the entry points coincide with regional structural lineations in the margin, the process of canyon formation was significantly enhanced.

The open slope areas in both margins allowed undisturbed rapid sediment build-up which gave rise to sediment instabilities arising primarily from underconsolidation of the deposited sediments. Build-up of excess pore-pressures appears to be the most important trigger mechanism for large-scale mass sediment failures in both margins. Furthermore, both margins display widespread distribution of lithological weak layers which were exploited as glide planes for mass sediment movement. Whereas the Uruguayan margin additionally receives organic matter from the fluvial source at present times, the Mauritanian margin currently does not receive any fluvial input. However, the occurrence of the Cap Timiris Canyon and its postulated coupling to an ancient river as well as the fact that the mouth of the Senegal River was located further to the North during Miocene/Pliocene times also suggest significant fluvial input to this margin in past times. It appears high marine productivity has been very instrumental in significantly elevating the organic inputs into both margins which enhanced the generation of excess pore pressures and also, perhaps, introduced more organic matter into the formation of the mud-rich lithologic weak layers.

The thesis provides fundamental insights for understanding canyon processes and open slope mass sediment movement along passive continental margins influenced by high productivity. Results from the Cap Timiris Canyon call for further research efforts to completely establish the temporal and spatial relationships between canyon origin and its fluvial source. The resulting information could be a useful proxy for resolving the paleo-climatic evolution of the Sahara Desert since Neogene time. In addition, a detailed investigation is required of the distal channel segment of the canyon and its associated levees as well as the down-system depositional environment for a complete understanding of the role the canyon has played in the sedimentary dynamics of the margin. New data addressing these aspects were collected during Meteor-Cruise M65/2 in July 2005.

In the case of the Mauritania slide Complex, further work should investigate the temporal and spatial relationships between diapiric growths and sediment destabilization in the slide area. Further data coverage is needed for especially the distal parts of the slide in order to completely constrain the seafloor map of the slide complex. A more detailed data coverage of the slide would also allow a much closer investigation of the sediment flow mobility history of the slide complex.

Whilst the study of the Uruguayan margin provides new insights for understanding controls on slope processes, sediment transport mechanisms and re-deposition along the margin, a complete understanding of the sedimentation process history of the margin would require a more detailed and broader seismic investigation, also including age calibrations of key reflectors. Future research efforts should in particular expand coverage to the presumed source area of the debris flows in order to allow firm conclusions to be drawn about the mode of sediment failures that have given rise to the extensive debris flow distribution. In addition the cause of the bathymetric swell as well as its influence on sedimentation processes should be of great interest for further investigations. A pre-proposal for a Meteor-Cruise with the aim of studying the sediment transport at this margin from the shelf to the deep sea was successfully reviewed and the full proposal is to be submitted by the end of this year. The proposed work includes acoustic, sedimentological and geochemical investigations for a detailed characterization of the sedimentary process of the margin. Additionally, geotechnical analyses including in situ pore pressure measurements of selected slides and their glide planes should examine the slope stability and therefore potential trigger mechanisms.

## General acknowledgements

I am deeply grateful to Prof. Dr. Volkhard Spieß for offering me the opportunity to undertake this PhD research study which is under the frame of Project C2 of the Research Center Ocean Margins (RCOM). I am also very thankful to him for being my advisor. It is through his generously provided guidance and support that this work has been realized. I also gratefully acknowledge Prof. Dr. Rüdiger Henrich for agreeing to be a referee to this thesis.

I acknowledge with deep thanks to Dr. Sebastian Krastel for being a very supportive and readily cooperative co-advisor. This work benefited greatly from very useful and stimulating discussions during Project C2 meetings with colleagues including Prof. Dr. Katrin Huhn, Dr. Till Hanebuth, Dr. Martin Kölling, Dr. Christine Holz, Ingo Kock, and Katharina Wien, and I am very grateful to these persons as well. I deeply cherish the excellent cooperation and good working relationship I enjoyed among colleagues within my research group, AG Spieß. I specially thank Angelika Rinkel for her kind and ready support. The research study was funded by the DFG Research Center 'Ocean Margins'

And finally, I need to specially commend my family, my wife, Akos and daughters, Gloria, Andrea and Alfreda, especially for their patience, understanding and care which have always provided me the basis to reach for a higher dream!